

ADA 039754

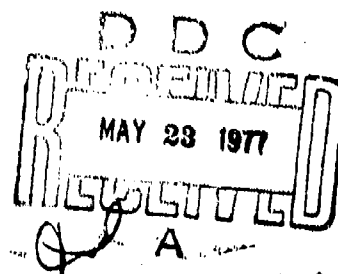
AFML-TR-76-153

**THE MECHANISMS OF ELEVATED TEMPERATURE PROPERTY
LOSSES IN HIGH PERFORMANCE STRUCTURAL EPOXY
RESIN MATRIX MATERIALS AFTER EXPOSURES TO HIGH
HUMIDITY ENVIRONMENTS**

*COMPOSITE AND FIBROUS MATERIALS BRANCH
NONMETALLIC MATERIALS DIVISION*

MARCH 1977

TECHNICAL REPORT AFML-TR-76-153
FINAL REPORT FOR PERIOD JUNE 1974 - JULY 1976



Approved for public release; distribution unlimited

AIR FORCE MATERIALS LABORATORY
AIR FORCE WRIGHT AERONAUTICAL LABORATORIES
AIR FORCE SYSTEMS COMMAND
WRIGHT-PATTERSON AIR FORCE BASE, OHIO 45433

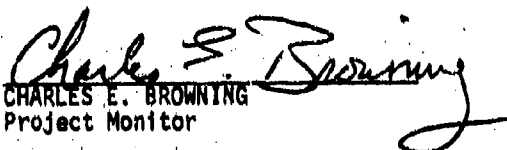
DDC FILE COPY

NOTICE


When Government drawings, specifications, or other data are used for any purpose other than in connection with a definitely related Government procurement operation, the United States Government thereby incurs no responsibility nor any obligation whatsoever; and the fact that the government may have formulated, furnished, or in any way supplied the said drawings, specifications, or other data, is not to be regarded by implication or otherwise as in any manner licensing the holder or any other person or corporation, or conveying any rights or permission to manufacture, use, or sell any patented invention that may in any way be related thereto.

This report has been reviewed by the Information Office (IO) and is releasable to the National Technical Information Service (NTIS). At NTIS, it will be available to the general public, including foreign nations.

This technical report has been reviewed and is approved for publication.


CHARLES E. BROWNING
Project Monitor

FOR THE COMMANDER


T. J. REINHART, JR., Chief
Composite and Fibrous Materials Branch
Nonmetallic Materials Division

Copies of this report should not be returned unless return is required by security considerations, contractual obligations, or notice on a specific document.

UNCLASSIFIED

SECURITY CLASSIFICATION OF THIS PAGE (When Data Entered)

REPORT DOCUMENTATION PAGE		READ INSTRUCTIONS BEFORE COMPLETING FORM
1. REPORT NUMBER AFML-TR-76-153	2. GOVT ACCESSION NO.	3. RECIPIENT'S CATALOG NUMBER
4. TITLE (and Subtitle) THE MECHANISMS OF ELEVATED TEMPERATURE PROPERTY LOSSES IN HIGH PERFORMANCE STRUCTURAL EPOXY RESIN MATRIX MATERIALS AFTER EXPOSURES TO HIGH HUMIDITY ENVIRONMENTS.	5. TYPE OF REPORT & PERIOD COVERED Technical Report, Jun 74-Jul 76	6. PERFORMING OR REPORT NUMBER
7. AUTHOR Charles Edward Browning	8. CONTRACT OR GRANT NUMBER(s)	
9. PERFORMING ORGANIZATION NAME AND ADDRESS Air Force Materials Laboratory Air Force Systems Command Wright-Patterson Air Force Base, Ohio 45433	10. PROGRAM ELEMENT, PROJECT, TASK AREA & WORK UNIT NUMBERS 734003AB	
11. CONTROLLING OFFICE NAME AND ADDRESS Air Force Materials Laboratory Nonmetallic Materials Division Composite & Fibrous Materials Branch	12. REPORT DATE Mar 1977	13. NUMBER OF PAGES 187
14. MONITORING AGENCY NAME & ADDRESS (if different from Controlling Office) 12 188p.	15. SECURITY CLASS. (of this report) Unclassified	15a. DECLASSIFICATION/DOWNGRADING SCHEDULE
16. DISTRIBUTION STATEMENT (of this Report) Approved for public release; distribution unlimited.		
17. DISTRIBUTION STATEMENT (of the abstract entered in Block 20, if different from Report)		
18. SUPPLEMENTARY NOTES		
19. KEY WORDS (Continue on reverse side if necessary and identify by block number) Moisture High Humidity Exposures Creep Glass Transition Effects Epoxy Resin Matrix Materials High Performance Composites		
20. ABSTRACT (Continue on reverse side if necessary and identify by block number) The objective of this research program was the determination of the mechanisms by which epoxy resins utilized in high performance composites and adhesives exhibit losses in their elevated temperature properties as a result of exposure to a humid environment. The study specifically considered an epoxy resin formulation that is characteristic of a variety of composite and adhesive systems. The moisture absorption and diffusion characteristics of this resin system were first investigated		

DD FORM 1 JAN 75 1473

EDITION OF 1 NOV 65 IS OBSOLETE

UNCLASSIFIED

SECURITY CLASSIFICATION OF THIS PAGE (When Data Entered)

012320

JF

UNCLASSIFIED

SECURITY CLASSIFICATION OF THIS PAGE(When Data Entered)

20. Abstract (Contd)

as a function of simple humidity environments and simulated real-life environments which included thermal spikes. In addition, the effect of absorbed moisture on the resin system's glass transition temperature, T_g was determined as a function of both simple humidity and real-life exposures. This was followed by a study into the tensile and creep behavior of the epoxy resin as a function of absorbed moisture. A variety of experimental techniques were utilized to accomplish these studies: constant strain rate and dynamic tensile measurements, infrared spectroscopy, heat distortion tests, bomb creep tests, scanning electron microscopy, polarized-light photomicroscopy, and ESCA.

The results established that moisture plasticized this particular epoxy resin, causing a lowering of the T_g which in turn affected mechanical response, such as by shifting the relaxation moduli to shorter times. This phenomenon is described and quantified in terms of an existing free volume theory relationship. Weight-gains greater than equilibrium amounts were observed without accompanying T_g changes which is attributed to moisture entrapment during microcracking in the resin.

Creep studies performed underwater at 300°F established an addition mechanism for loss of elevated temperature properties. This loss is characterized by the appearance and growth of cracks in the material. The observed failure processes are described in terms of an existing theory for rupture of cross-linked rubbers. The process is governed by the synergistic effects of moisture, temperature, and stress. Moisture changes the viscoelastic response of the material so that stress-induced crack formation and growth is facilitated. Also, it is inferred from the creep studies that no significant, chemically-induced chain scission is taking place; however, very localized chemical chain scission at such areas as crack tips cannot be completely ruled out.

UNCLASSIFIED

SECURITY CLASSIFICATION OF THIS PAGE(When Data Entered)

TABLE OF CONTENTS

SECTION	PAGE
I INTRODUCTION	1
II HISTORICAL	3
1. Moisture Absorption and Transmission in Epoxies	4
2. Moisture Effects on the Physical/Mechanical Properties of Epoxies	19
3. Reversible Processes	22
4. Irreversible Processes	27
III RESEARCH PLAN	29
IV RESULTS AND DISCUSSION	31
1. Materials Selection and Preparation	31
2. Absorption and Diffusion Studies	32
a. Sample Configurations	33
b. Constant Temperature and Humidity Exposures	33
c. Real-Life Environmental Exposures	62
d. Absorption Anomalies	64
e. Swelling	74
3. Glass Transition Temperature Studies	78
a. Background	78
b. Experimental	82
c. Results and Discussion	84
4. Stress-Strain Studies	94
a. Tensile Tests	94
b. Near Infrared Studies	108
c. Environmentally Induced Stresses	112

PRECEDING PAGE BLANK NOT FILMED

TABLE OF CONTENTS (Contd)

SECTION	PAGE
5. Creep Studies	114
a. Background	114
b. Experimental	129
c. Results and Discussion	133
V CONCLUSIONS	152
APPENDIX HDT CURVES	157
REFERENCES	171

LIST OF ILLUSTRATIONS

FIGURE	PAGE
1. Effect of Oxygen Content on Water Absorption of Metaphenylenediamine Cured Epoxy Castings (Reference 8)	5
2. The Effective Fractional Water Absorption as a Function of the Square Root of Time for E-293 and X-904 Epoxy Resins (Reference 3)	10
3. Diffusion of H ₂ O into Epoxy X-904 Plate at Room Temperature and 75% RH (Reference 3)	11
4. Diffusion of H ₂ O into Epoxy E-293 Plate at Room Temperature and 75% RH (Reference 3)	12
5. Moisture Absorption in a 4-Ply Graphite/Epoxy Laminate at 120°F (Reference 10)	14
6. Effect of Relative Humidity on Equilibrium Moisture Content (Reference 10)	15
7. Moisture Absorption in a 4-Ply Graphite/Epoxy Laminate (Reference 10)	16
8. A "Real-Life" Environmental Exposure Cycle (Reference 10)	17
9. Comparison of Real-Life and Simple Humidity Absorption Behavior (Reference 10)	18
10. Types of Relaxation Unit Processes Which a Polymer Sample May Undergo (Reference 16)	20
11. Barcol Hardness vs. Temperature for Dry and Humidity Aged Epoxy Specimens (Reference 20)	23
12. HDT Measurements for Dry and Humidity Aged Epoxy Samples (Reference 2)	24
13. HDT Curves for Dry and Humidity Aged Epoxy Specimens (Reference 20)	25
14. Dilatometer Results on Dry and Humidity Aged Epoxy Specimens (Reference 21)	26
15. Weight-Gain vs. Time for Different Temperatures at 100% RH	35

LIST OF ILLUSTRATIONS (Contd)

FIGURE	PAGE
16. Weight-Gain vs. Time for Different Temperatures at 75% RH	36
17. Weight-Gain vs. Time for Different Humidity Conditions	37
18. Equilibrium Weight-Gain vs. Relative Humidity	38
19. Fraction of Equilibrium Weight-Gain as a Function of Square Root of Time for 100% RH	39
20. Diffusion Coefficient vs. Reciprocal of Absolute Temperature for 100% RH	40
21. Fraction of Equilibrium Weight-Gain as a Function of Square Root of Time for 75% RH	43
22. Diffusion Coefficient vs. Reciprocal of Absolute Temperature for 75% RH	44
23. Diffusion of Water into a 0.125-Inch Thick Plate of Epoxy Resin at 100°F and 100% RH	45
24. Diffusion of Water into a 0.25-Inch Thick Plate of Epoxy Resin at 100°F and 100% RH	46
25. Diffusion of Water into a 0.500-Inch Thick Plate of Epoxy Resin at 100°F and 100% RH	47
26. Diffusion of Water into a 0.125-Inch Thick Plate of Epoxy Resin at 75°F and 75% RH	48
27. Diffusion of Water into a 0.25-Inch Thick Plate of Epoxy Resin at 75°F and 75% RH	49
28. Diffusion of Water into a 0.500-Inch Thick Plate of Epoxy Resin at 75°F and 75% RH	50
29. Epoxy Moisture Absorption - 160°F/100% RH	52
30. TANH Treatment of Epoxy Moisture Absorption for 100% RH	54
31. TANH Treatment of Epoxy Moisture Absorption for 100% RH	55
32. TANH Treatment of Epoxy Moisture Absorption for 100% RH	56

LIST OF ILLUSTRATIONS (Contd)

FIGURE	PAGE
33. TANH Treatment of Epoxy Moisture Absorption for 100% RH	57
34. Diffusion Coefficient vs. Reciprocal of Absolute Temperature for 100% RH TANH Treatment	59
35. Predicted Epoxy Moisture Absorption According to Different Solutions of Fick's Law	61
36. Epoxy Moisture Absorption as a Function of Real-Life Exposure Conditions	63
37. The Effect of Thermal-Spikes on Epoxy Moisture Absorption (160°F/100% RH)	65
38. The Effect of Thermal-Spikes on the Moisture Absorption (160°F/100% RH) of Several Epoxy Castings	66
39. Moisture Absorption for Several Epoxy Castings - 160°F/100% RH	67
40. SEM of Epoxy Specimen after Exposure to 160°F/ 100% RH - 5.6% Weight-Gain (2000 X)	69
41. SEM of Epoxy Specimen after Exposure to 160°F/ 100% RH/1 Daily Thermal-Spike - 6.7% Weight-Gain (2000 X)	69
42. SEM of Epoxy Specimen after Exposure to 160°F/ 100% RH/ 1 Daily Thermal-Spike - 6.7% Weight-Gain (600 X)	70
43. SEM of Epoxy Specimen after Exposure to 160°F/ 100% RH/4 Daily Thermal-Spikes - 7.4% Weight-Gain (300 X)	70
44. SEM of Epoxy Specimen after Exposure to 160°F/ 100% RH/4 Daily Thermal-Spikes - 7.4% Weight-Gain (3000 X)	71
45. SEM of Epoxy Specimen after Exposure to 160°F/ 100% RH/4 Daily Thermal-Spikes - 7.4% Weight-Gain (60 X)	71
46. SEM of Fracture Surface of Epoxy Specimen after Exposure to 160°F/100% RH/4 Daily Thermal-Spikes- 7.4% Weight-Gain (100 X)	72

LIST OF ILLUSTRATIONS (Contd)

FIGURE	PAGE
47. SEM of Fracture Surface of Epoxy Specimen after Exposure to 160°F/100% RH/4 Daily Thermal-Spikes - 7.4% Weight-Gain (200 X)	72
48. SEM of Fracture Surface of Epoxy Specimen after Exposure to 160°F/100% RH/4 Daily Thermal-Spikes - 7.4% Weight-Gain (80 X)	73
49. Photomicrograph of Epoxy Surface after Exposure to 160°F/100% RH/4 Daily Thermal-Spikes - 7.4% Weight-Gain	75
50. Photomicrograph of Epoxy Surface after Exposure to 160°F/100% RH/4 Daily Thermal-Spikes - 8.3% Weight-Gain	75
51. Thickness Increase as a Function of Moisture Absorption	77
52. Modulus vs. Temperature Curve for Typical Visco-elastic Cross-Linked Amorphous Polymer	79
53. T_g Measurement from Specific Volume vs. Temperature Plot	81
54. Diagram of HDT Test Apparatus	83
55. T_g Determination from HDT Test	85
56. HDT Curves as a Function of Absorbed Moisture - 160°F/100% RH	86
57. HDT Curves as a Function of Absorbed Moisture for 180°F/75% RH Exposure	87
58. T_g as a Function of Absorbed Moisture for 100% RH Exposure	88
59. T_g as a Function of Absorbed Moisture for 75% RH Exposure	89
60. T_g vs. Equilibrium Weight-Gain	91
61. HDT Curves as a Function of Absorbed Moisture for 160°F/100% RH/1 Daily Thermal-Spike Exposure	92

LIST OF ILLUSTRATIONS (Contd)

FIGURE	PAGE
62. T_g as a Function of Absorbed Moisture for 160°F/ 100% RH/1 Daily Thermal-Spike Exposure	93
63. Constant Strain-Rate Tensile Test Coupon	94
64. Stress-Strain Behavior of Dry, Control Epoxy Specimens	96
65. Stress-Strain Behavior of Wet (Equilibrium Weight- Gain) Epoxy Specimens	97
66. Relaxation Modulus as a Function of Temperature for Dry, Control Specimens	98
67. Relaxation Modulus as a Function of Temperature for Wet (Equilibrium Weight-Gain) Specimens	99
68. Relaxation Modulus Master Curves, Reference Temperature = 300°F	100
69. Determination of Shift Factor from Different Modulus - Temperature Curves	101
70. Tan δ vs. Temperature for Dry, Control Sample	104
71. Storage Modulus (E') and Loss Modulus (E'') vs. Temperature for Dry, Control Sample	105
72. Tan δ vs. Temperature for Specimen Exposed to Equilibrium Weight-Gain and Then Dried	106
73. Storage Modulus (E') and Loss Modulus (E'') vs. Temperature for Specimen Exposed to Equilibrium Weight-Gain and Then Dried	107
74. Near IR Spectra of Dry, Control Specimen and Aged (300°F/Underwater/1 HR) Specimen	109
75. Near IR Spectra of Epoxy Resin as a Function of Cure- (1) 1 HR at 250°F, (2) 3 HRS at 250°F, (3) 3 HRS at 250°F + 1 HR at 300°F, (4) 3 HRS at 250°F + 1 HR at 300°F + 1/2 HR at 350°F	110
76. Qualitative Determination of Gradients and Stress States for Thermal-Spike/Humidity Environment	113
77. Typical Creep Curves for a Cross-Linked Rubber (Reference 18)	115

LIST OF ILLUSTRATIONS (Contd)

FIGURE	PAGE
78. Stress-Relaxation Behavior of a Cross-Linked Rubber at 100°C (Reference 19)	117
79. Stress-Relaxation Behavior of a Cross-Linked Rubber at 120°C in Air and Purified Nitrogen (Reference 19)	118
80. Stress-Relaxation Behavior of a Cross-Linked Rubber as a Function of Temperature (Reference 19)	119
81. Effect of Temperature on the Rupture Stress of Cross-Linked Rubbers (Reference 40)	122
82. Creep-Rupture Stress vs. Time for Different Test Temperatures (Reference 40)	124
83. Hypothetical Rupture Stress vs. Time Curves at a Constant Temperature	125
84. Hypothetical Critical Fracture Stress vs. Crack Length Curves	126
85. Number of Cracks per cm vs. Applied Stress for Rubbers Having Pre-Existent Flaws-(1) = RAZOR-CUT, (2) = DIE-CUT (Reference 43)	128
86. Bomb Creep Test Specimen Configuration	130
87. Bomb Creep Test Apparatus Mounted in an Oven	132
88. Elongation vs. Time for Bomb Creep Tests at 300°F and Underwater (Saturation)	134
89. Stress and Elongation vs. Time-To-Break for 300°F/Underwater (Saturation) Creep Tests	136
90. Polarized-Light Photomicrographs (20X) of 300°F/Underwater (Saturation) Creep Test Specimens	137
91. Polarized-Light Photomicrographs (20X) of 300°F/Underwater (Saturation) Creep Test Specimens	138
92. Polarized-Light Photomicrographs (20X) of 300°F/Underwater (Saturation) Creep Test Specimen	139

LIST OF ILLUSTRATIONS (Contd)

FIGURE	PAGE
93. Polarized-Light Photomicrographs (20X) of Dry, Control Specimens	140
94. Elongation vs. Time for Bomb Creep Test in Dry Nitrogen	141
95. Elongation vs. Time for Bomb Creep Tests at 300°F and Above Water (<Saturation)	142
96. Polarized-Light Photomicrographs (20X) of 300°F Above Water (<Saturation) Creep Test Specimens	143
97. Polarized-Light Photomicrographs (20X) of 300°F Above Water (<Saturation) Creep Test Specimen	144
98. Elongation vs. Time for Bomb Creep Tests at 200°F and Underwater	146
99. Polarized-Light Photomicrographs (20X) of 200°F/ Underwater Creep Test Specimens	147

LIST OF TABLES

TABLE	PAGE
1. Water Absorption and Oxygen Content of Metaphenylenediamine Cured Epoxy Castings	6
2. Results of Linear Solution to Fick's Law for 100% RH Exposures	42
3. Results of Linear Solution to Fick's Law for 75% RH Exposures	42
4. Results of TANH Solution to Fick's Law for 75% RH Exposures	58
5. Qualitative and Quantitative ESCA Results on Dry Control and Environmentally Aged Epoxy Samples	149
6. Chemical ESCA Results on Dry and Aged Epoxy Samples	150

SECTION I

INTRODUCTION

Structural composite materials derived from epoxy resins and fibrous reinforcements such as fiberglass, graphite, and boron filaments have found ever increasing importance in the field of commercial and military aircraft and space systems. This trend will undoubtedly continue with major interest concentrated on composites of graphite and boron. To derive the maximum benefit from these high performance reinforcements the resin matrices utilized must retain a high percentage of their initial physical properties under a wide range of temperature and humidity conditions. In the case of epoxy resins it has been shown (References 1 - 4) that their elevated temperature properties are adversely affected by high humidity to a degree that limits their ultimate potential.

The objective of this research program was to study the loss in elevated temperature mechanical properties exhibited by high performance composite matrix materials after exposure to high humidity environments and to examine associated pertinent phenomena. This study specifically included an epoxy resin that is common to a variety of composite and adhesive systems.

The epoxies, as a class of polymers, are one of the most important commercial engineering plastics, being used as matrix resins, adhesives, protective coatings, etc. They are playing a critical role in the ever increasing use of adhesives and high performance composites in current and future aerospace programs. The current limitation of epoxy resins is their substantial loss in elevated temperature (300-350°F) mechanical properties (tensile strength and modulus, flexural strength and modulus, etc.) as a result of moisture absorbed from high humidity environments. This property degradation was recently discovered (References 1-4) and has become increasingly important as high performance structural composites and adhesives are being applied in more critical applications to current and future aircraft. Historically, composite hardware has been so drastically overdesigned that this property loss would

probably not be a major concern. However, now that composites are being applied to primary aircraft structures, it would be very desirable to design the composites closer to their application requirements, resulting in a lighter structure and reduced materials and fabrication costs. This necessitates that the behavior of the composite materials, in particular the resin matrices, be well characterized with respect to their environmental responses and that they suffer no unpredictable loss of mechanical properties due to moisture and other environmental factors.

Several mechanisms have been postulated for the humidity related property losses shown by the epoxies (References 1, 3, 5). These included plasticization and chemical reactions such as chain scission leading to degradation. Plasticization needed to be validated, and the presence and extent of the other possibilities needed to be delineated. It should be noted that additional problems can arise in epoxy composites due to the presence of fibers. Included here would be fiber loading, fiber orientations (loading mode), wicking effects, interfacial adhesive problems, etc. It is essential, however, that the neat (pure) resin matrix materials be dealt with first in order to differentiate between composite structure engineering problems and the matrix materials related problems.

In the normal course of composite development, the candidate resins are characterized neat (without fibers or fillers) and until recently no allowance has been made for appropriate environmental exposures. The delineation of environmental effects (high humidity and high temperature, principally) and how they occur are generally not well understood. The objective of the research program described herein was to investigate the effects of environments on one particular epoxy composite matrix resin.

SECTION II

HISTORICAL

The deleterious effects of moisture on the elevated temperature properties of graphite fiber reinforced composites was first observed by investigators at General Dynamics and Fiberite Corporations in 1970 (Reference 6). In the course of a joint graphite/epoxy prepreg fabrication and evaluation program, it was found that composite specimens which had been inadvertently exposed to high humidity for several days prior to acceptance testing, lost a significant amount of their high temperature properties. Subsequent to this discovery, several workers (References 1-4) documented the effect of absorbed moisture on epoxy composite properties. Principal emphasis was placed on graphite/epoxy composites with very minimal efforts being directed toward the neat resin matrix. Most of these efforts centered about the evaluation of the effect of moisture on typical engineering properties with essentially no effort applied to the mechanisms of the phenomenon.

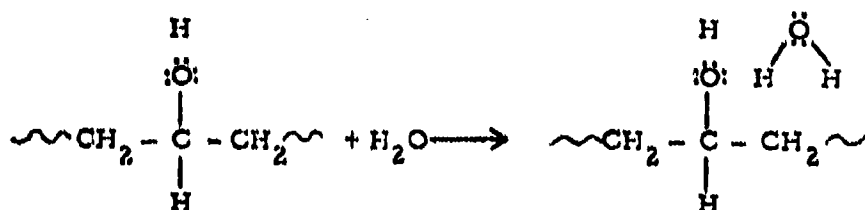
Concern about the environmental durability of epoxy resin systems has existed for many years. Some of the earliest investigations in the late 1950's were concerned with deleterious effects of humid, tropical environments on adhesive bonded metal lap joints (Reference 7). Subsequent to this, fiberglass/epoxy composites were examined as to any adverse effects of high relative humidity. With this type of work being performed over the last 20 years on the effects of humidity on epoxy systems, it is reasonable to ask why the epoxy-moisture phenomenon was not addressed much earlier. The reason simply was that in the earlier time period the vast majority of applications for epoxy structures were for ambient to low temperatures, and it is not until tests are conducted at elevated temperatures, near the glass transition temperature of the resin, that the effect of absorbed moisture becomes clearly evident.

With the advent of graphite and boron fibers, more stringent demands were placed on the resin matrix material. In order to effectively utilize the high strength and modulus of the reinforcement, the resin

matrix must have good adhesion to the fiber, high strength and stiffness, and furthermore, must maintain these properties to relatively high temperatures. It was during the elevated temperature testing, following exposure to high humidity environments, that the epoxy-moisture phenomenon became clearly evident.

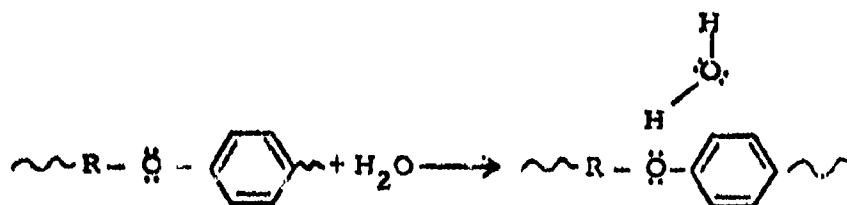
1. MOISTURE ABSORPTION AND TRANSMISSION IN EPOXIES

The absorption of water by epoxy resins and epoxy resin composites can in large part be attributed to the moisture affinity of specific functional groups of a highly polar nature in the cured resin. This is illustrated in Figure 1 and Table 1 (Reference 8). The three most important polar functional groups present in the epoxies and their respective associations with water are: (1) hydroxyl groups formed when curing agents add across the epoxide groups;



Hydroxyl Group/H₂O Association

(2) phenolic ether groups $(-\text{CH}_2 - \text{O} - \text{C}_6\text{H}_4 -)$ which are present in all bisphenol A or novolac based epoxies;



Ether/H₂O Association

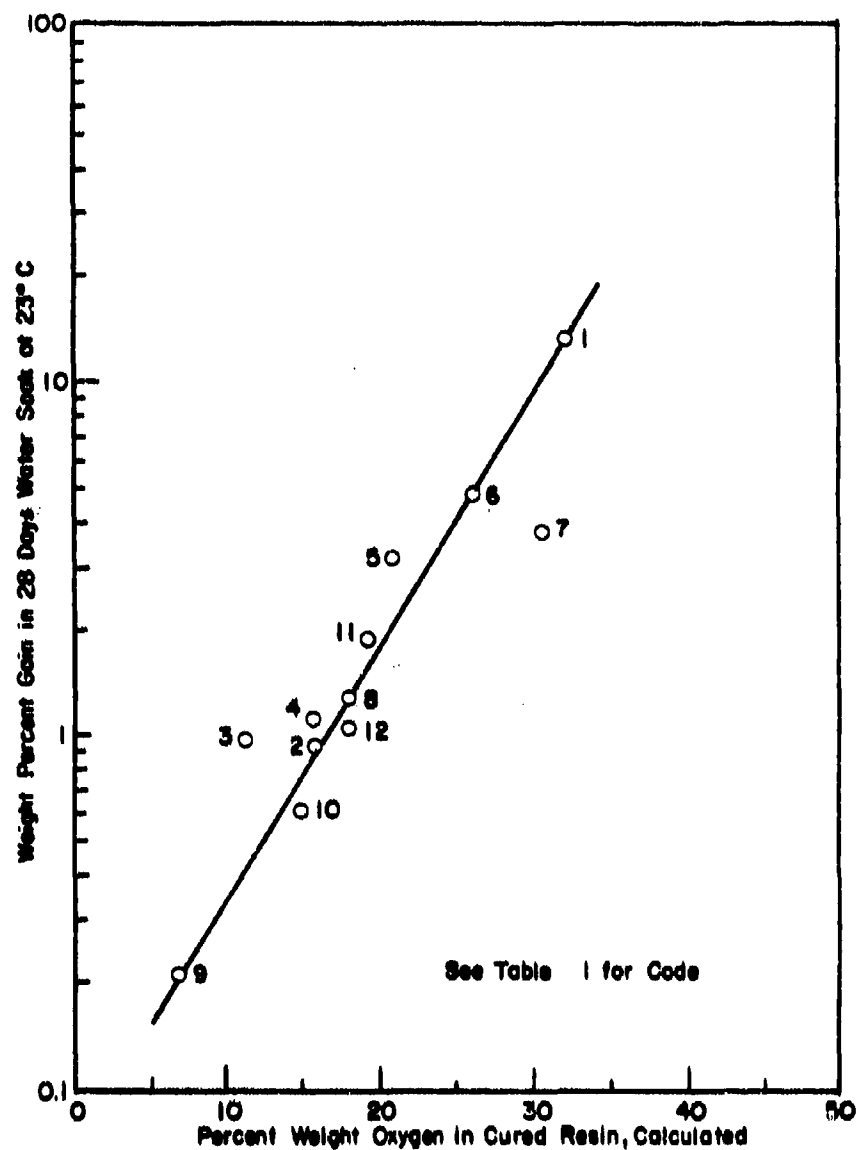


Figure 1. Effect of Oxygen Content on Water Absorption of Metaphenylenediamine Cured Epoxy Castings (Reference 8)

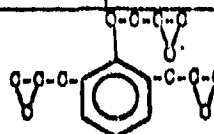
TABLE 1

WATER ABSORPTION AND OXYGEN CONTENT OF
METAPHENYLENEDIAMINE CURED EPOXY CASTINGS (Reference 8)

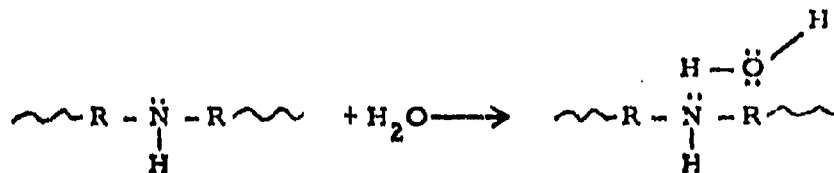
No.	Resin	Curing Agent, phr	Oxygen Content of Casting, %w (calcd)	Water Absorption at Room Temp., %wt Gain After 28 Day Soak in Distilled H ₂ O
1	Glycidyl glycidate	OL, ¹⁾ 37.5	32.0	13.0
2	EPON X-22 (Pure EPON 828)	OL, 13.6	16.3	0.97
3	Diglycidyl ether of 1,4 bis[2(p- hydroxyphenyl) 2- propyl] benzene	OL, 11.4	12.6	0.98
4	1,3 Divinylcyclo- pentane diepoxide (cis isomer)	OL, 34	15.5	0.98
5	Bis(2,3-epoxy- cyclopentyl)ether (trans)	OL, 28.4	20.5	3.2
6	Diglycidyl ether	OL, 40	26.0	4.7
7	Diglycidyl-4,5 epoxycyclohexane- 1,2 dicarboxylate	OL, 23.5	30.4	3.8
8	1,2,6,7 Diepoxy- heptane	OL, 40.5	17.8	1.3
9	Diglycidyltribromo- aniline	OL, 10	6.6	0.2
10	Diglycidylaniline	OL, 24.3	12.6	0.6
11	EPON X-801 ²⁾	OL, 24	19.7	1.9
12	1,2,7,8-Diepoxy- octane	OL, 37.5	16.4	1.1

1) OL = metaphenylenediamine.

2) 2,6(2,3-epoxypropyl)phenyl glycidyl ether



and (3) amino groups from amine curing agents



Amine/H₂O Association

Other polar species such as sulfone groups present in many curing agents or organometallic catalysts could also exhibit a high affinity for moisture.

Not only is hydrogen bonding important in the water absorption process, it is also important in providing high strength to resins and composites since hydrogen groups on the polymer chain can form hydrogen bonds to groups on other polymer chains. Bond strengths attributed to hydrogen bonding such as those illustrated are on the order of 4 - 9 kcal/mole (Reference 9), which may be compared to Van der Waals forces which are on the order of only 1 - 2 kcal/mole (Reference 9). Therefore, based on bond strengths, epoxy resins are approximately two to three times stronger than they would be if the polymer molecules were held together solely by Van der Waals forces.

The absorption and transmission of water molecules in a plastic material can be represented by Fick's law diffusion models. Recent studies (References 3, 10, 11) have applied Fick's second law to the study of epoxy resins and epoxy resin based composites. The general diffusion equation for one-dimensional diffusion, Fick's second law, is as follows:

$$\frac{\partial c}{\partial t} = D \frac{\partial^2 c}{\partial x^2} \quad (1)$$

where: c = concentration
 t = time
 x = distance
 D = diffusion coefficient

Van Amerongen (Reference 12) has summarized the solutions of this differential equation which have been developed for various conditions. For the simple case of a flat sheet absorbing a vapor from a constant environment at its two faces, the amount of penetrant absorbed as a function of time is

$$F = \frac{4}{l} \left(\frac{Dt}{\pi} \right)^{1/2} \quad (2)$$

where:

l = thickness of plate
 F = fraction of equilibrium amount absorbed in time, t

Equation 2 can then be rearranged to give

$$D = \frac{\pi F^2 l^2}{16t} \quad (3)$$

from which the diffusion coefficient can be obtained. The most appropriate way to determine D is to utilize Equation 2 and make a plot of F versus $t^{1/2}$ which gives a straight line of slope, s , given by

$$s = \frac{4}{l} (D/\pi)^{1/2} \quad (4)$$

Rearranging Equation 4 gives the following:

$$D = \frac{\pi s^2 l^2}{16} \quad (5)$$

from which D , the diffusion coefficient, can be obtained.

In the experimental process, the equilibrium absorption value is found by exposing finely powdered resin samples to a high humidity environment until a constant weight-gain is achieved. Moisture absorption values are then measured on cast resin plates. These values together with the equilibrium value give the experimental absorption fractions, the F values, which are then plotted versus the square root of time.

Diffusivities of 4.77×10^{-9} and 11.3×10^{-9} cm^2/sec were determined (Reference 3) for two different "state-of-the-art" epoxy resin systems using the aforementioned procedure where, in each case, the data were found to be accurately described by straight lines (Figure 2). These values are of the same magnitude as values previously reported in the literature (References 13, 14) for the diffusion of water in epoxy.

These values of the water diffusion coefficients were then used in a computer program (Hercules Incorporated's 1-D Multicomponent Diffusion Computer Program No. 61014) to determine the water concentration profiles through 1-cm-thick cast epoxy plates (Figures 3 and 4). The computer program uses the Crank-Nicolson finite difference method to solve Fick's second law of diffusion. Examination of Figures 3 and 4 illustrates that the rate of diffusion of water through the resin materials is relatively slow. Resin A requires four years and Resin B two years for the center of a 1 cm plate to reach the equilibrium level of absorbed water in a 75% RH, RT environment. The curves also predict that after only four weeks exposure, a steep concentration gradient exists with essentially all of the absorbed water concentrated in the outer 0.2 cm of the specimens.

It should be noted that the diffusivity value will be dependent on the chemical structure of the particular resin system (i.e., the base epoxy resin structure, specific curing agent, catalysts, accelerators, etc.) as well as its fabrication history.

The aforementioned diffusion study was subsequently extended to epoxy composites reinforced with both graphite fibers (Reference 3)

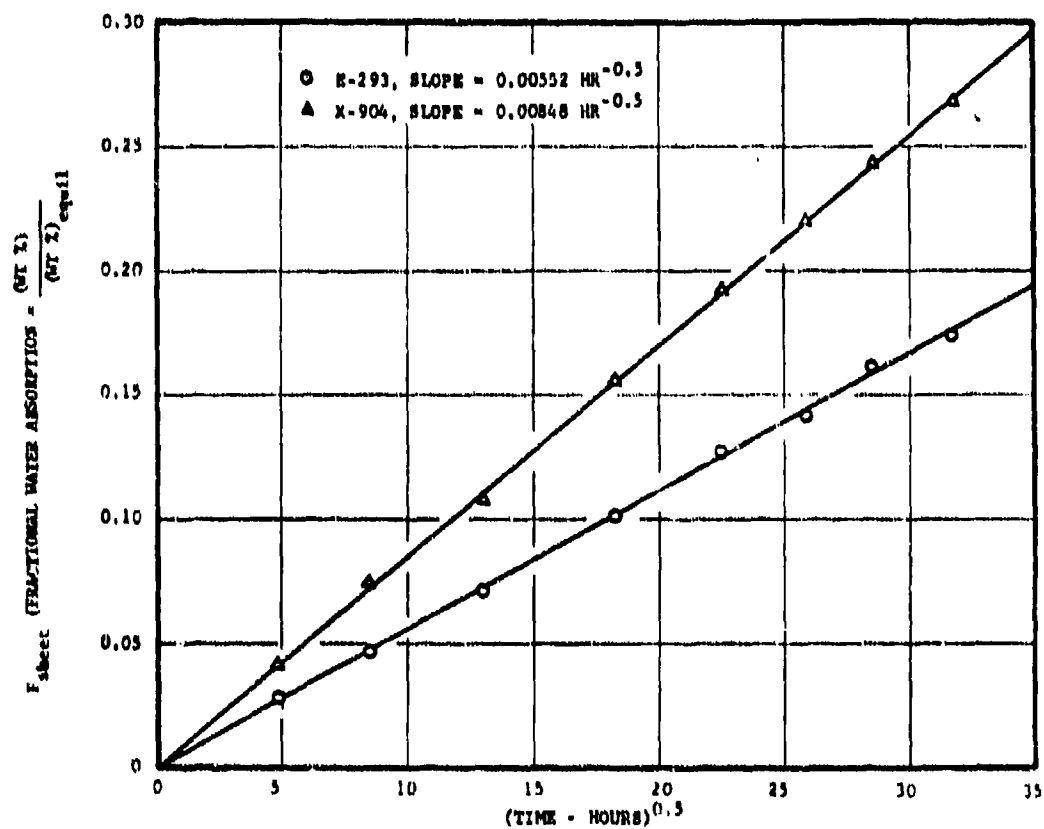


Figure 2. The Fractional Water Absorption as a Function of the Square Root of Time for E-293 and X-904 Epoxy Resins (Reference 3)

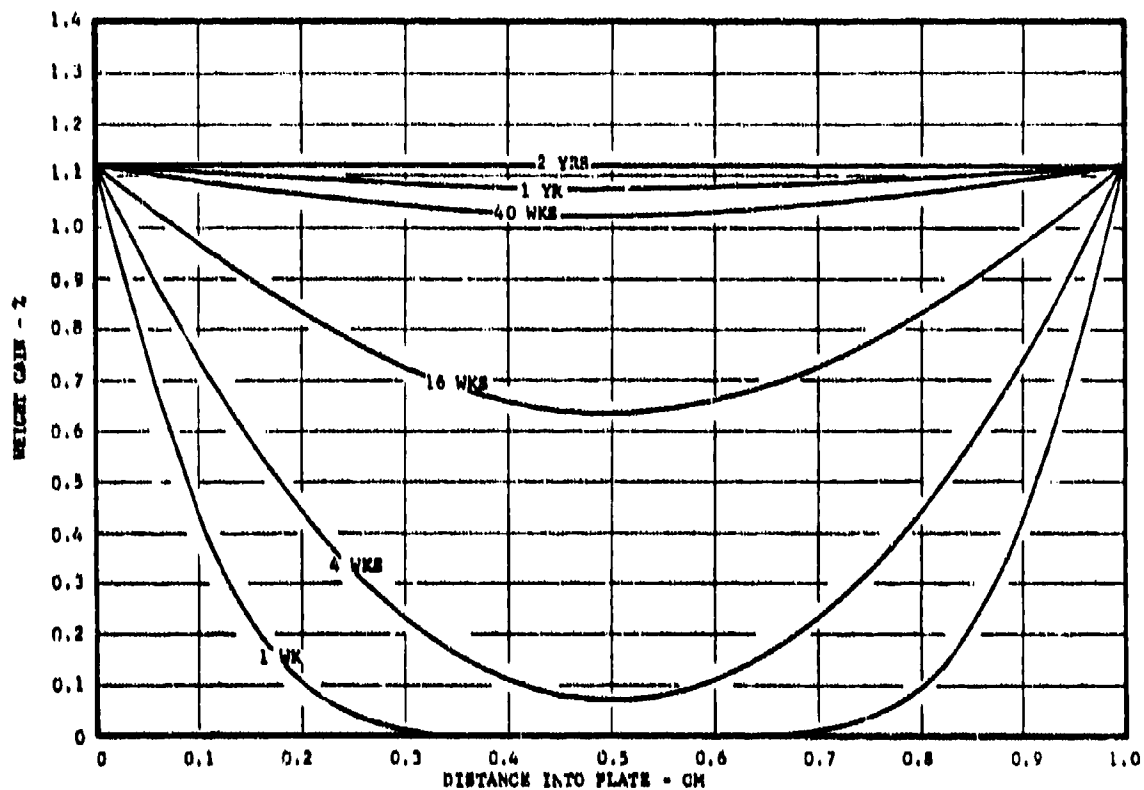


Figure 3. Diffusion of H_2O into Epoxy X-904 Plate at Room Temperature and 75% RH (Reference 3)

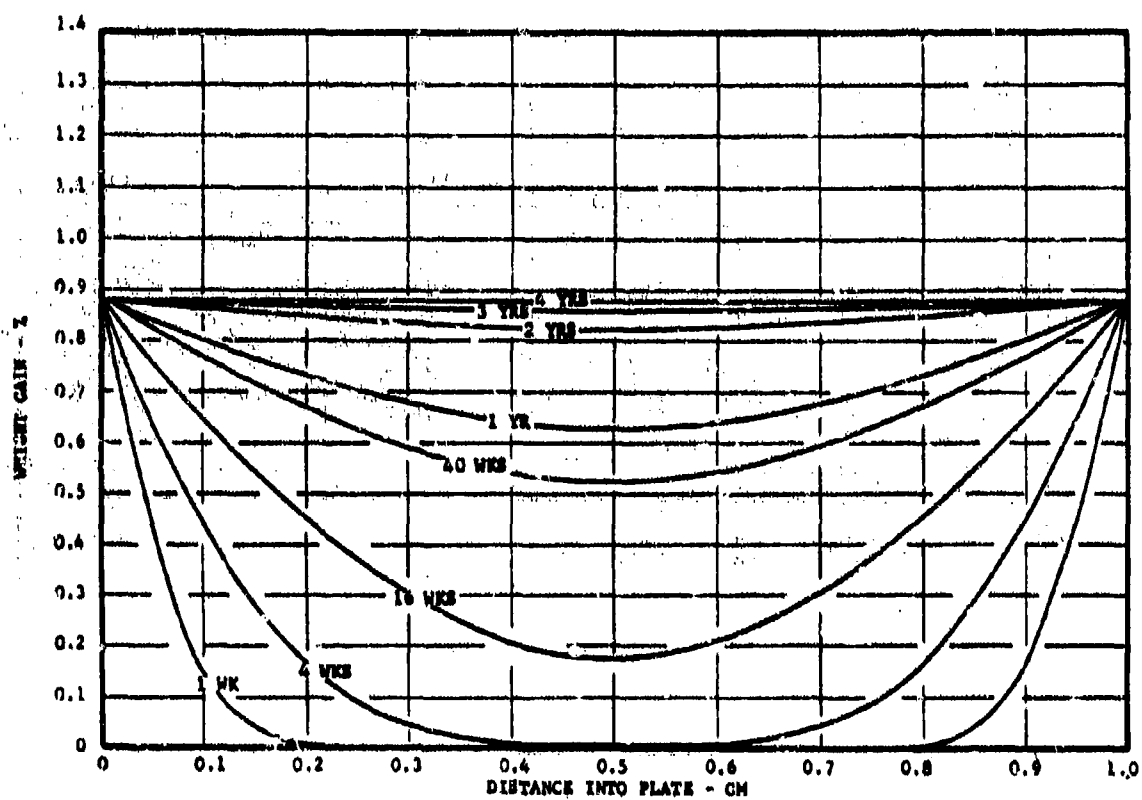


Figure 4. Diffusion of H_2O into Epoxy E-293 Plate at Room Temperature and 75% RH (Reference 3)

and boron filaments (Reference 11). In each case Fickian behavior identical to that of the neat resins, excluding volume effects, was found. Straight-line plots of F vs. $t^{1/2}$ were found, as were similar water concentration profile vs. thickness plots. This is highly indicative of the importance of understanding the matrix material's behavior, since an understanding of its behavior would allow one to predict the composite's behavior.

Subsequent studies (Reference 10) into the diffusion of water into epoxy/graphite composites found that at very high values of F , the moisture content vs. $t^{1/2}$ curves asymptotically approach the equilibrium moisture contents (Figure 5) instead of remaining linear. Apparently previous workers were operating at relatively lower values of F (lower moisture contents) where the curves of F vs. $t^{1/2}$ are linear.

To adequately describe this asymptotic behavior of F , a curve fitting form of Equation 2 was empirically arrived at (Reference 10):

$$F = \text{TANH} \left[\frac{4}{L} \left(\frac{Dt}{\pi} \right)^{1/2} \right] \quad (6)$$

As time approaches infinity, the hyperbolic tangent forces the value of F to approach 1.0. The ability of this equation to adequately describe the moisture pick-up process in neat resins has never been investigated.

In this same study (Reference 10), it was found that the equilibrium amount of absorbed moisture is directly proportional to the relative humidity or water vapor concentration (Figure 6). This dependence of equilibrium moisture content on relative humidity and independence with respect to temperature was further illustrated in Figure 7 for 75% RH and 100% RH exposures at different temperatures.

These same workers extended their study to include the moisture absorption process in graphite/epoxy composites as a function of real-life service environments. The exposure cycle shown in Figure 8 was developed by General Dynamics (Reference 10) and is considered

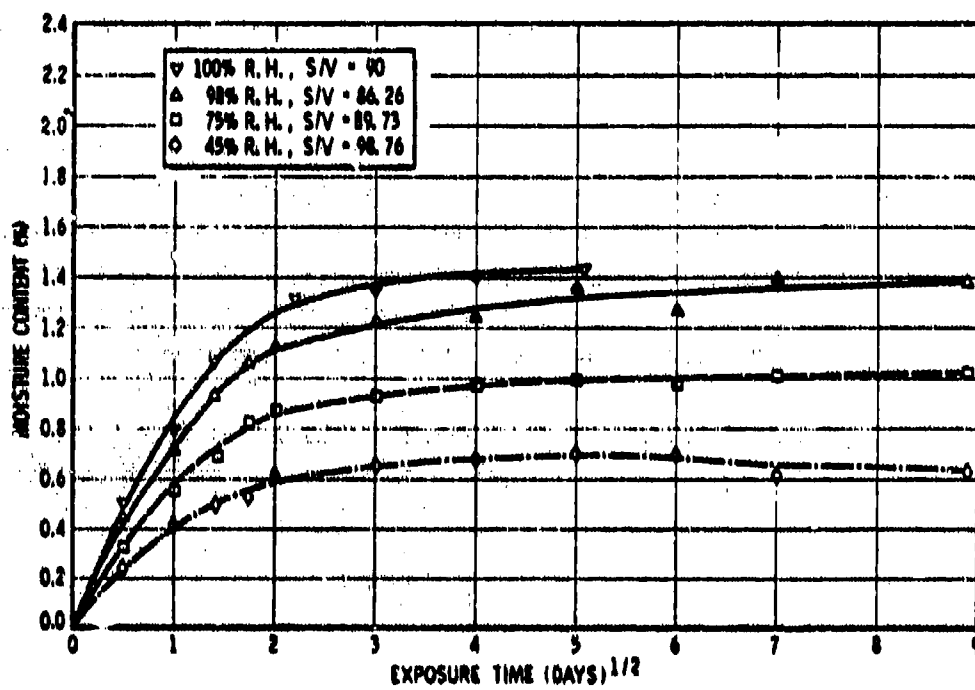


Figure 5. Moisture Absorption in a 4-Ply Graphite/Epoxy Laminate at 120°F (Reference 10)

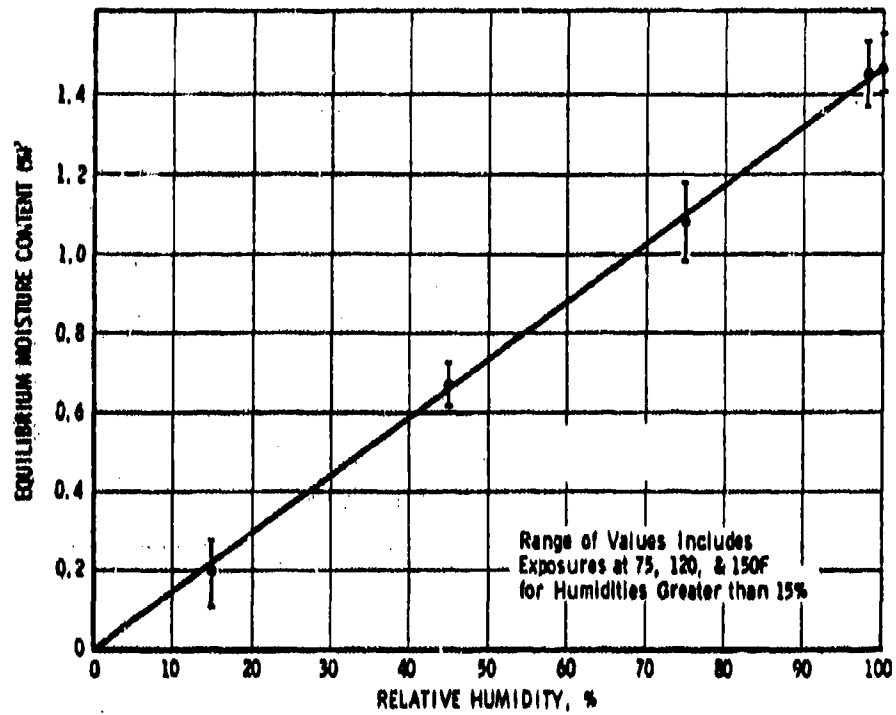


Figure 6. Effect of Relative Humidity on Equilibrium Moisture Content (Reference 10)

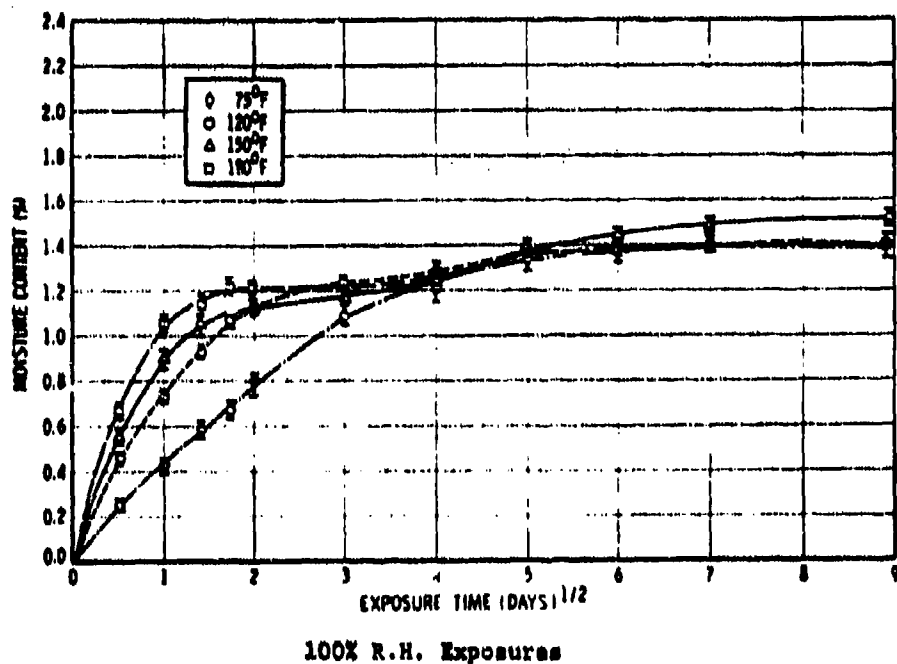
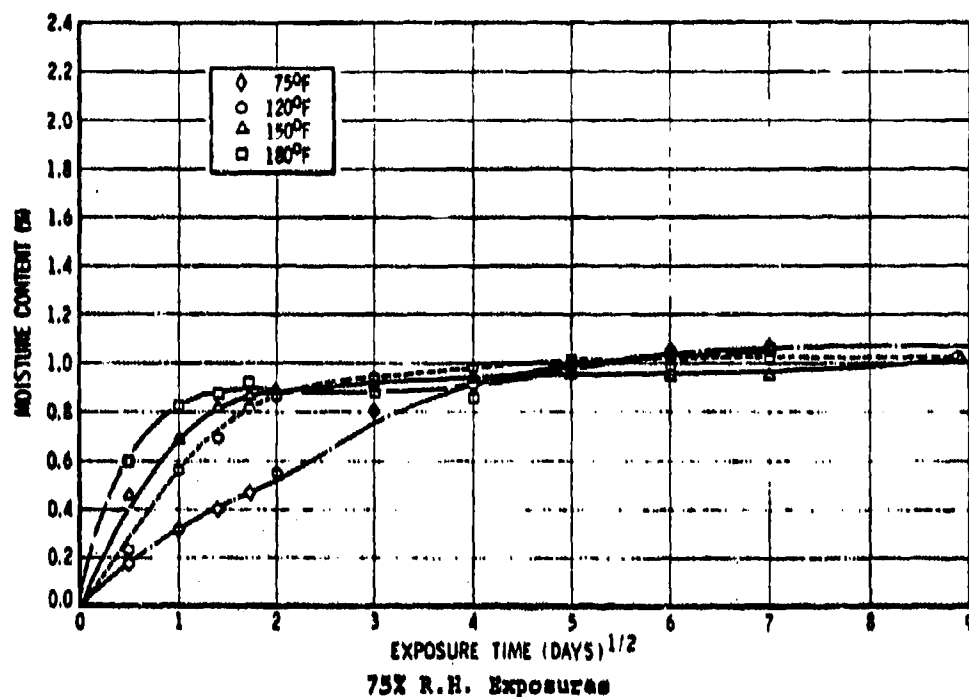


Figure 7. Moisture Absorption in a 4-Ply Graphite/Epoxy Laminate (Reference 10)

• FLORIDA RUNWAY CONDITIONS (75% R.H. AT 75°F), 7 DAYS PER WEEK

• MONDAY AND THURSDAY

- ✓ Rain (3-1/2 Hours Each Day)
- ✓ Subsonic Flight (-65°F for 90 Minutes)

• TUESDAY AND FRIDAY

- ✓ Rain (3-1/2 Hours Each Day)
- ✓ Subsonic Flight (-15°F for 45 Minutes)
- ✓ Supersonic Dash (Spike to 300°F)

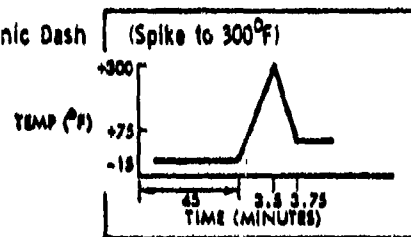


Figure 8. A "Real-Life" Environmental Exposure Cycle (Reference 10)

to be an environment that is quite representative of a typical flight profile for a supersonic aircraft. The results of absorption studies on 8-ply laminates are shown in Figure 9 with real-life data plotted along with humidity only results. It is apparent that the real-life environment has caused an acceleration of the moisture absorption rate and raised the absorption level to values higher than equilibrium values for humidity only conditions. It was subsequently found that the one variable that led to this type of behavior was the supersonic heating spike (Reference 10).

The real-life environment was not applied to neat resin specimens to examine matrix behavior. Further, the mechanism by which the heat spike causes the increase in the weight-gain process was not investigated.

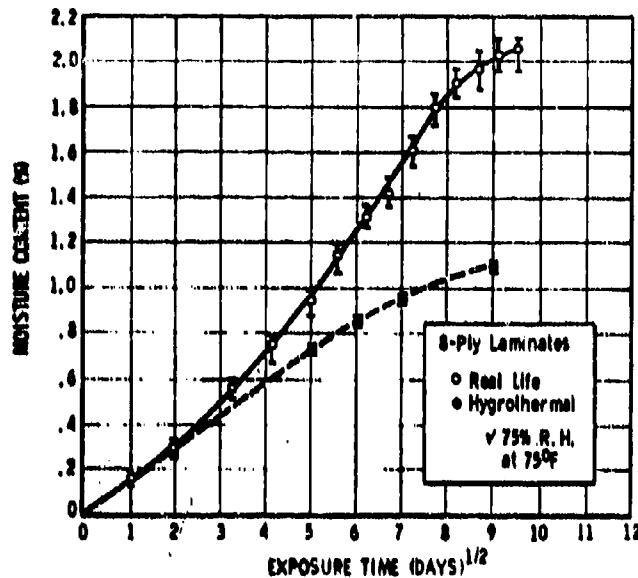


Figure 9. Comparison of Real-Life and Simple Humidity Absorption Behavior (Reference 10)

The most recent study (Reference 15) into the diffusion of moisture into graphite/epoxy composites utilized the series solution of Equation 1, previously described in Van Amerongen (Reference 12), to determine the percent moisture content, M , of the material as a function of time, t . It was found that the value of M is given by

$$M = G (M_m - M_i) + M_i \quad (7)$$

where M_i is the initial moisture content, M_m is the equilibrium moisture content, and G is a time dependent parameter given by:

$$G = 1 - \frac{8}{\pi^2} \sum_{j=0}^{\infty} \frac{\exp \left[- (2j+1)^2 \pi^2 \left(\frac{Dt}{4L^2} \right) \right]}{(2j+1)^2} \quad (8)$$

Equation 8 can be approximated by

$$G = 1 - \exp \left[-7.3 \left(\frac{Dt}{4l^2} \right)^{0.75} \right] \quad (9)$$

This treatment yields curves equivalent to those shown in Figure 5 for M vs. $t^{1/2}$.

This particular treatment of Fick's Second Law was never extended to the resin matrix material.

As a final note to this background discussion of prior diffusion studies, it is worthwhile to point out that all of these treatments have the one common feature of determining the value of the diffusion coefficient from the linear portion of the F vs. $t^{1/2}$ curve. In essence then, if one is applying a finite-element analysis to the absorption process in order to determine moisture concentration profiles, it makes no difference which technique is used.

2. MOISTURE EFFECTS ON THE PHYSICAL/MECHANICAL PROPERTIES OF EXPOXIES

It is important to reemphasize that the problem under consideration is the loss in elevated temperature mechanical properties exhibited by epoxy resins and composites after the absorption of moisture from high humidity exposures. Prior to considering potential mechanisms by which moisture may cause a loss in mechanical properties, consider the resin in a "dry", unexposed condition. In the absence of water, the only environmental condition of any importance is temperature (excluding chemical degradation such as oxidation).

The discussion then comes down to what possible processes exist by which stresses may be relieved in the polymer due to temperature. In general, there are five basic types of relaxation processes possible in a polymer system (Reference 16), and these are illustrated in Figure 10.

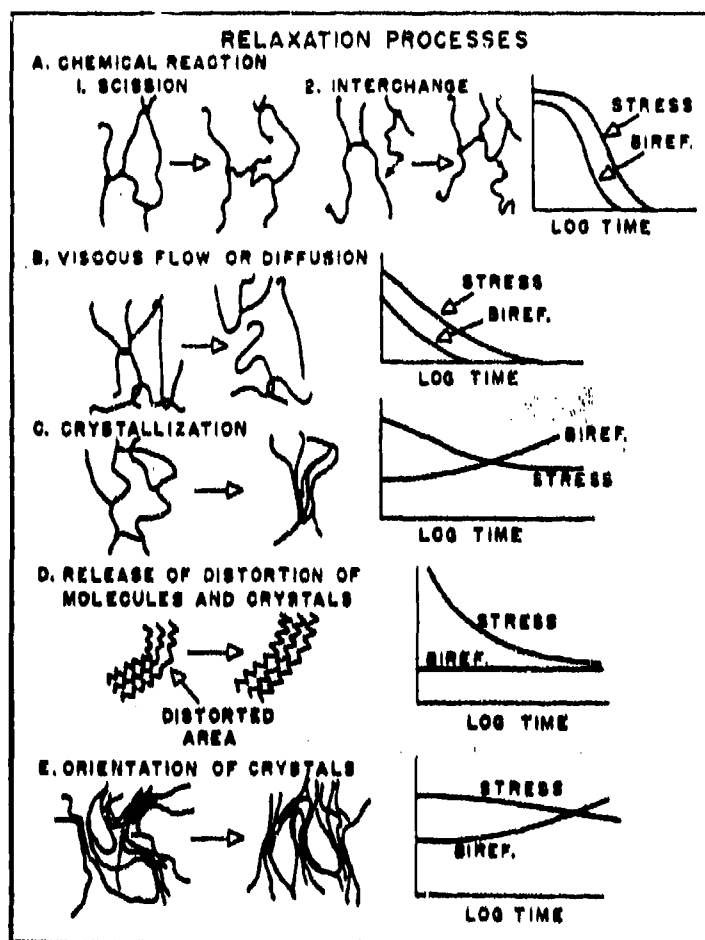


Figure 10. Types of Relaxation Unit Processes Which a Polymer Sample May Undergo (Reference 16)

Processes "C", "D", and "E" can be eliminated since the resins we are concerned with are amorphous, not crystalline (Reference 17). Also, since these resins are cured and post-cured at temperatures several degrees higher than their use temperatures, process "A" should not be important here. Likewise, as long as these polymeric materials are used at temperatures sufficiently below their glass transition temperature, T_g (i.e., at temperatures where they retain their structural integrity) process "B" should not be of concern. In essence then, these materials should not exhibit any significant property loss under normal use conditions.

If an epoxy resin containing a certain weight percent water is considered to be a polymer plus diluent system, the stress relaxation processes previously discussed (Figure 10) could be applied. Processes "C", "D", and "E" can still be eliminated since the material is still amorphous. Then this leaves processes "A" and "B" as the principal candidates by which stress relaxation may take place. In other words, the presence of water could result in a weakening of the polymer due to chain scission at elevated temperatures (process "A"). Similarly, the presence of water could allow viscous flow or diffusion to take place at a lower temperature (Reference 18) (i.e., the material has been plasticized) so that the maximum use temperature of the material is lowered by process "B".

Chemical stress relaxation or chemical creep (process "A") is a mechanism that has been observed in several polymers (Reference 19) and involves the breakage of primary chemical bonds due to the combined effect of water, temperature, and stress. It has the characteristic feature of irreversibility. Stress relaxation due to viscous flow or diffusion as a result of absorbed moisture (i.e., plasticization) would have the characteristic feature of reversibility, that is, the original properties can be regenerated by removing the plasticizer (Reference 18). Therefore, it is appropriate to discuss the physical and mechanical behavior of epoxy systems in a moisture environment under the categories of reversible or irreversible processes.

3. REVERSIBLE PROCESSES

Studies of reversible behavior have generally centered about experimental measurements which yielded results that were either a direct or indirect measurement of the effect of the amount of absorbed moisture on a resin's or composite's T_g . Several techniques have been utilized. One of the first methods (Reference 20) to be employed was to measure the Barcol Hardness of the resin as a function of temperature and water absorption (Figure 11). Results showed that the hardness at temperature was lowered as a function of water content and could be restored upon drying the specimen to its original weight.

Another technique which has become very popular is to measure a specimen's deflection-temperature behavior under load as a function of its moisture content (References 2 and 20). These tests yield results such as those shown in Figures 12 and 13 for different moisture weight-gains. Analogous to the hardness measurements, there is a lowering of the deflection temperature curve due to absorbed moisture, and the original deflection temperature curve can be recovered upon drying of the specimen.

Epoxy resin T_g changes as a function of absorbed moisture have also been determined using the classical T_g measurement tool, the dilatometer (Reference 21), wherein the volumetric expansion of the resin is measured. Typical results are shown in Figure 14 for unaged and humidity aged specimens, showing the drop in T_g due to moisture absorption.

Similar changes in resin T_g as a result of absorbed moisture have been investigated using other techniques such as thermomechanical analysis (Reference 10), torsion braid analysis (Reference 22), and a variety of standard mechanical tests such as flexure, tensile, and shear measurements (References 2, 3, 23).

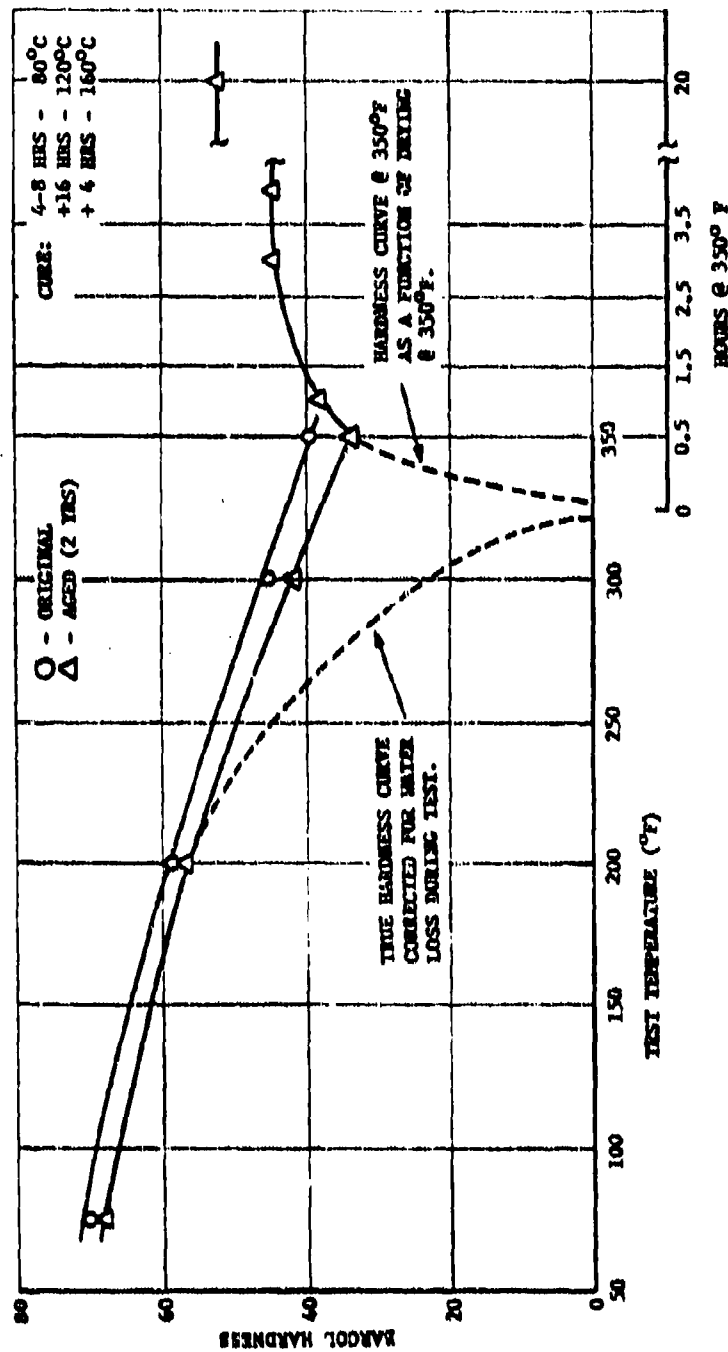


Figure 11. Barcol Hardness vs. Temperature for Dry and Humidity Aged Epoxy Specimens (Reference 20)

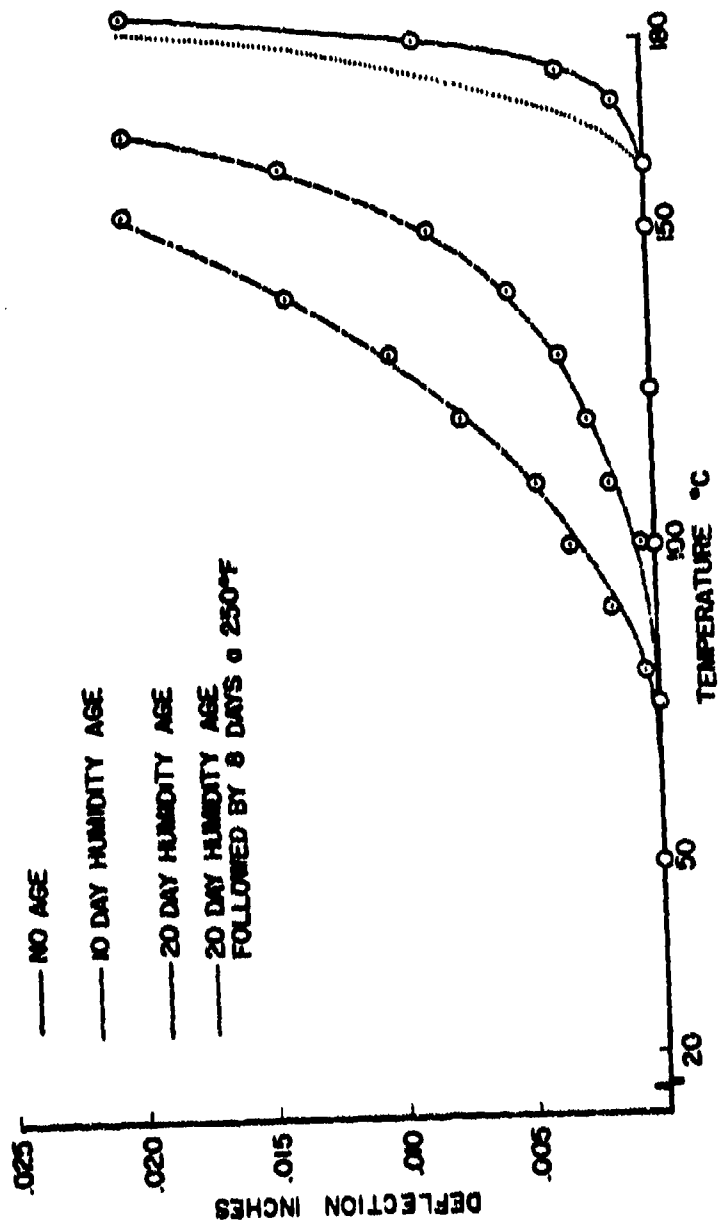


Figure 12. HDT Measurements for Dry and Humidity Aged Epoxy Samples (Reference 2)

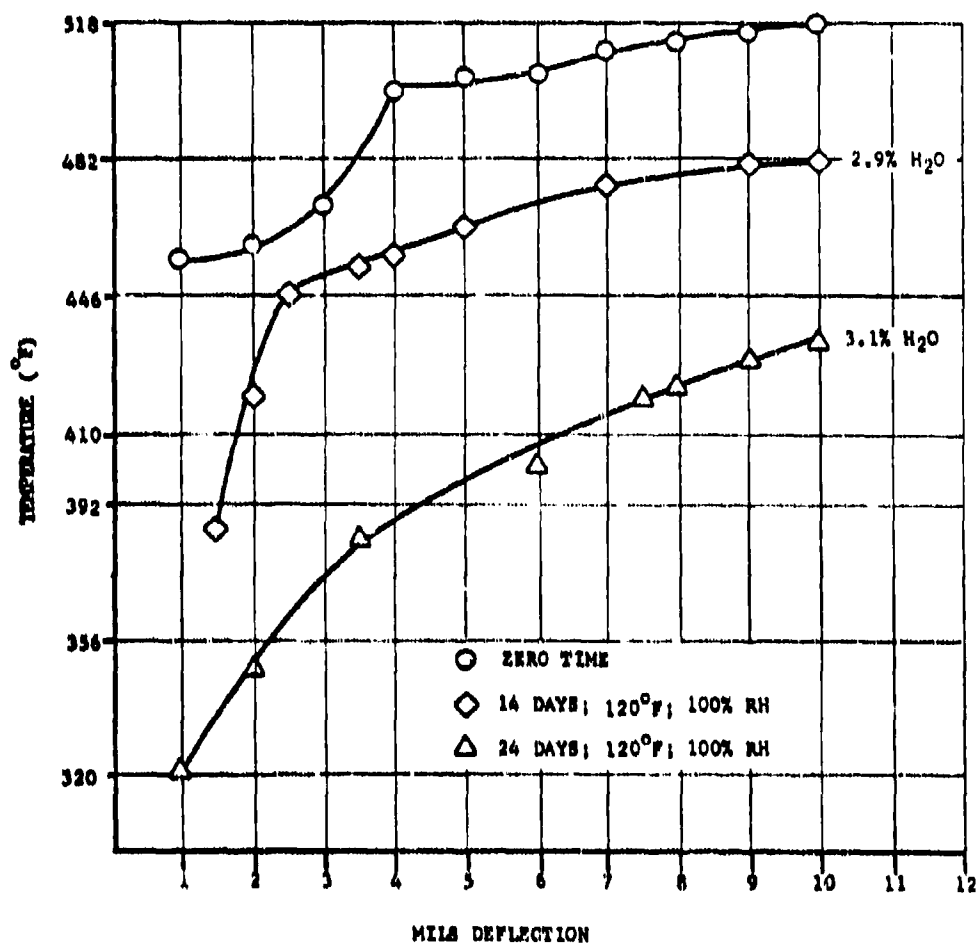


Figure 13. HDT Curves for Dry and Humidity Aged Epoxy Specimens (Reference 20)

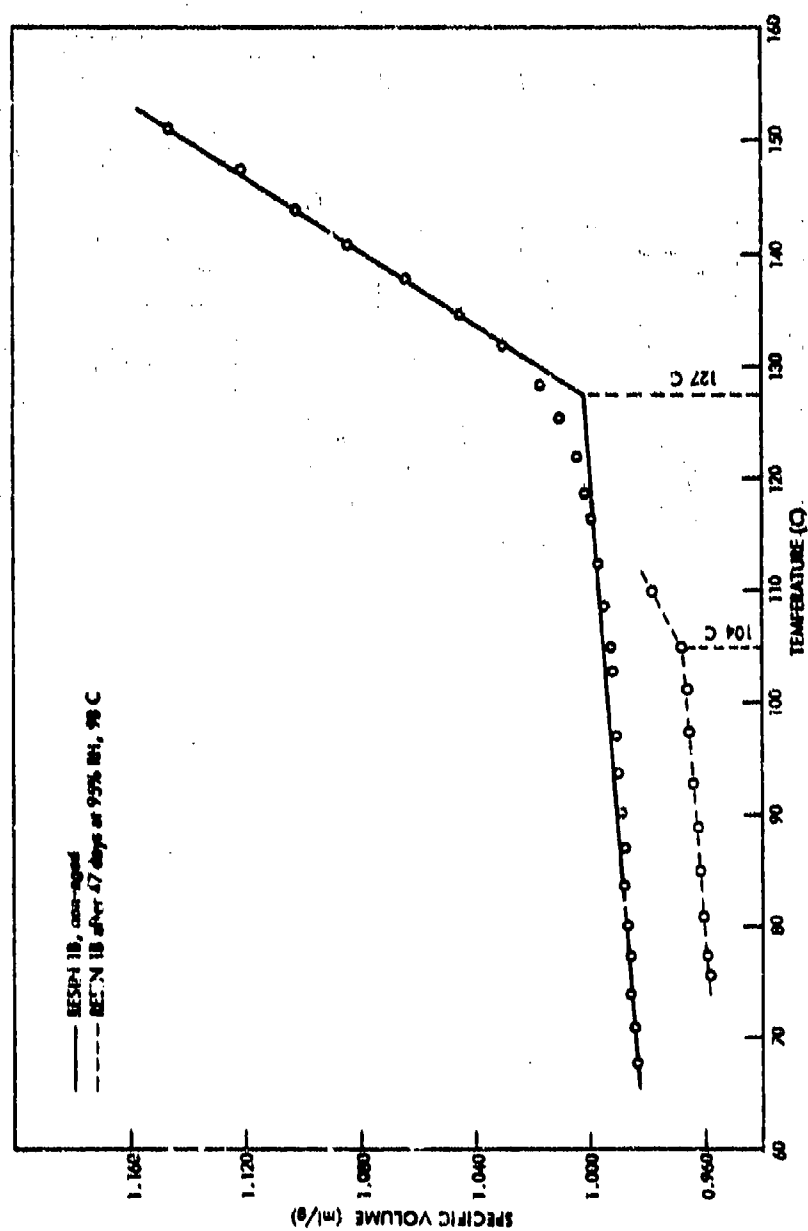


Figure 14. Dilatometer Results on Dry and Humidity Aged Epoxy Specimens (Reference 21)

In actuality, all of these investigators were measuring the effects of the same phenomenon - moisture induced plasticization of the epoxy resin. Therefore, in all cases similar behavior was observed - absorbed moisture lowers the resin T_g (plasticization) or T_g governed mechanical property, and, as would be anticipated, the T_g or mechanical property was found to be recoverable upon drying of the specimen to its original weight. The process is reversible.

This plasticization or lowering of the resin's T_g is fully reflected in matrix - dominated composite properties wherein substantial elevated temperature property losses are observed. This behavior has been well documented for different types of matrix controlled laminate orientations and tests (References 2, 23) and substantiates the need to understand the mechanisms by which the resin matrix material is affected by absorbed moisture.

4. IRREVERSIBLE PROCESSES

Studies of the irreversible degradation of epoxy resins have in the past been largely limited to thermally or thermo-oxidatively induced degradation (References 24-26). Irreversible hydrolytic degradation (moisture-induced chemical chain scission) has not been considered to be a problem of any great concern in the case of the amine-cured epoxies under investigation in this research program and of interest to the aerospace materials community. However, hydrolysis was a well-known occurrence in anhydride-cured epoxies (Reference 17) wherein moisture sensitive ester linkages are formed as a result of the cure reaction. With respect to the amine-cured systems, previous efforts, as pointed out earlier, have been limited to the effects of absorbed moisture on physical properties such as T_g , with no direct effort applied to the study of irreversible, chemical chain scission mechanisms.

A recently initiated study (Reference 27) into potential moisture - induced chemical reactions is using Fourier-Transform Infrared Spectroscopy to detect any evidence of chemical changes occurring

during stress-temperature-humidity exposures. This instrumental technique is a highly sophisticated spectroscopic method that is capable of detecting very minute changes in chemical functionality. Results to date show some minor decreases in the functionality associated with the curing agent. The reason for this has not been established.

In summary, the information available has shown that the T_g of epoxy resins is lowered as a result of absorbed moisture and that matrix-controlled composite properties are adversely affected. However, none of the previous studies considered the specific epoxy resin system investigated herein which is of paramount importance to the aerospace materials community. Furthermore, previous work was of a qualitative nature and did not attempt to explain or quantify the moisture absorption and T_g changes in terms of existing theoretical relationships. In addition, the influence of a real-life environment on the T_g of epoxy resins has not been investigated, nor were the relationships of T_g changes to changes in the other physical/mechanical phenomena such as tensile moduli, creep rupture, and moisture weight-gain. If epoxy resins are to be exploited to their fullest potential in primary structure applications as matrix resins and/or adhesives, then a fuller, more fundamental understanding of their response to a humid, high temperature environment must be obtained.

To achieve this understanding, it was necessary to determine the effect of absorbed moisture on the T_g of this particular epoxy resin system, to quantify this phenomenon in terms of an existing theoretical relationship, and to extend this investigation to include the effect of real-life environmental conditions on the T_g . Furthermore, the complete lack of any prior work illustrated the need for determining if other mechanisms might exist for the moisture-induced elevated temperature property losses in epoxy resin matrix materials.

SECTION III

RESEARCH PLAN

The investigation into the mechanisms of moisture-induced property losses in epoxy resins consisted of the following approach. After selection of the appropriate epoxy resin, its moisture absorption and diffusion characteristics would be thoroughly characterized. These results would then be utilized to determine the changes in the resin's T_g as a function of absorbed moisture. These T_g changes, combined with knowledge of diffusion behavior, would then be employed to guide the set-up and interpretation of subsequent tests such as tensile strength and modulus and creep behavior. Collectively, these data would provide the information needed to determine the mechanisms by which moisture affects the elevated temperature properties of epoxy resins.

To make the results of this research program meaningful, an epoxy resin was chosen which would evoke the highest interest possible from both the aerospace materials engineering and the polymer science communities. This resin would be fabricated into suitable test specimens for performing the remainder of the research program, which would consist of two basic areas: (1) determination of the absorption and diffusion characteristics of the epoxy resin and (2) determination of the resin's physical/mechanical response as a function of the absorbed moisture.

The particular epoxy resin investigated had not been examined previously relative to its moisture absorption and diffusion characteristics. Therefore, the first part of the program consisted of selecting an appropriate test specimen geometry, determining rates and amounts of moisture absorbed, the method of moisture transmission through the resin, and the geometric distribution of moisture within the epoxy sample. These objectives were to be investigated as a function of both simple humidity environments and real-life environment. In essence, this phase of the program would serve as the foundation to guide and aid in interpreting the results of the next phase. The results of the diffusion studies would provide needed experimental parameters such as

equilibrium weight-gains, times to reach specified weight-gains, the physical distribution of water in the specimen, and the amount of specimen swelling.

The first phase of the program would then be followed by physical/mechanical characterization as a function of absorbed moisture. The results of this second phase would provide the information necessary to determine the mechanisms of moisture-induced property losses in the epoxy system. The plan was to first determine the effect of absorbed moisture on resin T_g as a function of both simple humidity and real-life exposures. In the course of this study a plasticization phenomenon would be delineated and then explained and quantified in terms of existing, well-established theoretical relationships. Knowledge of how moisture affects the resin's T_g would be used to guide subsequent experimental tests (particularly with respect to test temperatures) and to help interpret their responses.

Several physical/mechanical tests were to be performed such as constant strain-rate tensile tests, dynamic mechanical tests, and creep. Relaxation moduli from the tensile tests would both verify the plasticization and quantify the magnitude of its effect on mechanical response. The creep tests were to be the principal mechanical test since their results would determine the existence of irreversible processes and possibly identify any unsuspected mechanisms of moisture-induced property losses. The test was to be performed in a controlled temperature/humidity environment at a temperature above the "wet" T_g of the epoxy as determined by the prior T_g studies. Experimentally, this would entail monitoring specimen response in a sealed bomb since the test temperature would exceed the boiling point of water.

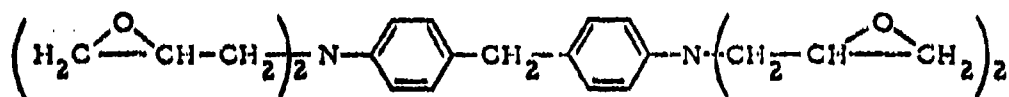
SECTION IV

RESULTS AND DISCUSSION

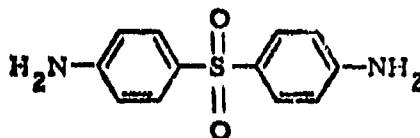
1. MATERIALS SELECTION AND PREPARATION

The epoxy resin studied in this program was chosen on the basis of its present and future commercial importance. This particular epoxy resin system was obtained in a formulated, commercially-available condition and, therefore, is typical of the commercial epoxy resins in use today in composite materials. Its formulation is as follows:

EPOXY RESIN



CURING AGENT (32phr)



CATALYST (1phr)



where phr refers to parts per hundred parts by weight of epoxy. This particular type of epoxy resin system is common to several resin systems used in high performance graphite composite materials and to several high performance adhesive systems (Reference 28). Because of this, research into the environmental behavior of this material is of substantial interest to the aerospace materials engineering community.

The epoxy plates used in the diffusion studies and in tensile testing were 0.125 in. thick and were prepared by casting the material between pyrex glass plates with 0.125 in. spacers. A seal around the periphery of the plates was made using Teflon spaghetti tubing.

Epoxy samples were fabricated by the following scheme. The as-received resin (which is stored at 0°F) was allowed to warm to room temperature. Approximately 200 grams of resin was poured into a large aluminum dish. This sample is then placed in a vacuum oven at room temperature (RT) under full vacuum and debulked until all volatile matter was removed as evidenced by the absence of bubble formation. Approximately 100 grams of this resin was poured via a funnel into the glass-plate casting mold. The casting mold was then placed in a vacuum oven at 200°F under full vacuum for two hours, heated to 250°F, and held under vacuum for 30 minutes. The vacuum was then removed and final cure allowed to take place at 350°F for 30 minutes. The sample was allowed to cool overnight to RT.

The plates were then machined into appropriate test specimens with diamond wheel saws and cutting and grinding tools. All specimens were examined with a polarizing microscope to ensure that no residual stresses or cracks were present.

In those instances where thin films (4-6 mils) were required (such as for IR, creep, and dynamic tensile testing) the above procedure was followed except that the spacers and seal material in the mold were 3.5 mils thick fluoroglass fabric.

2. ABSORPTION AND DIFFUSION STUDIES

The first phase of the research effort determined the absorption and diffusion characteristics of epoxy resin samples. The principal objectives were to determine the rates and amounts of moisture absorbed, the method of moisture transmission through the epoxy, and the geometric distribution of moisture within the epoxy as the absorption/diffusion

process is occurring. These objectives were investigated as a function of simple temperature/humidity environments and simulated real-life environments involving cyclic exposures.

a. Sample Configurations

Time-weight change studies were performed on samples whose dimensions were 2.0 in. x 2.0 in. x 0.125 in. These dimensions were chosen to obtain meaningful data within a reasonable time period. It is desirable to use a large surface area plate (relative to its thickness) to simplify the treatment of the diffusion process using Fick's Law, and further, it is desirable to use a thickness that is of sufficient size to permit the determination of moisture and temperature gradient effects within a reasonable length of time. These criteria are satisfied with specimens having the aforementioned dimensions. This was verified by other workers (References 4, 10, 23) and by the initial results in this phase of the program. Thin films (3-7 mils in thickness) were also examined and will be considered in the discussion accordingly.

b. Constant Temperature and Humidity Exposures

As described in Section II, diffusion of moisture into polymeric materials can be described by various solutions of Fick's Second Law of diffusion. For one-dimensional diffusion assuming a constant diffusion coefficient, the general diffusion equation was shown to be Equation 1:

$$\frac{\partial c}{\partial t} = D \frac{\partial^2 c}{\partial x^2} \quad (1)$$

For the simple case of a flat sheet absorbing a vapor from a constant environment at its two faces, the amount of penetrant absorbed as a function of time was shown to be given by Equation 2:

$$F = \frac{4}{\pi} \left(\frac{Dt}{\pi} \right)^{1/2} \quad (2)$$

which is the so-called linear solution, whose applicability to this particular epoxy resin will be described.

Weight-gains vs. time for varying temperature and humidity conditions are shown in Figures 15 and 16. Figure 15 shows the weight-gain vs. time for varying temperatures at 100% RH while Figure 16 shows similar data for 75% RH. The effects of increasing temperature on the rate of moisture pick-up can readily be seen. The equilibrium amounts of moisture absorption (M_{∞}) were taken from the maximum weight-gains found during the maximum temperature exposure for a given humidity. These particular weight-gain data are plotted in Figure 17 where it can be seen that for 100% RH, M_{∞} is 5.6% and for 75% RH, M_{∞} is 4.2%. A plot of M_{∞} vs. RH (Figure 18) shows that the equilibrium amount is directly proportional to the relative humidity. The values of M_{∞} were used in Fick's Law calculations to determine the fraction of equilibrium weight-gain, F ,

$$F = \frac{M_1}{M_{\infty}} \quad (10)$$

where M_1 = weight at time t .

Plots of F vs. $t^{1/2}$ are shown in Figure 19 for 100% RH. As previously discussed, the slopes of these curves were used to solve for the values of D , the diffusion coefficient (Equation 5). These data are summarized in Table 2. Using these data a plot of the log diffusion coefficient vs. the reciprocal of the absolute temperature can be made. The straight-line plot obtained (Figure 20) is indicative of the temperature dependence of the diffusion coefficient being in accordance with the theory of activated diffusion where the slope of the line is $[-E/2.303 R]$ as in

$$D = D_0 \cdot e^{-E/RT} \quad (11)$$

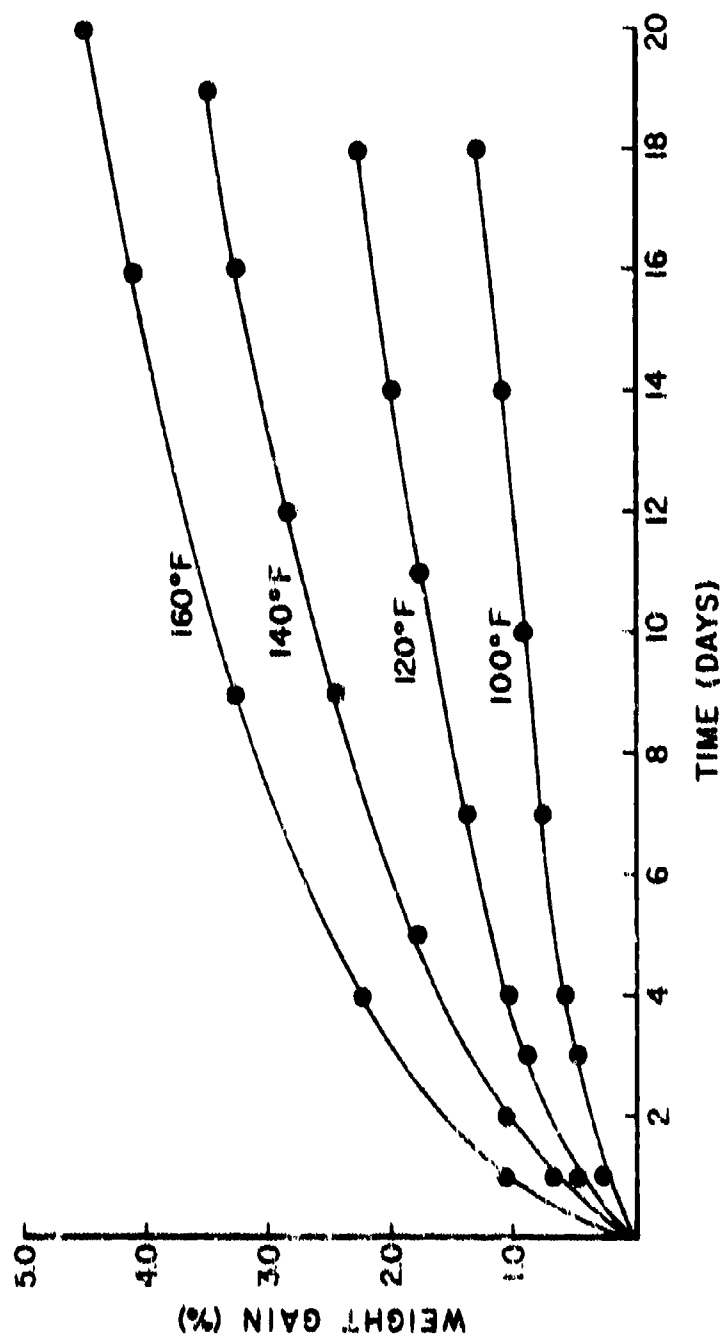


Figure 15. Weight-Gain vs. Time for Different Temperatures at 100% RH

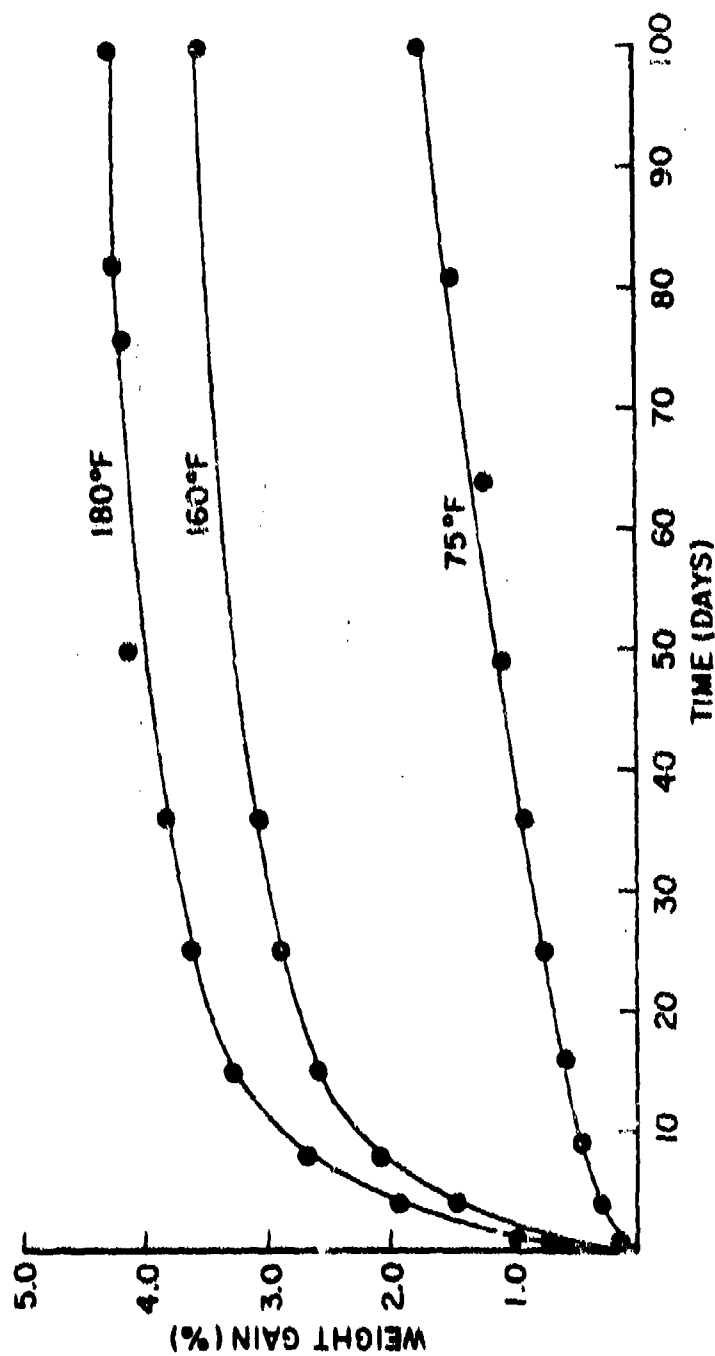


Figure 16. Weight-Gain vs. Time for Different Temperatures at 75% RH

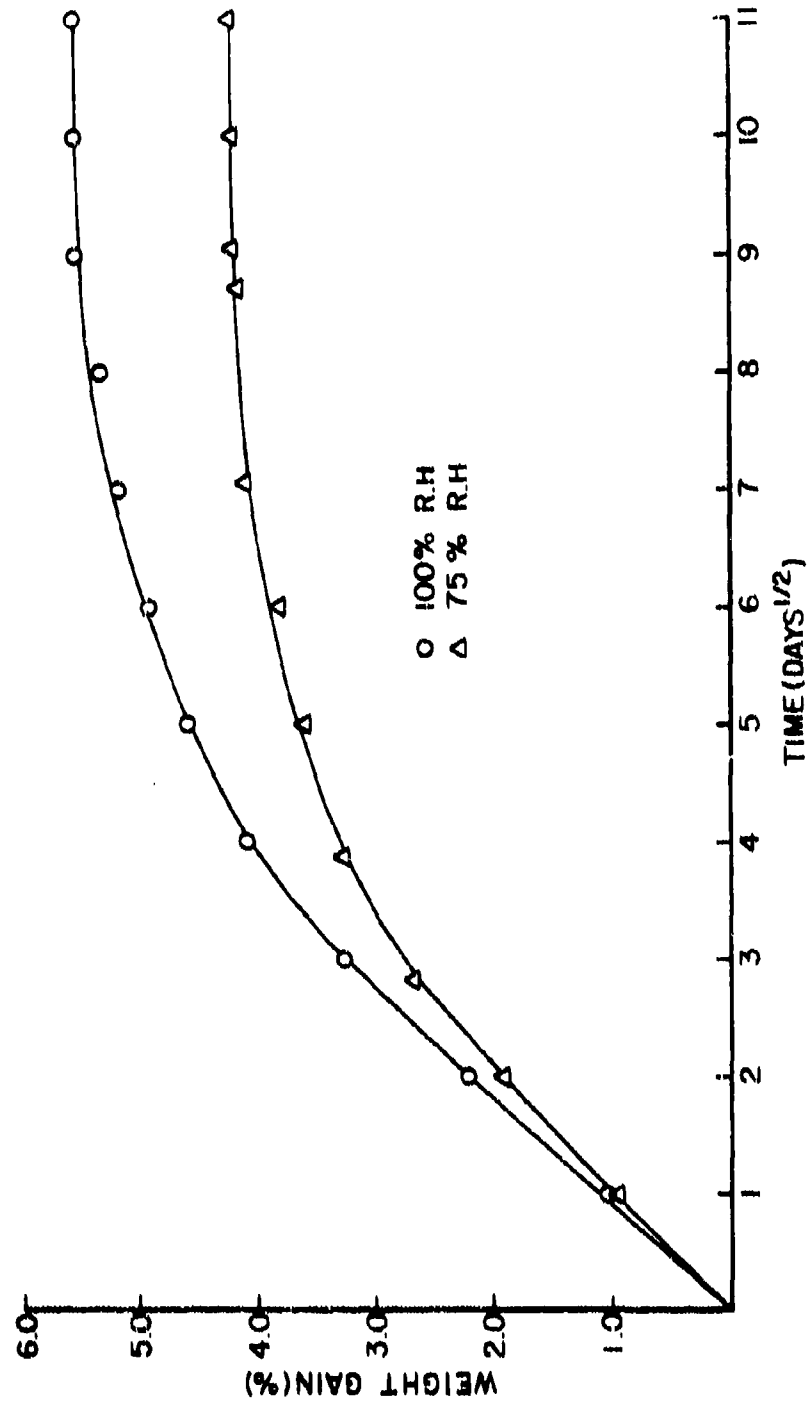


Figure 17. Weight-Gain vs. Time for Different Humidity Conditions

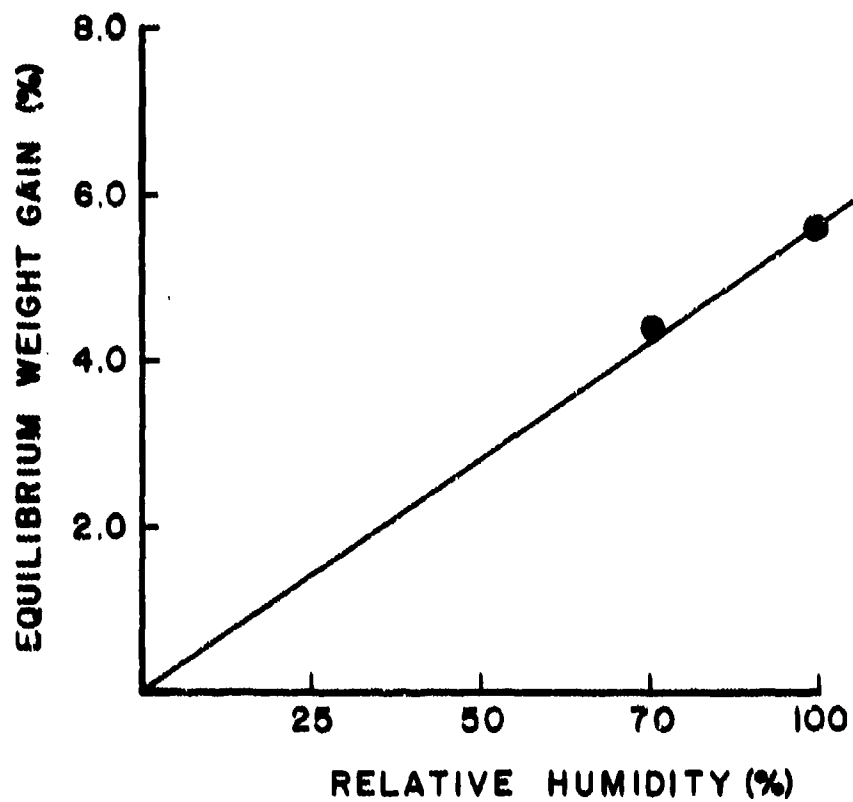


Figure 18. Equilibrium Weight-Gain vs. Relative Humidity

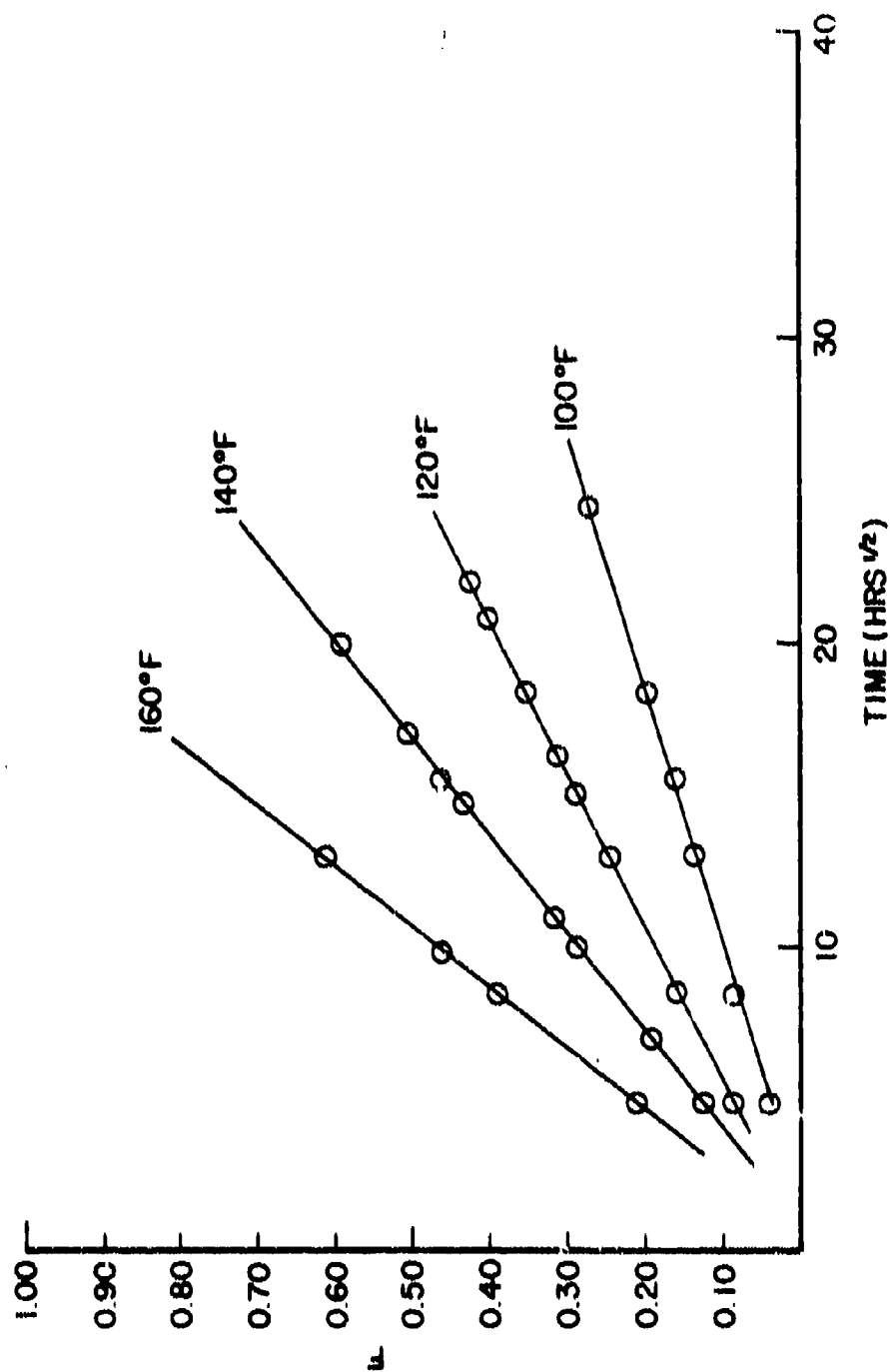
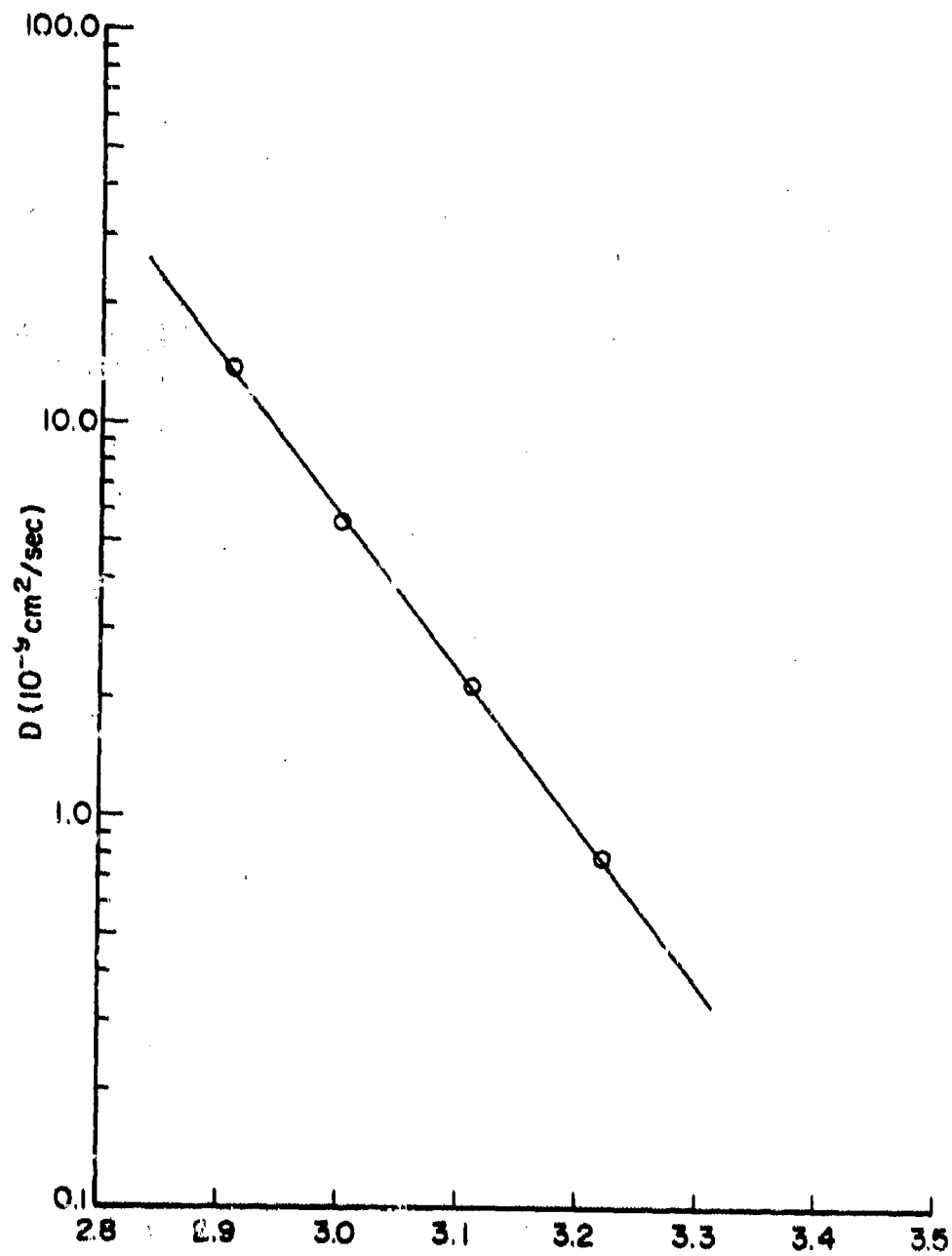


Figure 19. Fraction of Equilibrium Weight-Gain as a Function of Square Root of Time for 100% RH

AFML-TR-76-153



where D_0 = constant
 E = activation energy for diffusion
 T = absolute temperature

The value of E found is also shown in Table 2.

A similar treatment was also given to the data obtained at 75% RH. Figure 21 has plots of F vs. $t^{1/2}$ for different temperatures whose slopes were used to calculate the respective D 's. These values of D and the corresponding absolute temperature were used to prepare a $\log D$ vs. $1/T$ plot (Figure 22) from which the activation energy for diffusion at 75% RH can be calculated. The 75% RH data is summarized in Table 3.

The diffusivities shown in Tables 2 and 3 are of the same magnitude (i.e., 10^{-9} cm²/sec) as values found by other workers on various epoxy systems (Reference 3).

These values of the water diffusion coefficients were then used in a computer program (Reference 4) to determine the water concentration profiles through cast epoxy plates of varying dimensions. These results, shown in Figures 23-25, show the moisture concentration profiles or gradients that exist at conditions of 100°F and 100% RH and thicknesses of 0.125 in., 0.25 in. and 0.50 in., respectively. Similarly, Figures 26-28 show the gradients that exist at 75°F and 75% RH for thicknesses of 0.125 in., 0.25 in. and 0.50 in., respectively. As can be seen, for the 0.25-in. plate at 100% RH it takes 15 years to reach uniform moisture concentration through the thickness of the material. Until this equilibrium is reached, nonuniform stresses exist through the thickness of the specimen because of these moisture gradients. These stresses can lead to surface cracking and subsequent mechanical property losses under load. These effects will be specifically discussed in subsequent sections.

TABLE 2

RESULTS OF LINEAR SOLUTION TO FICK'S LAW
FOR 100% RH EXPOSURES

LINEAR SOLUTION

$$F = \frac{4}{l} \left(\frac{Dt}{\pi} \right)^{1/2}$$

T (°F)	R. H.(%)	D (cm ² /sec)
100	100	7.93 × 10 ⁻¹⁰
120	100	2.17 × 10 ⁻⁹
140	100	5.58 × 10 ⁻⁹
160	100	1.39 × 10 ⁻⁸

$$E_A = 18.4 \text{ KCAL / MOLE}$$

TABLE 3

RESULTS OF LINEAR SOLUTION TO FICK'S LAW
FOR 75% RH EXPOSURES

LINEAR SOLUTION

$$F = \frac{4}{l} \left(\frac{Dt}{\pi} \right)^{1/2}$$

T (°F)	RH (%)	D (cm ² /sec)
75	75	0.95 × 10 ⁻⁹
160	75	22.70 × 10 ⁻⁹
180	75	36.30 × 10 ⁻⁹

$$E_A = 13.20 \text{ KCAL / MOLE}$$

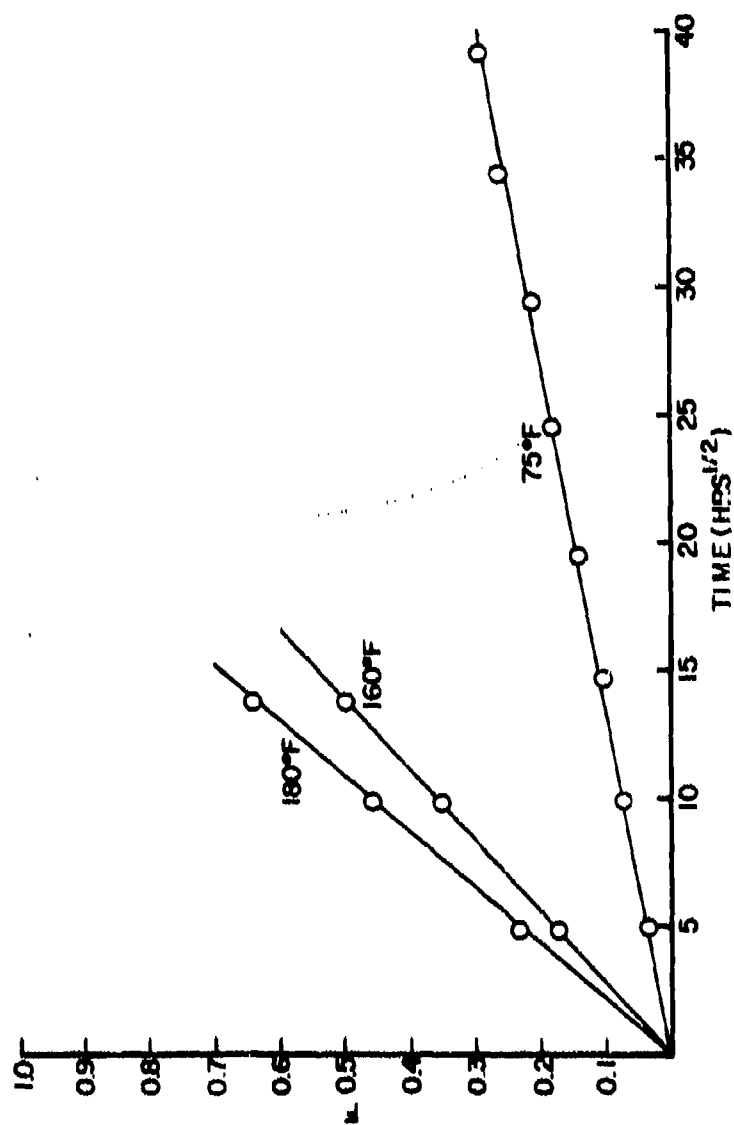


Figure 21. Fraction of Equilibrium Weight-Gain as a Function of Square Root of Time for 752 RH

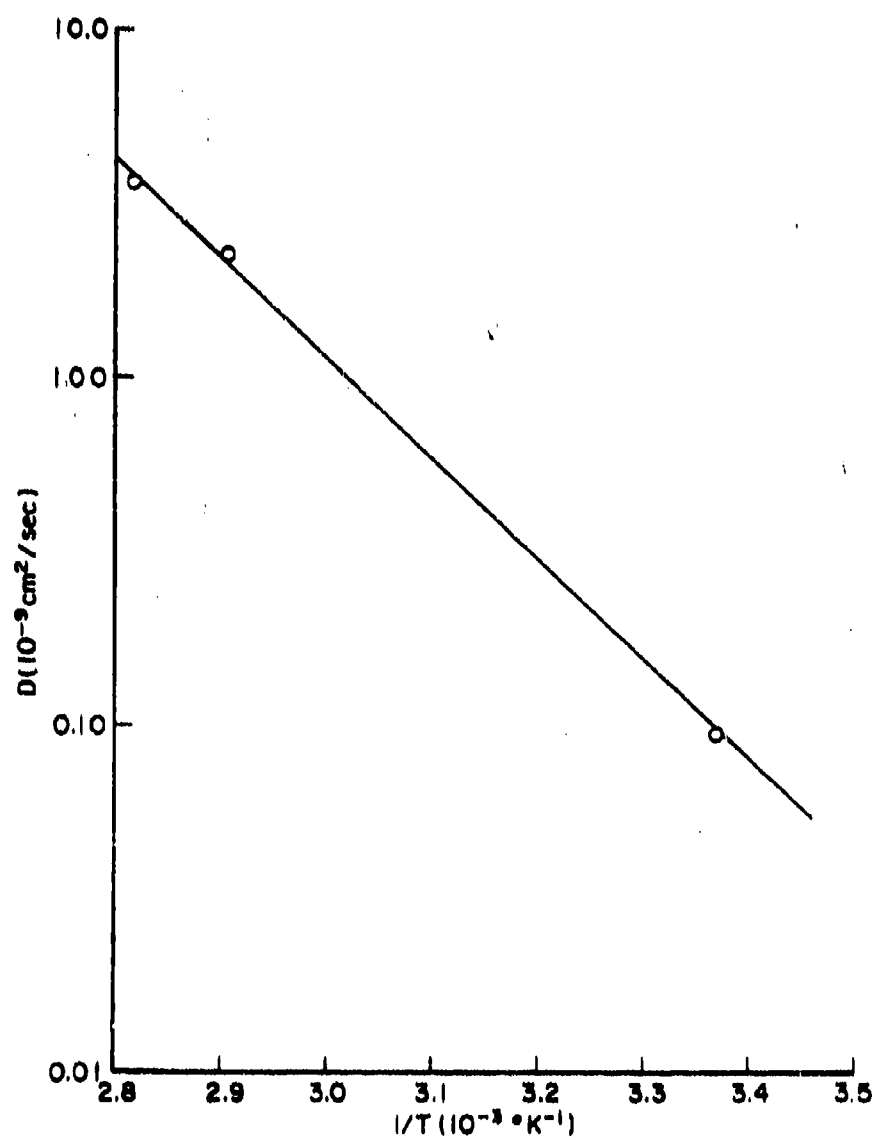


Figure 22. Diffusion Coefficient vs. Reciprocal of Absolute Temperature for 75% RH

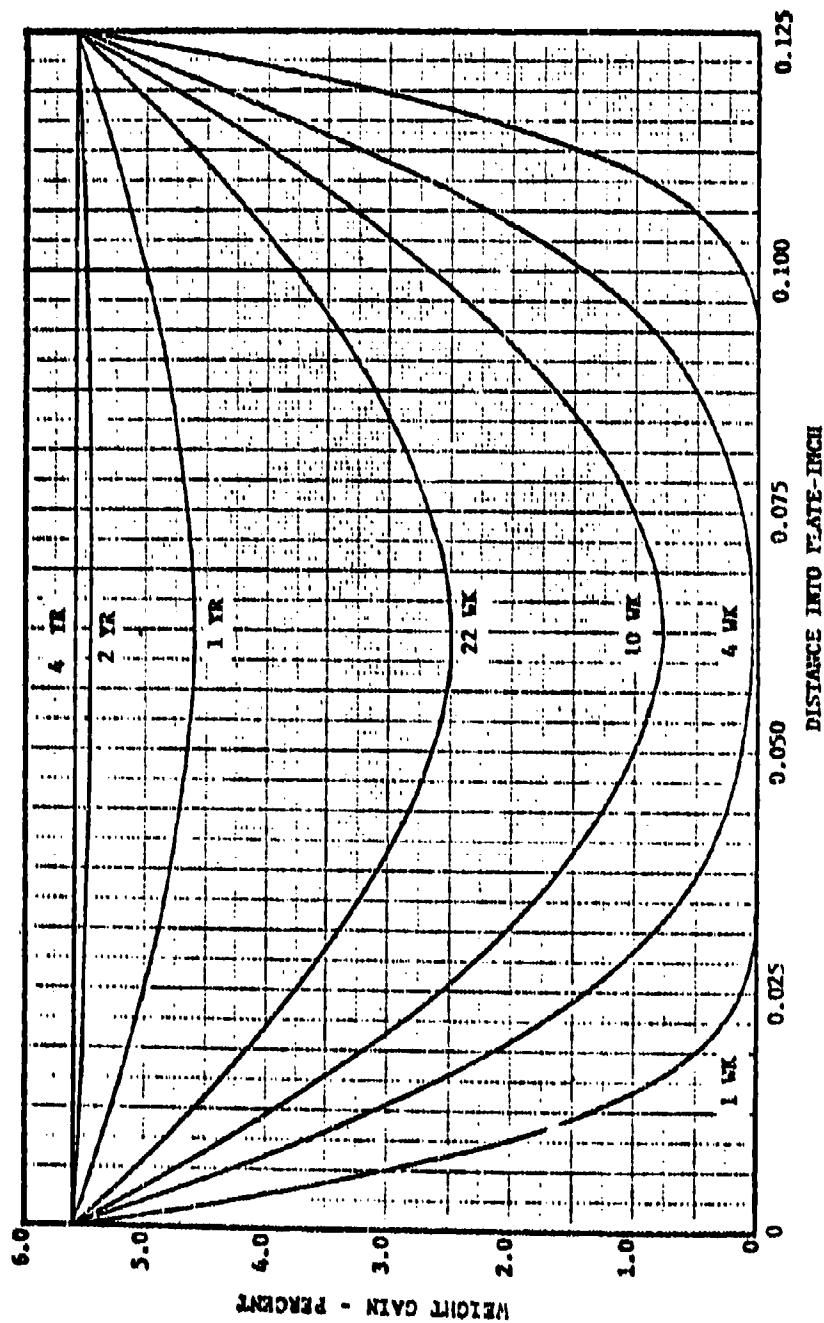


Figure 23. Diffusion of Water into a 0.125-Inch Thick Plate of Epoxy Resin at 100°F and 100% RH

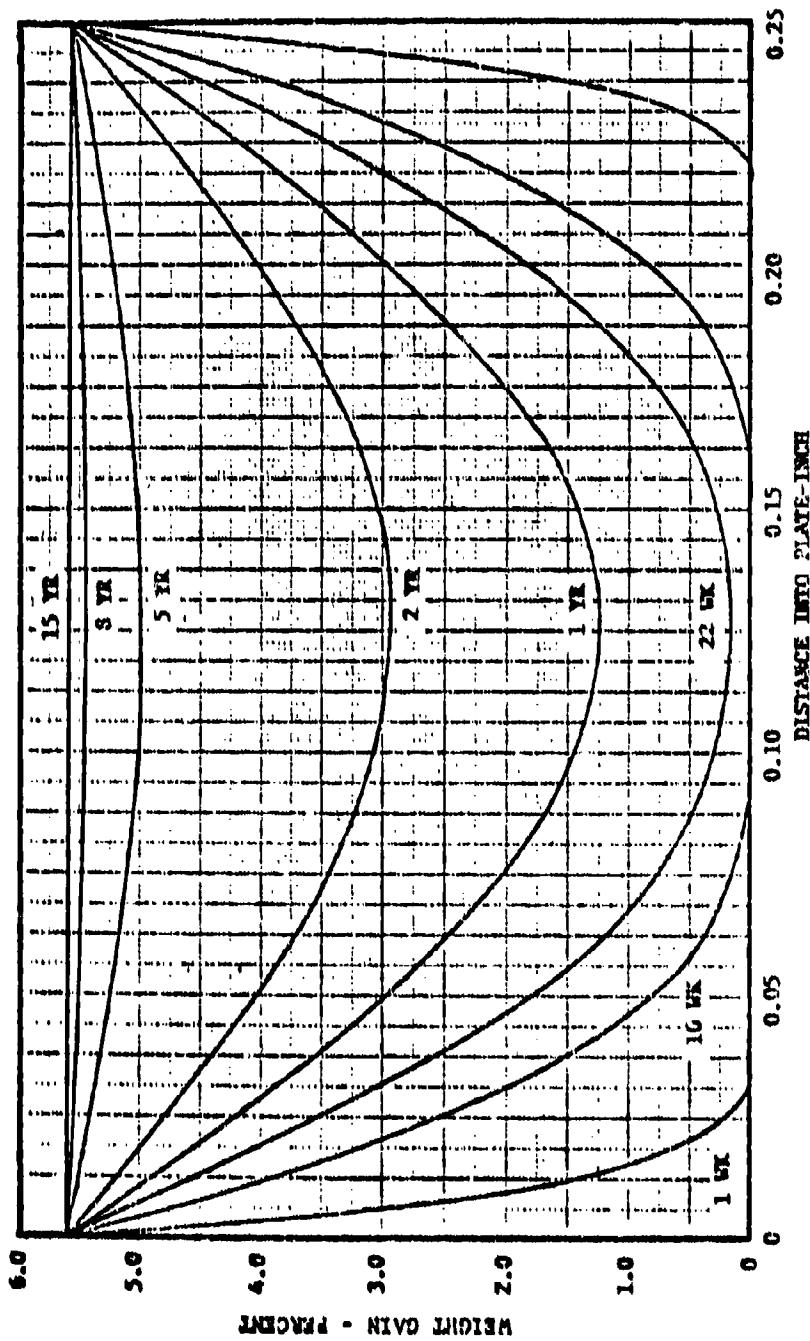


Figure 24. Diffusion of Water into a 0.25-Inch Thick Plate of Epoxy Resin at 100°F and 100% RH

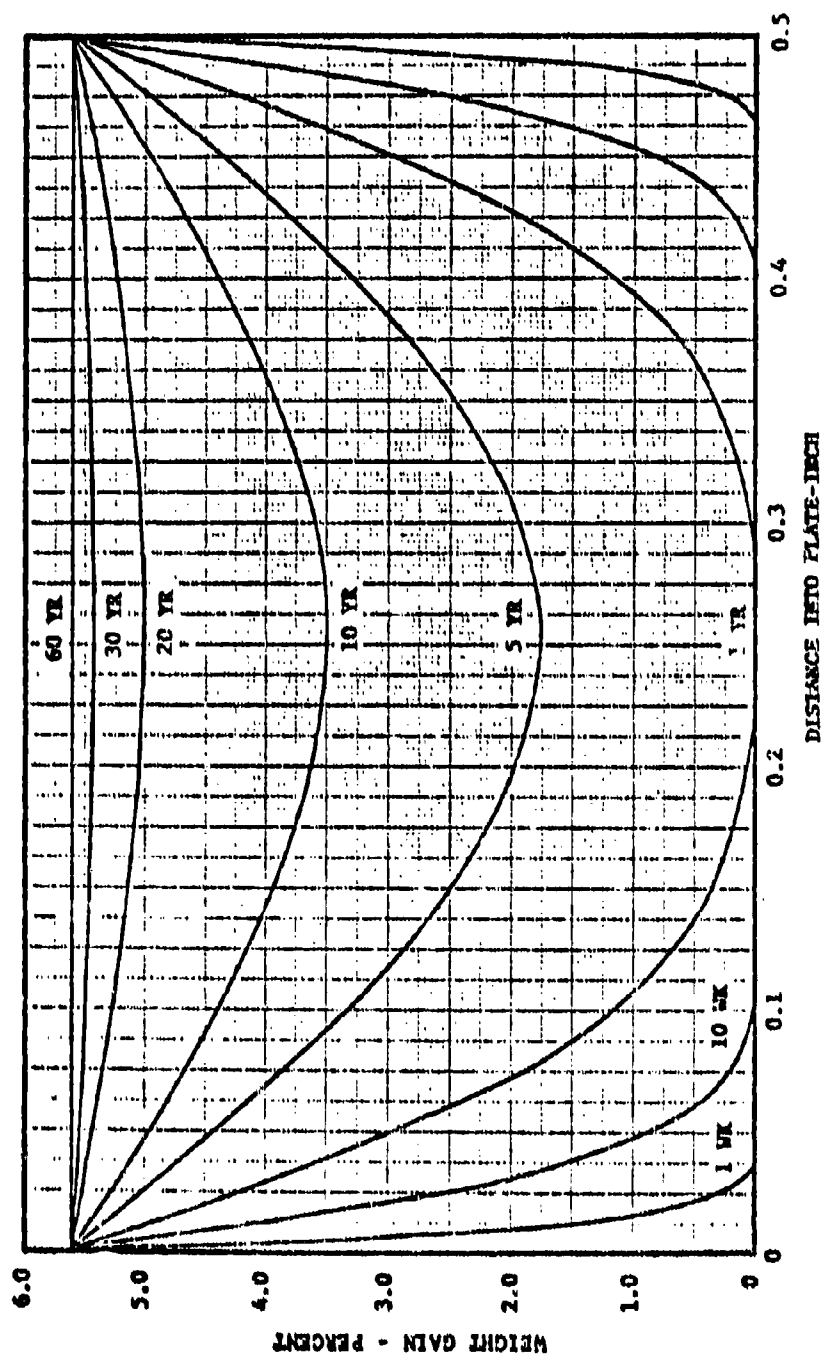


Figure 25. Diffusion of Water into a 0.500-Inch Thick Plate of Epoxy Resin at 100°F and 100% RH

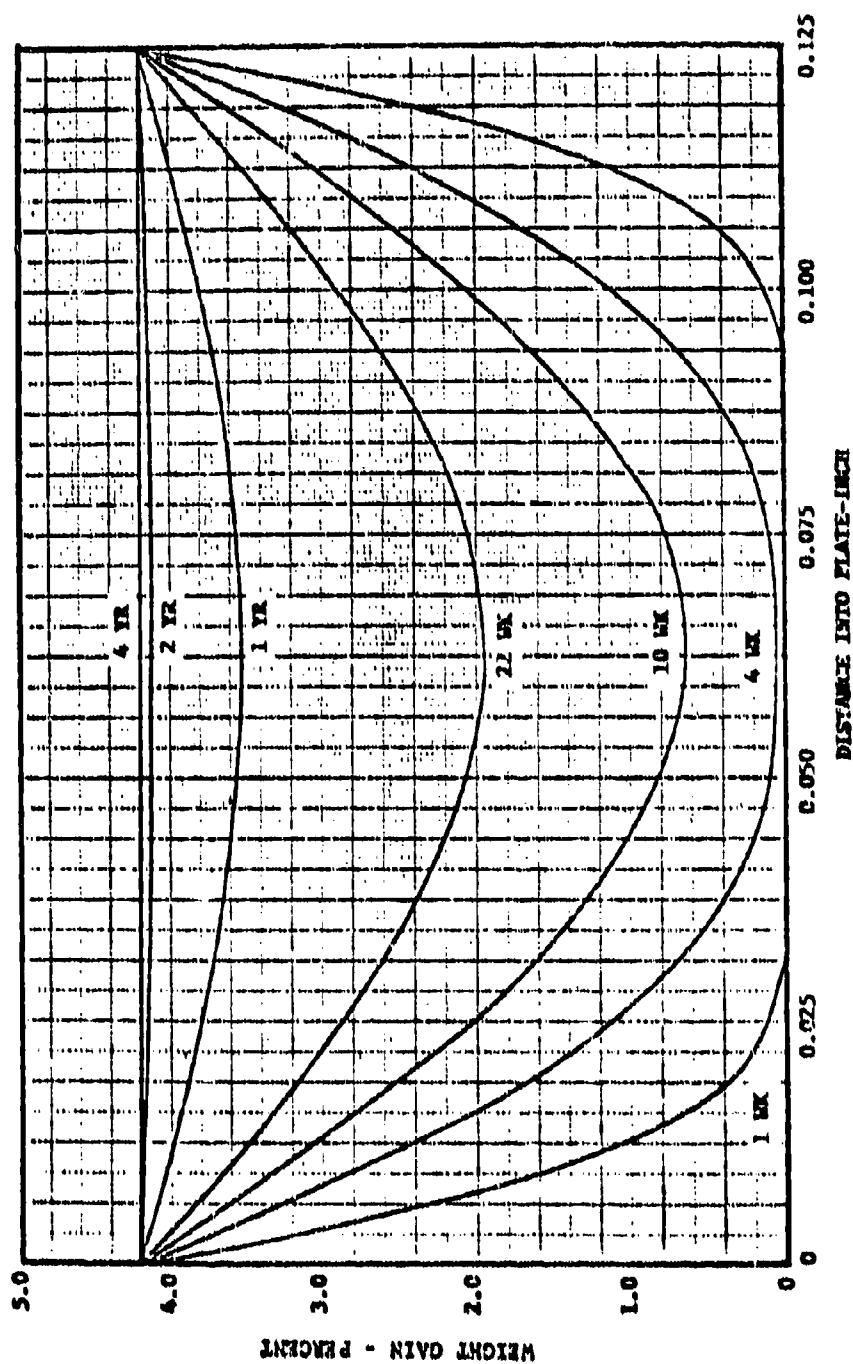


Figure 26. Diffusion of Water into a 0.125-inch Thick Plate of Epoxy Resin at 75°F and 75% RH

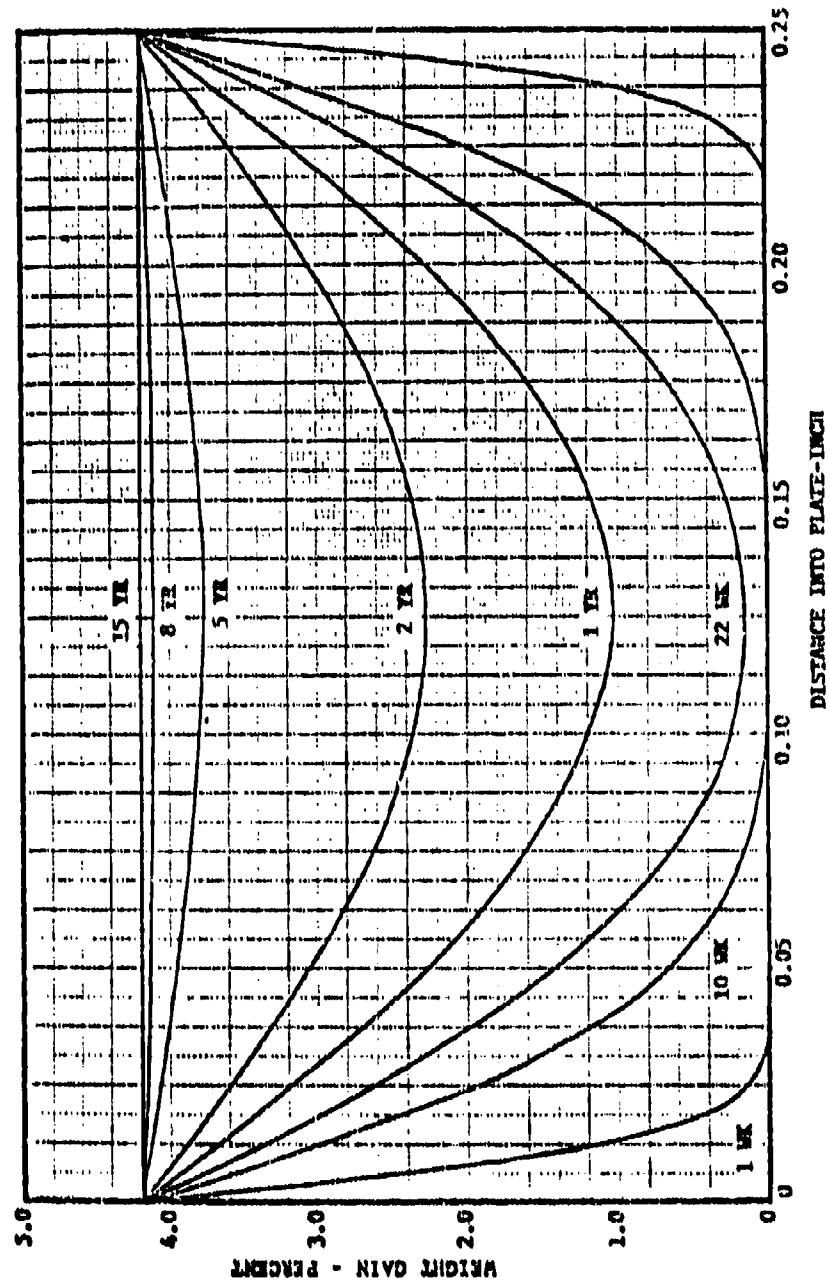


Figure 27. Diffusion of Water into a 0.25-Inch Thick Plate of Epoxy Resin at 75°F and 75% RH

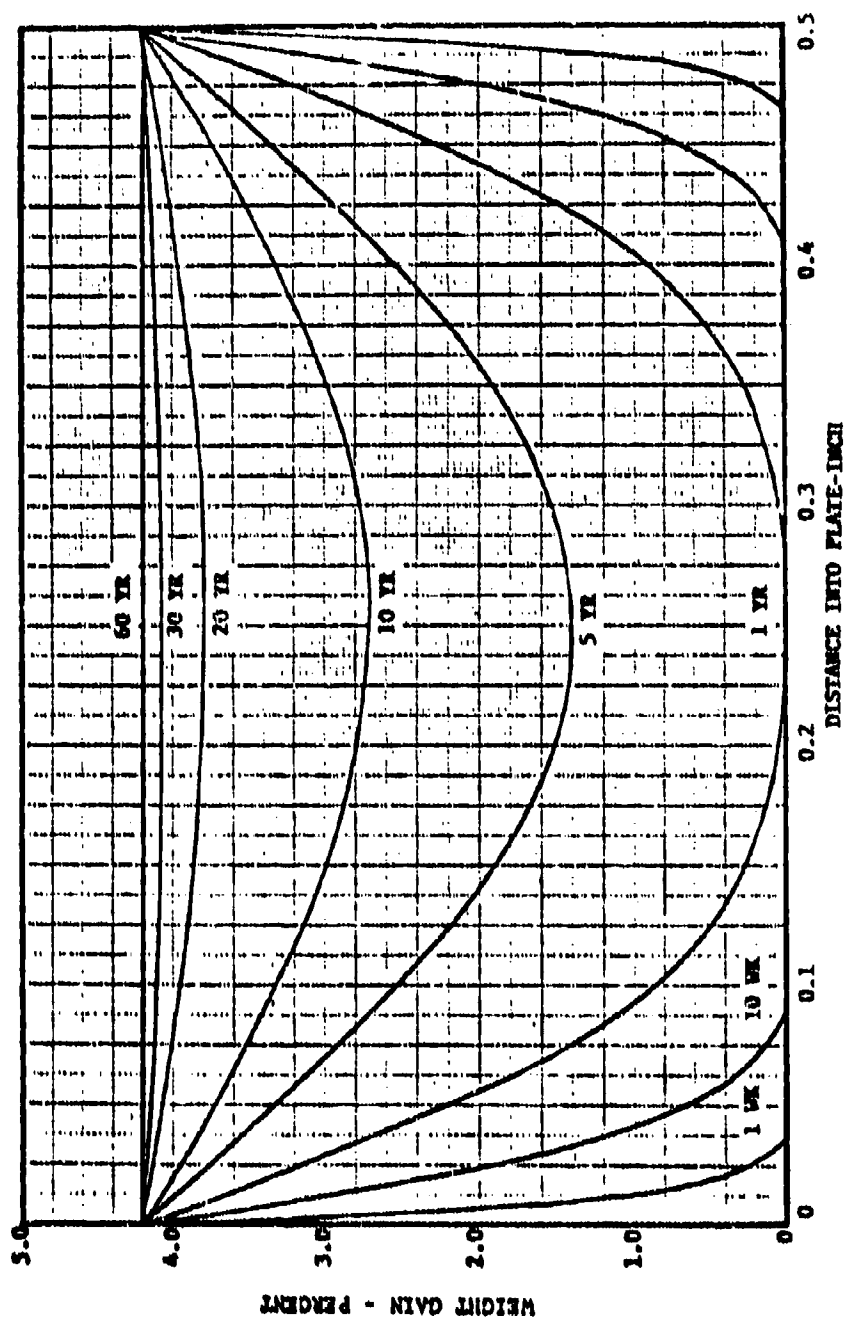


Figure 28. Diffusion of water into a 0.500-Inch Thick Plate of Epoxy Resin at 75°F and 75% RH

Similar diffusion coefficients and concentration profiles have been found for both graphite and boron composites (References 3, 4, 11, 23) when corrections were made for volume effects. These results substantiate the importance of the resin matrix in the diffusion/absorption process.

In summary, these results show that moisture is absorbed by epoxies and transmitted internally by a mechanism treatable by Fick's Law. Because of this behavior, concentration gradients, and in turn, stress gradients, exist through the thickness of the material.

Practically speaking, the linear solution to Fick's Law will not provide an accurate picture of the weight-gain process when F reaches a value of approximately 0.6 because at these values and higher the sheet can no longer be expected to behave as a semi-infinite plate (Reference 12) and consequently F is not linear with the square root of time. The problem with the linear model can be seen by considering Figure 29 where F is plotted against $t^{1/2}$ for the condition of 100% RH and 160°F. At values of F of 0.7 and greater the weight-gain process becomes nonlinear and asymptotically approaches the value of 1.0.

Because of this behavior a curve fitting model (Reference 10) was used which more accurately depicts the weight-gain process at high values of F . This model used the hyperbolic tangent of the linear solution

$$F = \text{TANH} \left[\frac{4}{L} \left(\frac{Dt}{\pi} \right)^{1/2} \right] \quad (6)$$

The hyperbolic tangent function forces the curve to go to a value of one asymptotically.

The hyperbolic tangent treatment was applied to the same data treated with the linear model for the case of 100% RH. In this case the following was done:

$$F = \text{TANH} \left[\frac{4}{L} \left(\frac{Dt}{\pi} \right)^{1/2} \right] \quad (6)$$

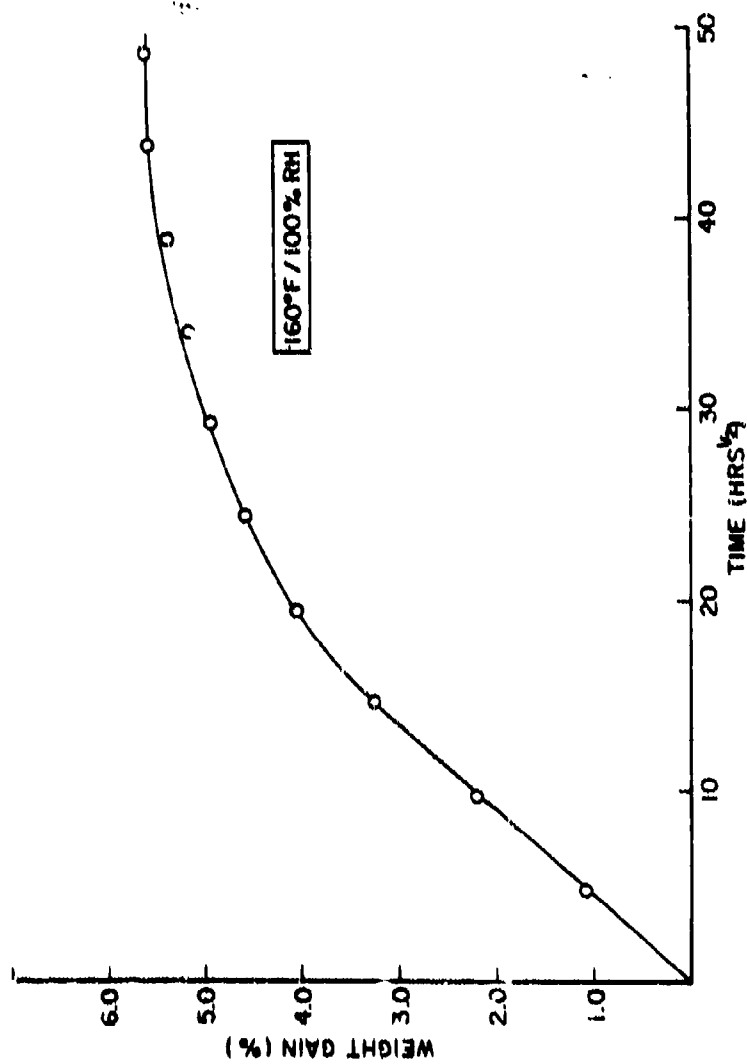


Figure 29. Epoxy Moisture Absorption - 160°F/100% RH

$$\text{TANH}^{-1}(F) = \frac{4}{L} \left(\frac{DM}{\pi} \right)^{1/2} \quad (12)$$

$$\left[\text{TANH}^{-1}(F) \right]^2 = \frac{16 \cdot Dt}{L^2 \pi} \quad (13)$$

Therefore, plots were made of $[\text{TANH}^{-1}(F)]^2$ vs. t . The slope, s , of the plots were used to calculate the values of D from:

$$s = \frac{16 \cdot D}{\pi L^2} \quad (14)$$

or

$$D = \frac{s \pi L^2}{16} \quad (15)$$

Figures 30 to 33 show the results of applying the TANH treatment to the 100% RH data at the temperatures of 100°F, 120°F, 140°F, and 160°F respectively. The values of the diffusion coefficients are summarized in Table 4. Similar to the linear treatment, a plot of $\log D$ vs. $1/T$ (Figure 34) was made to yield the activation energy for diffusion shown in Table 4. The data can be compared to the data obtained using the linear solution (Table 2). As can be seen, there is no significant difference between the two techniques for the lower temperatures.

Perhaps the most appropriate method for handling the diffusion problem is the calculation of a D using the linear model and then applying the series solution to Fick's Law to predict the absorption process. The utilization of the series solution has only recently been described (Reference 15) and is developed as follows:

Starting with the previously described general diffusion equation:

$$\frac{\partial c}{\partial t} = D \frac{\partial^2 c}{\partial x^2} \quad (1)$$

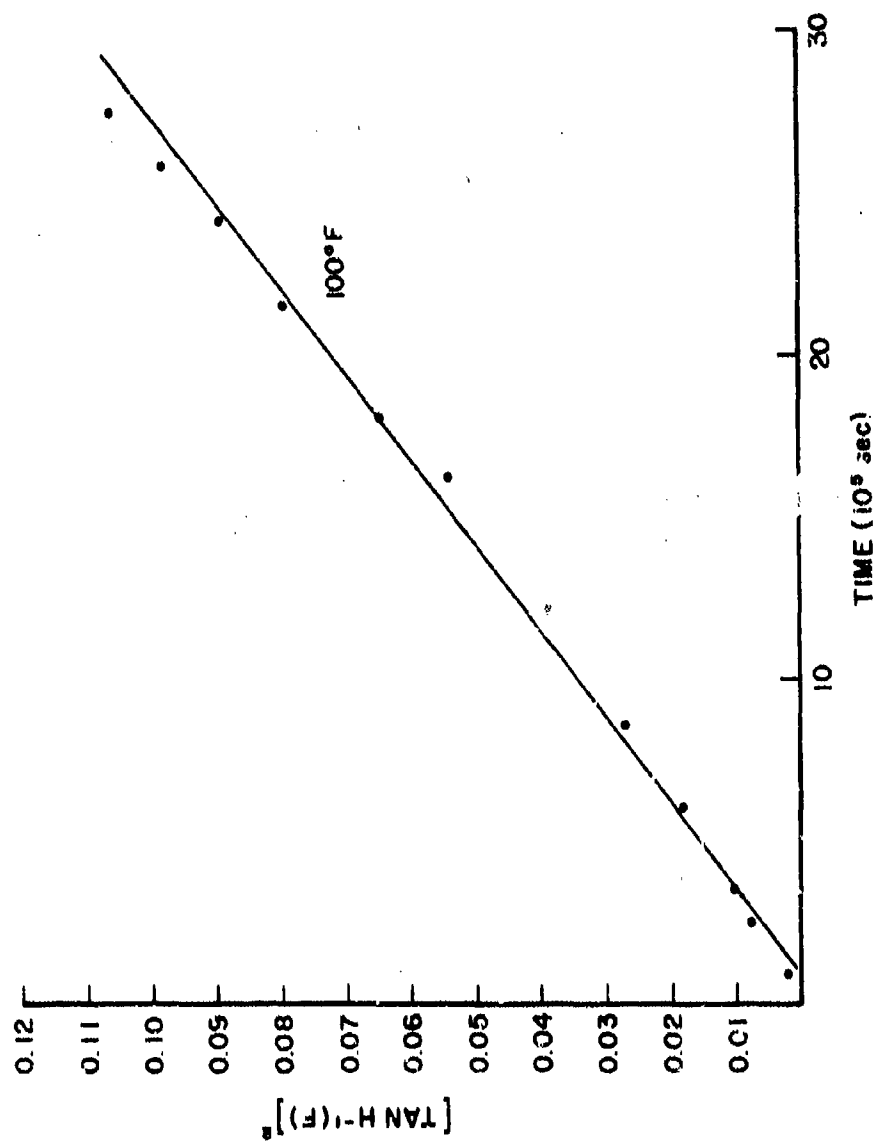


Figure 30. TANH Treatment of Epoxy Moisture Absorption for 100% RH

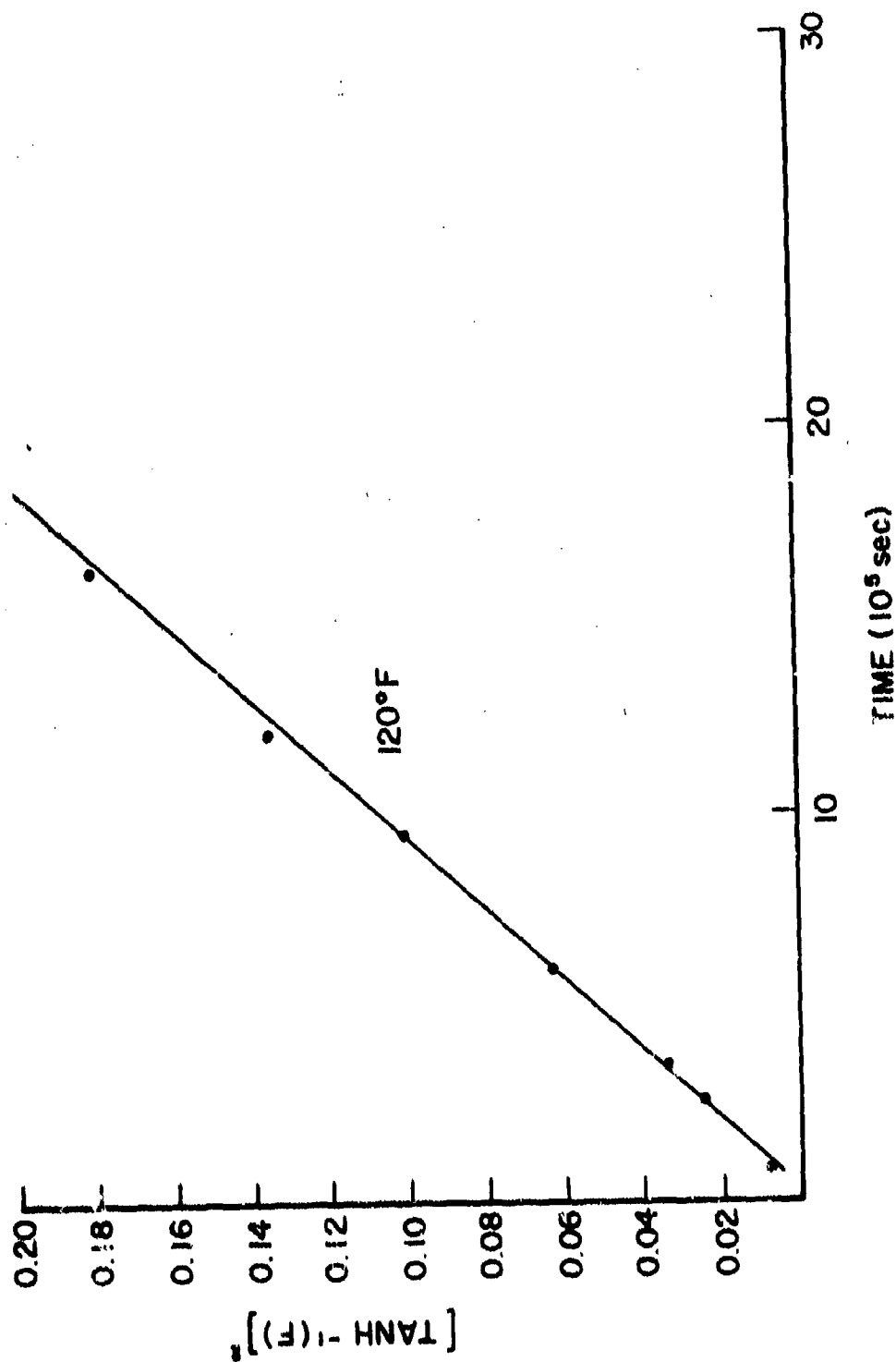


Figure 31. TANH Treatment of Epoxy Moisture Absorption for 100% RH

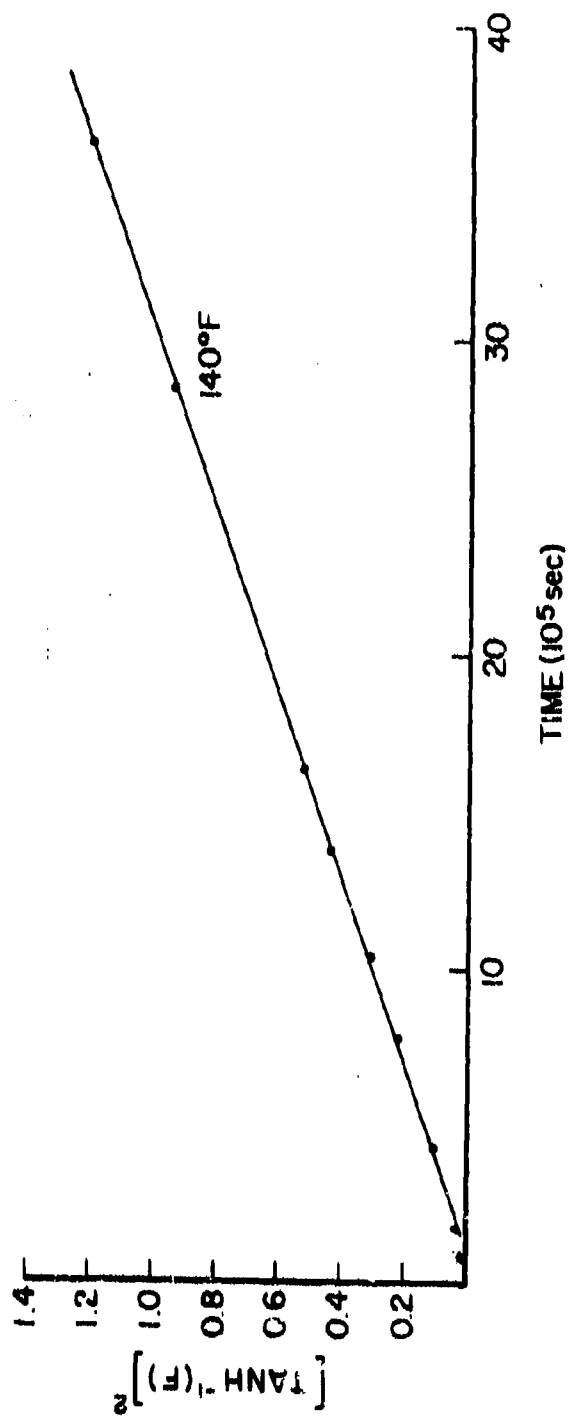


Figure 32. TANH Treatment of Epoxy Moisture Absorption for 100% RH

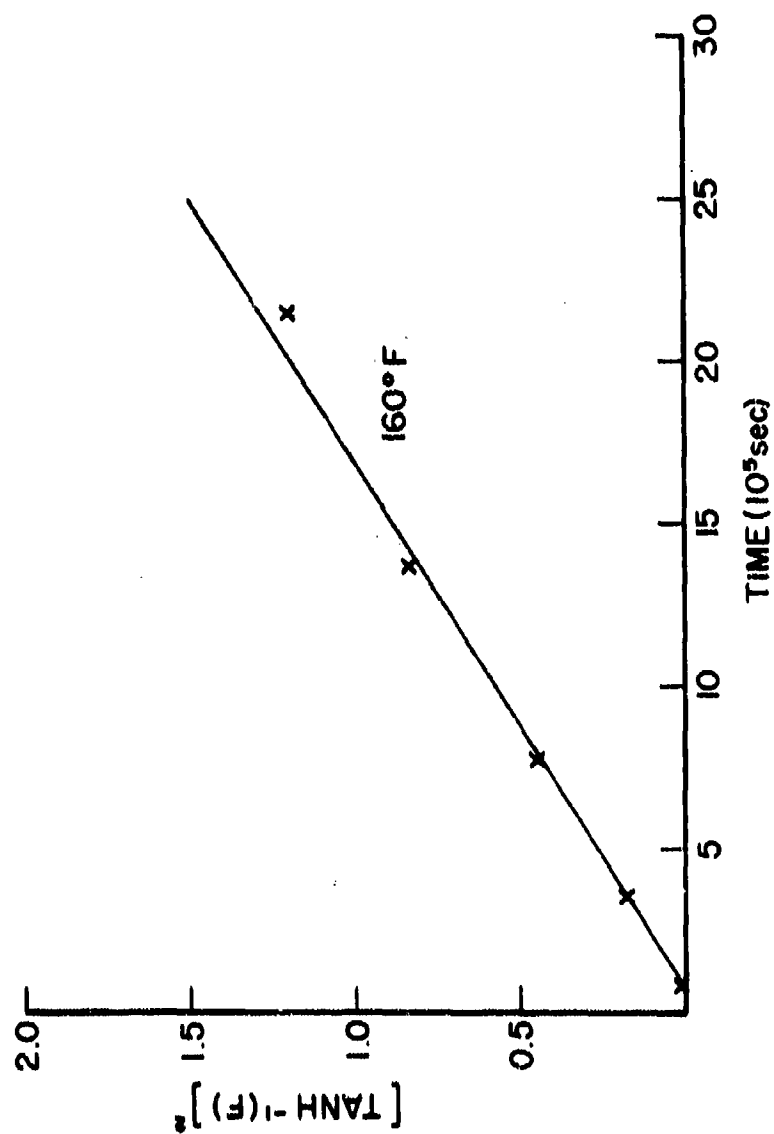


Figure 33. TANH Treatment of Epoxy Moisture Absorption for 100% RH

TABLE 4
RESULTS OF TANH SOLUTION TO FICK'S LAW
FOR 75% RH EXPOSURES

TANH SOLUTION

$$F = \text{TANH} \left[\frac{4}{\ell} \left(\frac{Dt}{\pi} \right)^{1/2} \right]$$

T (°F)	R. H. (%)	D (cm ² /sec)
100	100	1.09×10^{-9}
120	100	2.29×10^{-9}
140	100	7.10×10^{-9}
160	100	1.25×10^{-8}

$$E_A = 15.6 \text{ KCAL / MOLE}$$

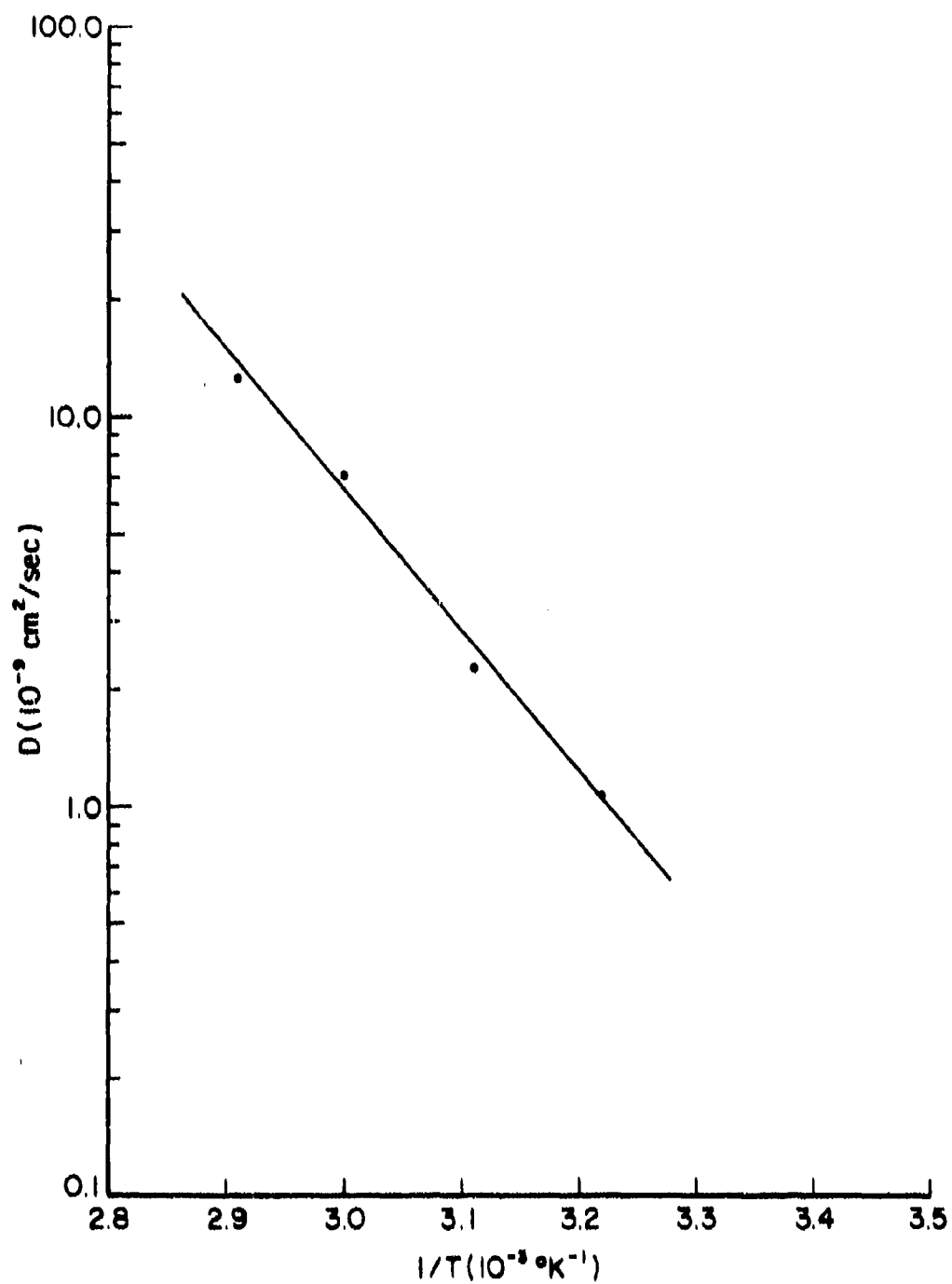


Figure 34. Diffusion Coefficient vs. Reciprocal of Absolute Temperature for 100% RH TANH Treatment

the following boundary and initial conditions for a plate of thickness, h , are used:

$$\begin{aligned} C(x, 0) &= C_i \\ C(0, t) &= C(h, t) = C_a \end{aligned} \quad (16)$$

where C_i is the initial moisture concentration in the material and C_a is the ambient moisture concentration. Classical separation of variables in conjunction with Equation 1 and Equation 16 yields the following:

$$\frac{C - C_i}{C_a - C_i} = 1 - \frac{4}{\pi} \sum_{n=0}^{\infty} \frac{1}{(2i+1)} \sin \frac{(2i+1)\pi x}{h} \cdot \exp \left[\frac{-(2i+1)^2 \pi^2 D t}{h^2} \right] \quad (17)$$

The total weight of the moisture in the material is given by

$$M = \int_0^h C \, dx \quad (18)$$

Integration of Equation 18 gives

$$G = \frac{M - M_i}{M_a - M_i} = 1 - \frac{8}{\pi^2} \sum_{n=1}^{\infty} \frac{\exp \left[(2i+1)^2 \pi^2 \left(\frac{D t}{h^2} \right) \right]}{(2i+1)^2} \quad (19)$$

In terms of percent weight-gain in the material, M , Equation 19 can be written in the form

$$M = G(M_a - M_i) + M_i \quad (20)$$

where the M 's are as previously described. For most problems of concern convergence of these series can be obtained with a maximum of ten terms.

This series treatment was applied to the data obtained for exposure at 160°F and 100% RH. The predicted values of M versus \sqrt{t} using both the linear and the hyperbolic tangent model are shown in Figure 35 along with the experimental data. As can be seen, at values of M greater than

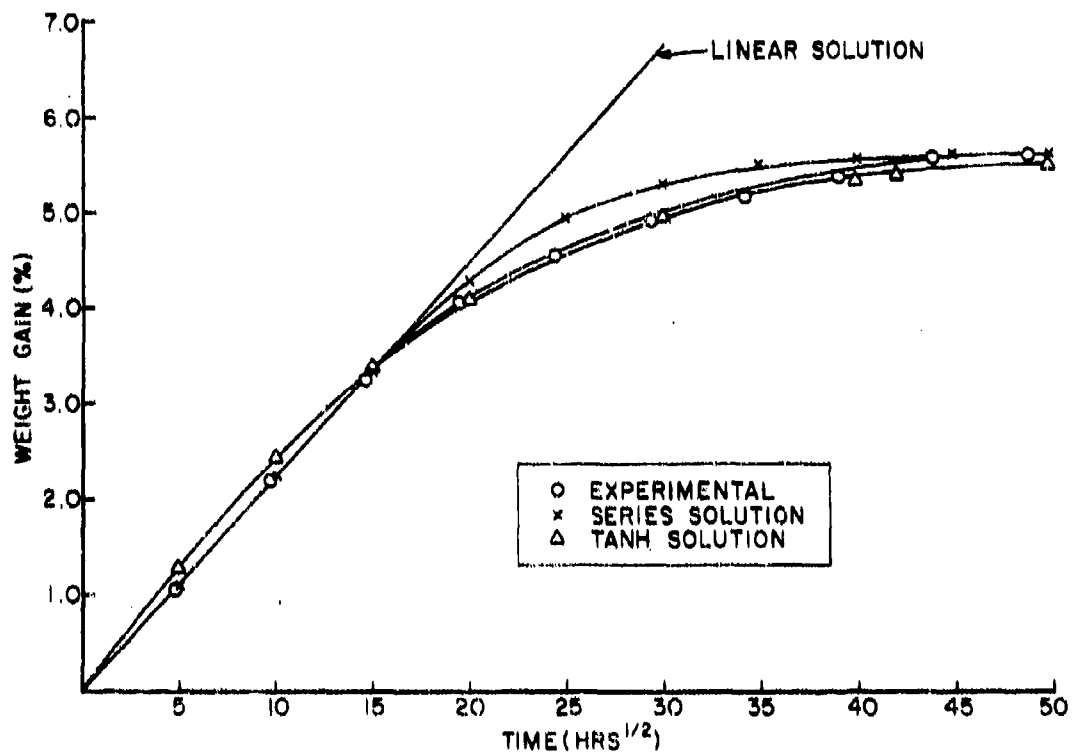


Figure 35. Predicted Epoxy Moisture Absorption According to Different Solutions of Fick's Law

60% of M_{∞} the linear treatment is no longer valid. Both the hyperbolic tangent and series treatments give predictions very close to the experimentally measured values.

The most important results to be gained from this study were that the absorption and diffusion process can be treated using Fick's Second Law and that good representations of the moisture concentration profiles or gradients within the epoxy samples can be determined.

c. Real-Life Environmental Exposures

All of the previous results and discussions were concerned with constant temperature/humidity environments. In actual usage in a real-world environment that an aircraft would see, these materials would be subjected to varying environmental excursions, temperature in particular. To simulate this, specimens were subjected to the real-life environmental exposure cycle shown in Figure 8. This environmental cycle was developed by General Dynamics (Reference 10) and is considered to be an environment that is representative of a typical flight profile for a supersonic aircraft. Of particular concern in this cycle is the 300°F thermal spike which simulates a supersonic dash maneuver. The profile in general simulates the aircraft sitting on the runway (75°F/75% RH and RAIN), flying at high altitudes (-65°F or -15°F) and then diving in on a supersonic, low altitude run (temperature to 300°F in 3 1/2 minutes).

In the course of this investigation, specimens were also subjected to the constant temperature/humidity conditions of the real-life environment (75°F/75% RH) and to all other phases of the real-life cycle except for the cold whose effect could be deduced from the results of the other phases. The results of the exposures to these conditions (rain/humidity/thermal spike/cold; rain/humidity/thermal spike; humidity only) are shown in Figure 36. It is quite obvious that the thermal spike has increased both the rate and amount of moisture absorbed.

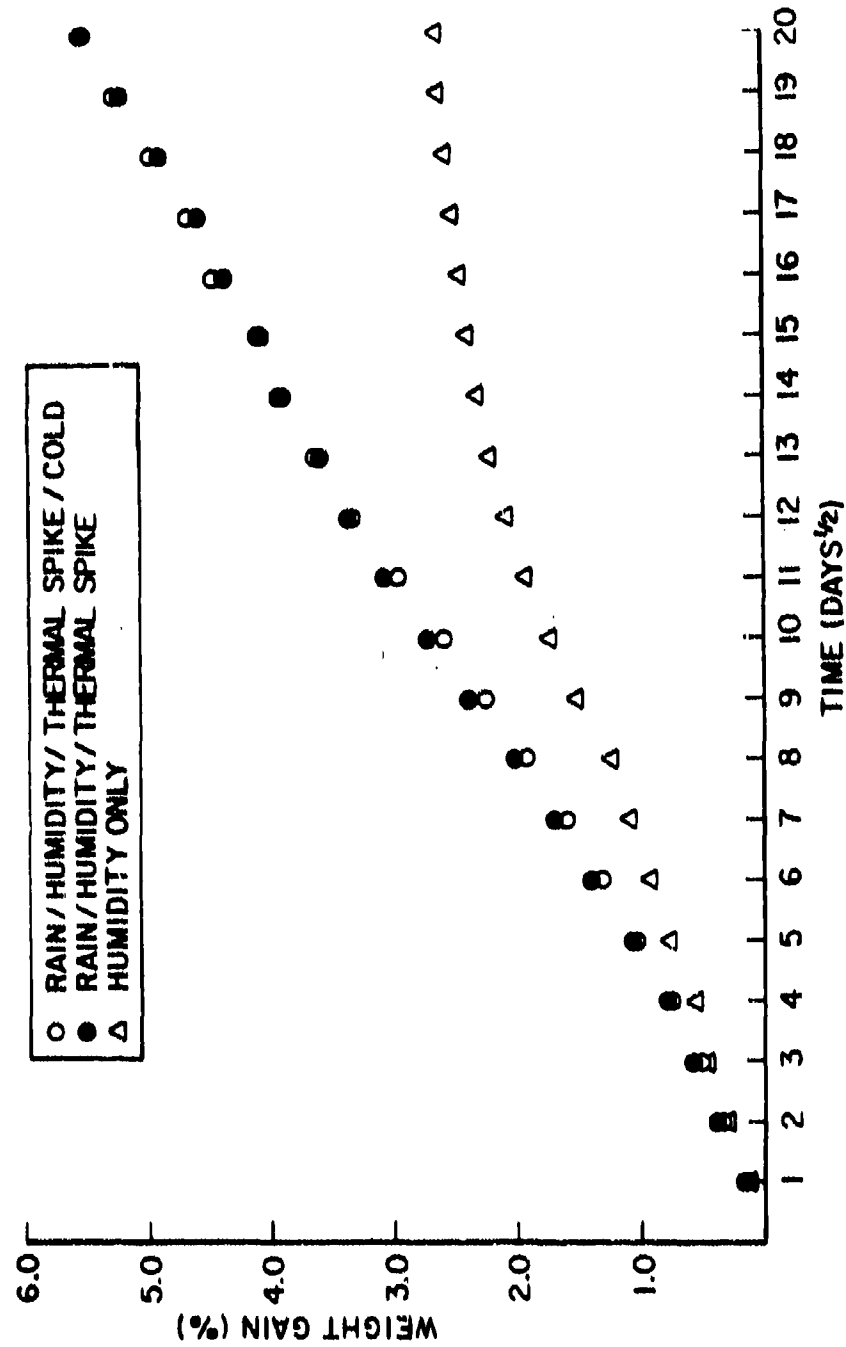


Figure 36. Epoxy Moisture Absorption as a Function of Real-Life Exposure Conditions

To further study the influence of the thermal-spike on the weight-gain process, specimens were subjected to the following exposures:

1. Constant temperature/humidity only (160°F/100% RH)
2. (1.) + 1 daily thermal-spike
3. (1.) + 4 daily thermal-spikes

These results are illustrated in Figure 37. It is obvious that the weight-gains are proportional to the number of thermal-spikes experienced by the specimens. These two figures also show that the thermal-spike is the single most important factor in this environment causing increased moisture pick-up.

d. Absorption Anomalies

Various anomalies in the weight-gains as a function of time were noted during this investigation. The data shown in Figure 37 for the long time period exhibit irregular behavior. Figure 38 shows similar weight-gain vs. time plots for three different castings with all specimens being exposed to 160°F/100% RH and one thermal-spike daily. Once the weight-gains exceed M_{∞} , the data become quite irregular with time. Figure 39 shows weight-gain data for 160°F/100% RH exposures only (no thermal-spikes), where for the long-term data points, some "scatter" is apparent when M_{∞} (5.6%) is exceeded.

This type of behavior where irregular weight-gains are observed when the M_t values exceed the M_{∞} values, can be attributed to micro-cracking in the specimens. Scanning electron microscopy (SEM) was performed on specimens which had been given the exposures:

1. Constant temperature/humidity only (160°F/100% RH)
2. (1.) + 1 daily thermal-spike
3. (1.) + 4 daily thermal-spikes

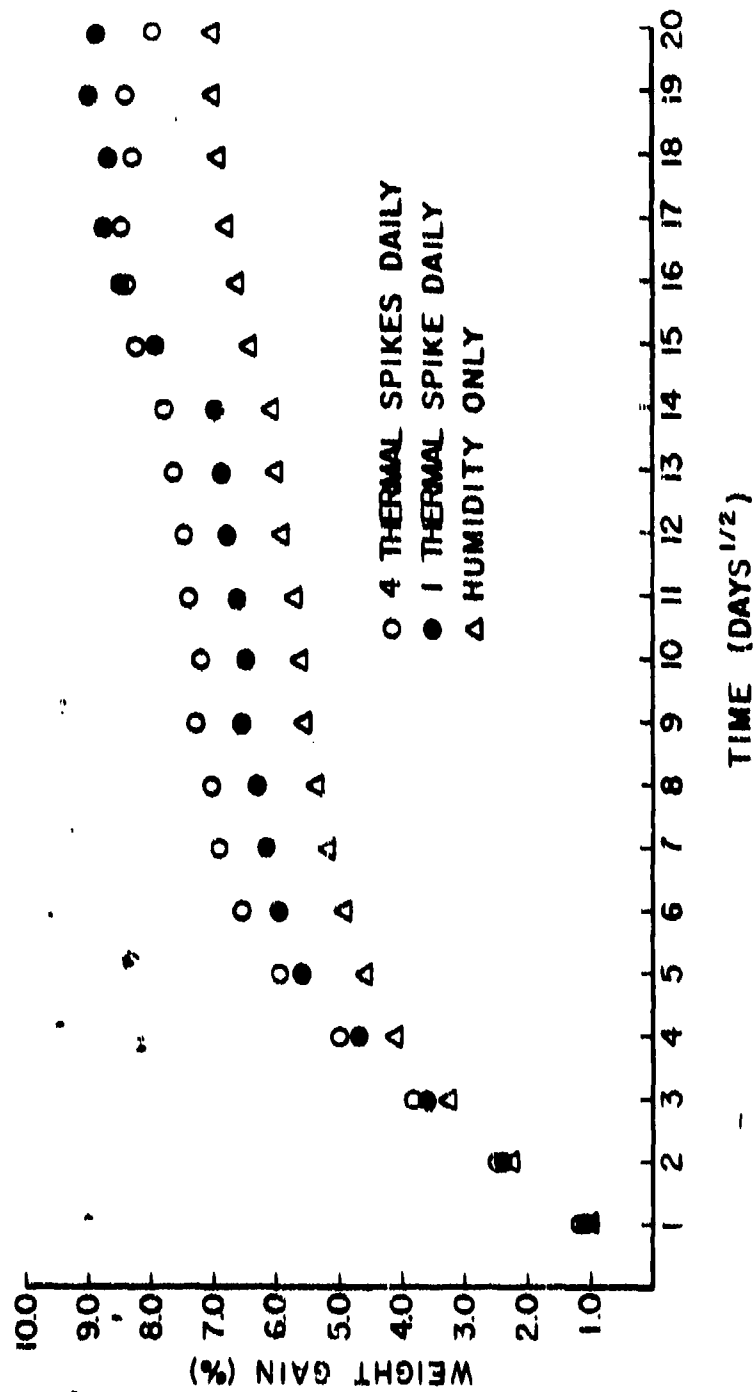


Figure 37. The Effect of Thermal-Spikes on Epoxy Moisture Absorption
(160°F/100% RH)

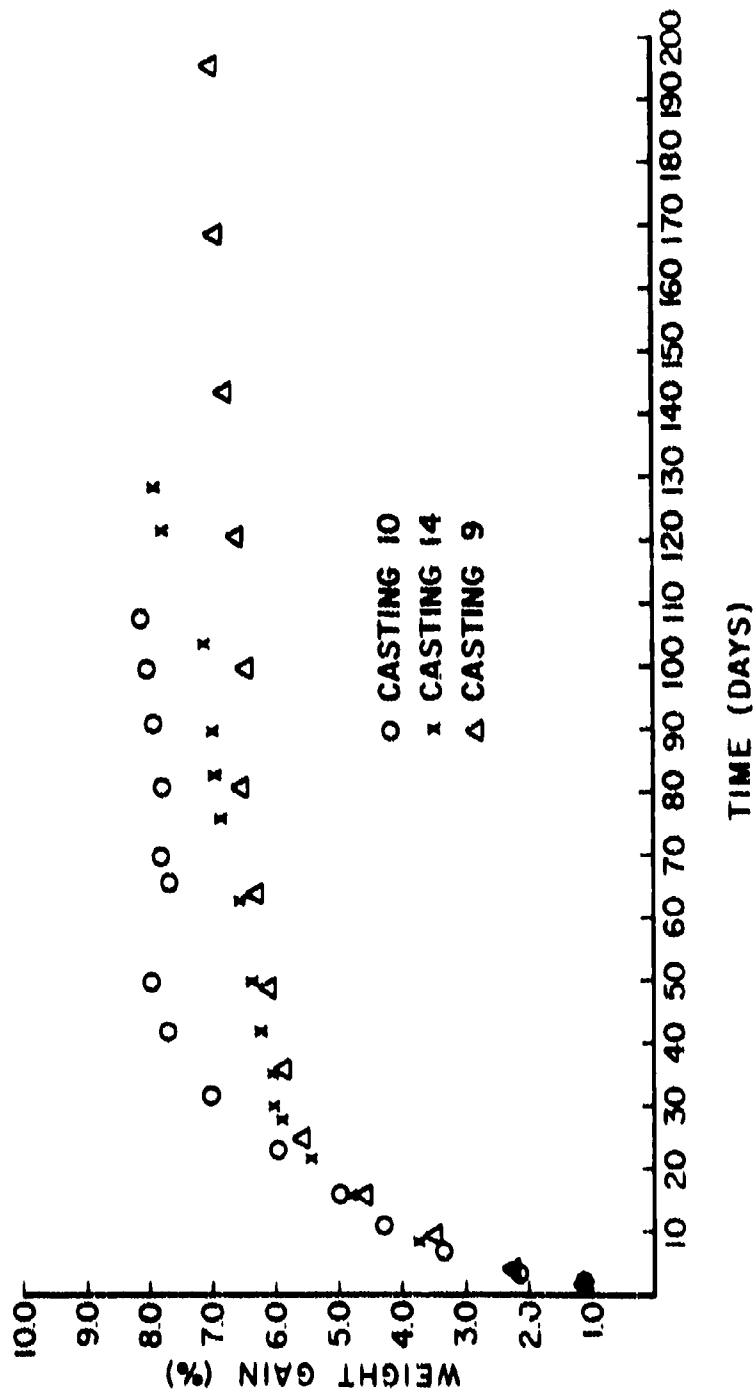


Figure 38. The Effect of Thermal-Spikes on the Moisture Absorption (160°F/100% RH) of Several Epoxy Castings

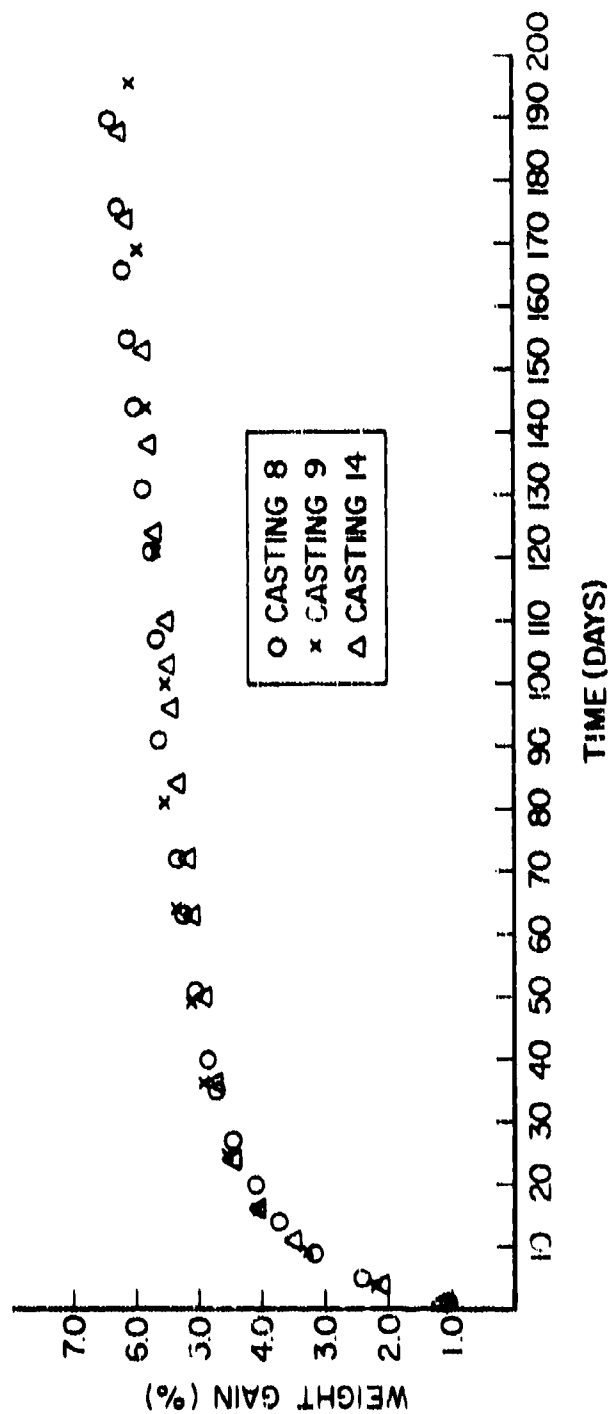


Figure 39. Moisture Absorption for Several Epoxy Castings - 160°F/100% RH

The weight-gains for each of these were 5.6%, 6.7%, and 7.4% for exposures 1., 2., and 3, respectively. The SEM photographs of these specimens are shown on the next several pages.

No cracks were apparent for type one exposures (160 °F/100% RH, 5.6% water). However, as shown in Figure 40, some material is being compressed or forced out of the surface of the specimen by the swelling forces of the absorbed moisture. Specimens which had been given Exposure 2 (Exposure 1. + 1 daily thermal-spike, 6.7% water) exhibited cracking around these compressed regions (Figure 41). Figure 42, for this same exposure, shows that substantial numbers of surface cracks are present. Specimens which had been given Exposure 3 (Exposure 1. + 4 daily thermal-spikes, 7.4% water) exhibited the greatest amount of surface cracking. Figure 43 shows that the compressed material has given way completely to cracks. A close-up of this region is seen in Figure 44. Figure 45 is a general surface view illustrating the degree of surface cracking.

A specimen from Exposure 3 was fractured by hand and the two fracture surfaces were mated together for the SEM study. A view of the two surfaces is shown in Figure 46 where the crack depth is on the order of 0.4 cm. Figure 47 shows a close-up of a crack tip where the presence of fibrils can be seen at the base of the classic river patterns which are associated with brittle fracture. These fibrils would be indicative of the highly plasticized state of the polymer in that the usually brittle epoxy has undergone sufficient plastic flow during fracture to yield fibrils. Figure 48 shows another view of a fracture surface around a crack. The striations or river patterns emanating from the crack perimeter are classical brittle fracture behavior (Reference 29).

Further evidence to support the contention that weight-gains exceeding the equilibrium amount were due to water trapped in microcracks was obtained through the use of a Quantimet 720 equipped with an Epidiascope. This instrument optically scans the surface of a specimen or a photomicrograph of a specimen and can yield information such as



Figure 40. SEM of Epoxy Specimen after Exposure to 160°F/100% RH - 5.6% Weight-Gain (2000 X)



Figure 41. SEM of Epoxy Specimen after Exposure to 160°F/100% RH/1 Daily Thermal-Spike - 6.7% Weight-Gain (2000 X)



Figure 42. SEM of Epoxy Specimen after Exposure to 160°F/100% RH/1 Daily Thermal-Spike - 6.7% Weight-Gain (600 X)

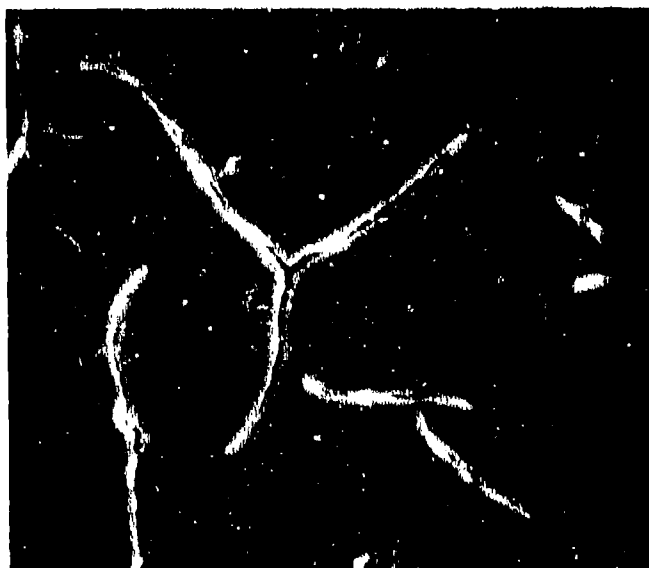


Figure 43. SEM of Epoxy Specimen after Exposure to 160°F/100% RH Daily Thermal-Spikes - 7.4% Weight-Gain (300 X)



Figure 44. SEM of Epoxy Specimen after Exposure to 160°F/100% RH/4 Daily Thermal-Spikes - 7.4% Weight-Gain (3000 X)

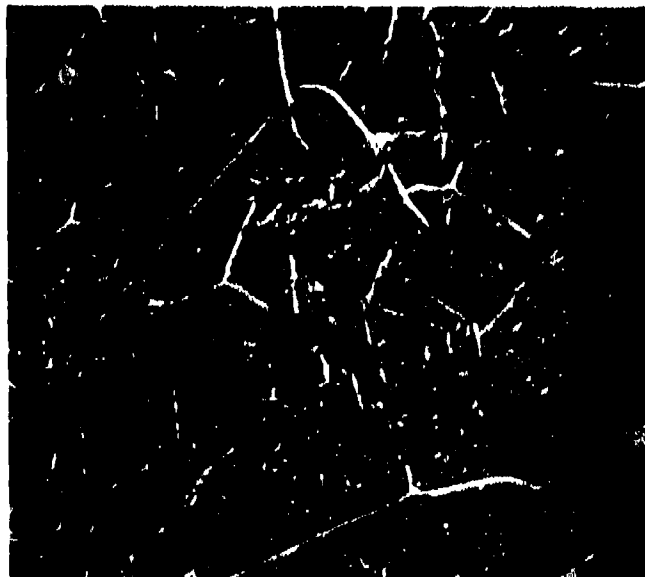


Figure 45. SEM of Epoxy Specimen after Exposure to 160°F/100% RH/4 Daily Thermal-Spikes - 7.4% Weight-Gain (60 X)

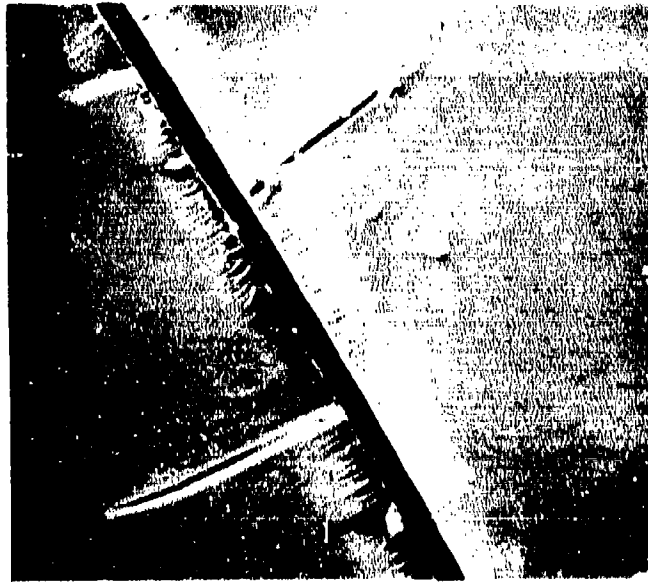


Figure 46. SEM of Fracture Surface of Epoxy Specimen after Exposure to 160°F/100% RH/4 Daily Thermal-Spikes - 7.4% Weight-Gain (100 X)

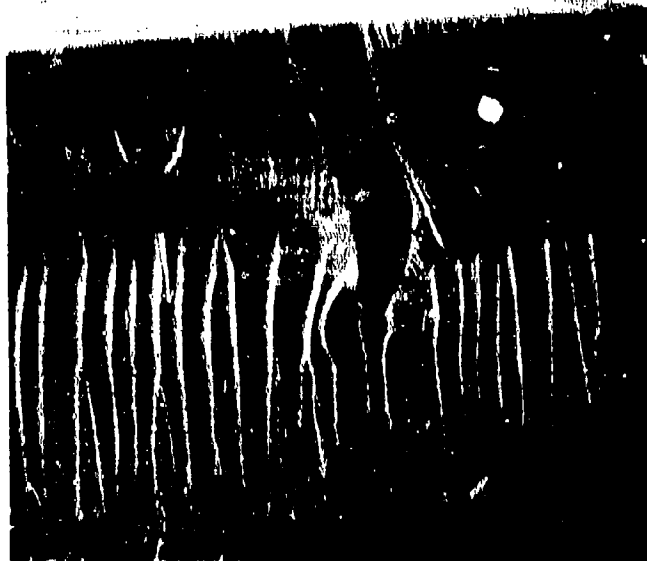


Figure 47. SEM of Fracture Surface of Epoxy Specimen after Exposure to 160°F/100% RH/4 Daily Thermal-Spikes - 7.4% Weight-Gain (200 X)

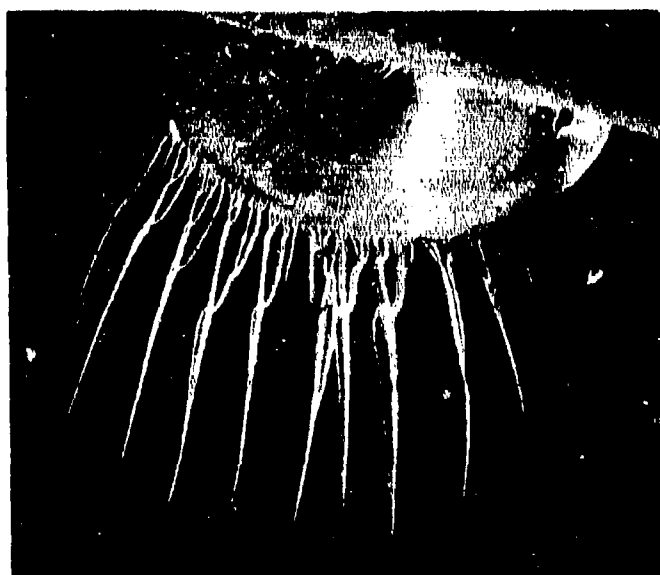


Figure 48. SEM of Fracture Surface of Epoxy Specimen after Exposure to 160°F/100% RH/4 Daily Thermal-Spikes - 7.4% Weight-Gain (80 X)

the perimeter or surface area of regions of differing optical contrast. Because of insufficient contrast with the actual specimens, high contrast photomicrographs of specimens were used in the Epidiascope attachment. Figure 49, with the lesser amount of cracks, had an associated weight-gain of 7.4% while Figure 50 had a weight-gain of 8.3%. The Quantimet reading on the 7.4% specimen showed surface cracks accounted for 4% of the surface area while the 8.3% specimen had 19.6% of its surface covered with cracks. If the shapes of these cracks were loosely assumed to be rectangular voids then one could crudely estimate the crack volume by multiplying the surface area by the crack depth. Using the crack depth of 0.4 cm found in the SEM study, crack volumes of 0.68 cm^3 and 3.34 cm^3 were calculated for the 7.4% and 8.3% weight-gain specimens, respectively. The ratio of these two values shows that sufficient cracks and fissures are present to account for the additional amounts of water.

It was also observed during this study that no significant differences in weight-gains between the spiked and nonspiked specimens are apparent until a weight-gain on the order of 1.5 to 2.0% had been attained. This can be seen in Figure 37 and by comparing Figures 38 and 39. By referring to the T_g versus weight-gain plot in Figure 60, it can be seen that this 1.5 to 2.0% weight-gain coincides with a lowering of the resins T_g below the spiking temperature. In other words, once the plasticized resin's T_g is below the spike temperature there is a substantial increase in the rate of moisture pick-up (Figure 37). This is possible because the lower T_g resin is a "softer" medium for water to diffuse through and can more easily deform or undergo viscous flow to accommodate the water than its higher T_g counterpart. It is also likely that microcracking is occurring simultaneously with the T_g lowering and also contributing to the increased rate of moisture pick-up.

e. Swelling

Another consequence of the moisture absorption process is that the specimen undergoes swelling to accommodate the water. Figure 51 shows a plot of specimen thickness increase vs. percent water absorbed.

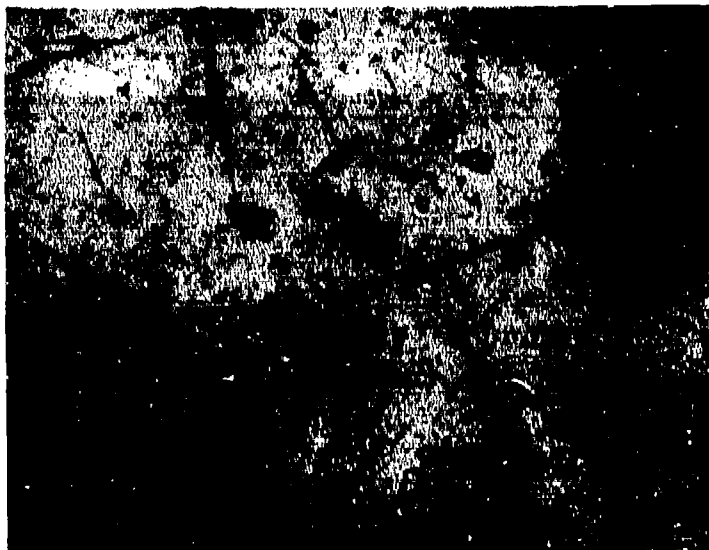


Figure 49. Photomicrograph of Epoxy Surface after Exposure to 160°F/100% RH/4 Daily Thermal-Spikes - 7.4% Weight-Gain

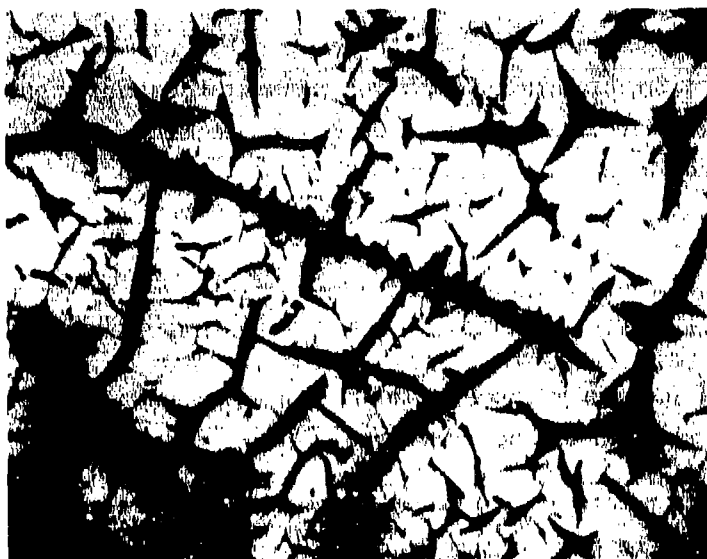


Figure 50. Photomicrograph of Epoxy Surface after Exposure to 160°F/100% RH/4 Daily Thermal-Spikes - 8.3% Weight-Gain

For the case of humidity-only exposures (160°F/100% RH) the thickness increase is linear with absorbed moisture until M_{∞} (5.6%) is reached. Above M_{∞} the thickness increase is greater than linearity which is believed to be the consequence of crack formation.

Data are also shown in Figure 51 for specimens which had received one daily thermal-spike in addition to constant temperature and humidity (160°F/100% RH). As previously noted, once the weight-gain reaches 1.5 to 2.0% the spiked specimens show increased moisture weight-gains. In the same weight-gain range, thermal-spiked specimens also exhibit a substantially larger rate of thickness increase. These very large increases in thickness to levels significantly higher than those for humidity only, M_{∞} levels, is due to microcracking as previously discussed. To further illustrate, specimens which had increased in thickness by 4.6% at a weight-gain of 8.4% were dried at 200°F under vacuum to constant weight. After drying, these specimens still had a residual thickness increase of 1.75%, which can be attributed to cracks and fissures in the specimen.

The effects of both the constant temperature/humidity environment and the thermal-spike environment on various mechanical properties will be discussed in the next section. To sum up the results of this phase of the investigation, the following have been determined:

- 1) The moisture absorption and transmission can be treated according to Fick's Second Law.
- 2) An accurate picture of the moisture concentration profile within the material can be determined.
- 3) As a result of the moisture concentration gradients, stress gradients will be present through the thickness of the material.
- 4) Real-life environments dramatically affect the moisture pick-up process.

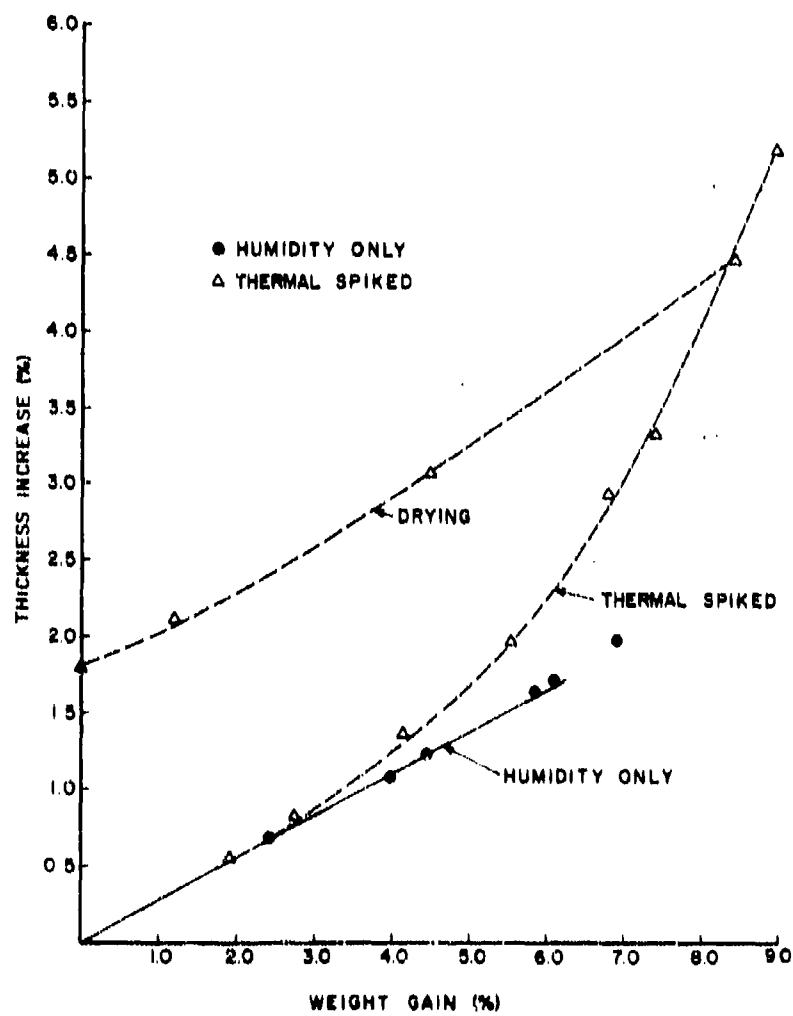


Figure 51. Thickness Increase as a Function of Moisture Absorption

- 5) The thermal-spike in the real-life cycle is the most important factor causing increased moisture pick-up.
- 6) Weight-gains exceeding the equilibrium amounts can be attributed to microcracking of the resin.
- 7) Increased weight-gains due to thermal-spiking occur when the T_g of the system is below the spike temperature.
- 8) There is a concurrent swelling due to moisture absorption.
- 9) Thermal-spikes accelerate the microcracking and swelling processes.

3. GLASS TRANSITION TEMPERATURE STUDIES

a. Background

The glass transition temperature, T_g , is one of the most important characteristic parameters of amorphous polymers such as the epoxies. Below T_g the polymer behaves like a "glassy" solid (e.g., high modulus) and above T_g it behaves like a "rubbery" material (e.g., relatively low modulus). In other words, T_g represents a temperature where the polymer is undergoing a significant, rapid change in physical properties. In actuality, the T_g occurs over a narrow temperature range of about 10-20°F rather than at a sharp temperature such as might be associated with the melting of ice.

One method of determining T_g is to examine the relaxation modulus (E_r) behavior of the polymer. The modulus vs. temperature curve shown in Figure 52 is typical for a viscoelastic, cross-linked amorphous polymer. At lower temperatures, Region (1), the polymer exhibits mechanical behavior described as "glassy" and is hard and brittle with E_r being on the order of 10^{10} dynes/cm². At higher temperatures, in Region (2), the transition region, the modulus varies between 10^{10} and 10^6 dynes/cm². The physical properties in Region (2) are described as "leathery". At still higher temperatures, Region (3), the polymer's

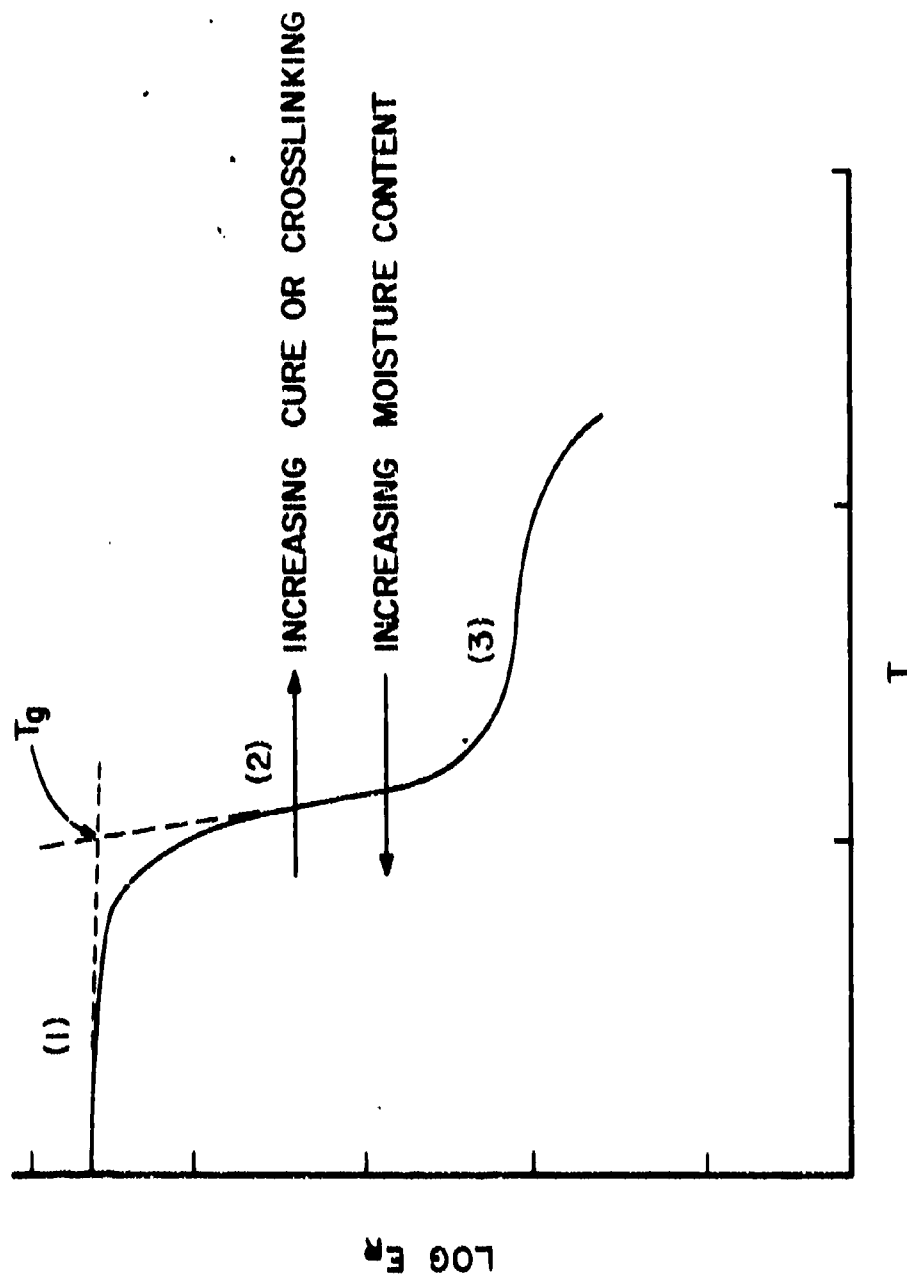


Figure 52. Modulus vs. Temperature Curve for Typical Visco-Elastic Cross-Linked Amorphous Polymer

modulus remains constant, about 10^6 dynes/cm². This region is termed the rubbery plateau and the physical properties of the polymer are described as "rubbery" in this region.

The T_g is obtained from the modulus vs. temperature curves by extrapolating the linear parts of the glassy region and transition region moduli as shown in Figure 52. The point of intersection is taken as the T_g .

There are several other methods of determining T_g . One method entails measuring the specific volume, \bar{V} , of the polymer as a function of temperature. Such measurements yield plots similar to the one shown in Figure 53. The temperature at which the break in the curve occurs is defined as the T_g . Below T_g the free volume (total macroscopic volume less the molecular volume of the polymer molecules) of the polymer is relatively small and the polymer segments of the molecules are only capable of local type motions. Above T_g there is an increase in the free volume with the result that the polymer molecules are capable of long-range type motions.

There are several factors which can affect the T_g of a polymer, but the one of prime interest is associated with changes arising from the absorption of water into the cured epoxy structure. It is an accepted theory (Reference 18) that at and below the T_g , 1/40 of the total volume of the material is free volume (total volume less molecular volume). If this is true, then the T_g can be altered by changing the polymer's free volume at a given temperature. If a polymer were mixed with a miscible liquid that contains more free volume than the pure polymer, then the T_g will be lowered. In particular, if it is further assumed that the free volumes are additive, then the polymer-diluent mixture will contain more free volume at a given temperature than would the polymer alone. As a result, plasticized polymers must be cooled to a lower temperature in order to reduce their free volume to 1/40 of the total volume of the polymer-diluent combination. This is the process which is proposed to occur when moisture is absorbed into an epoxy resin.

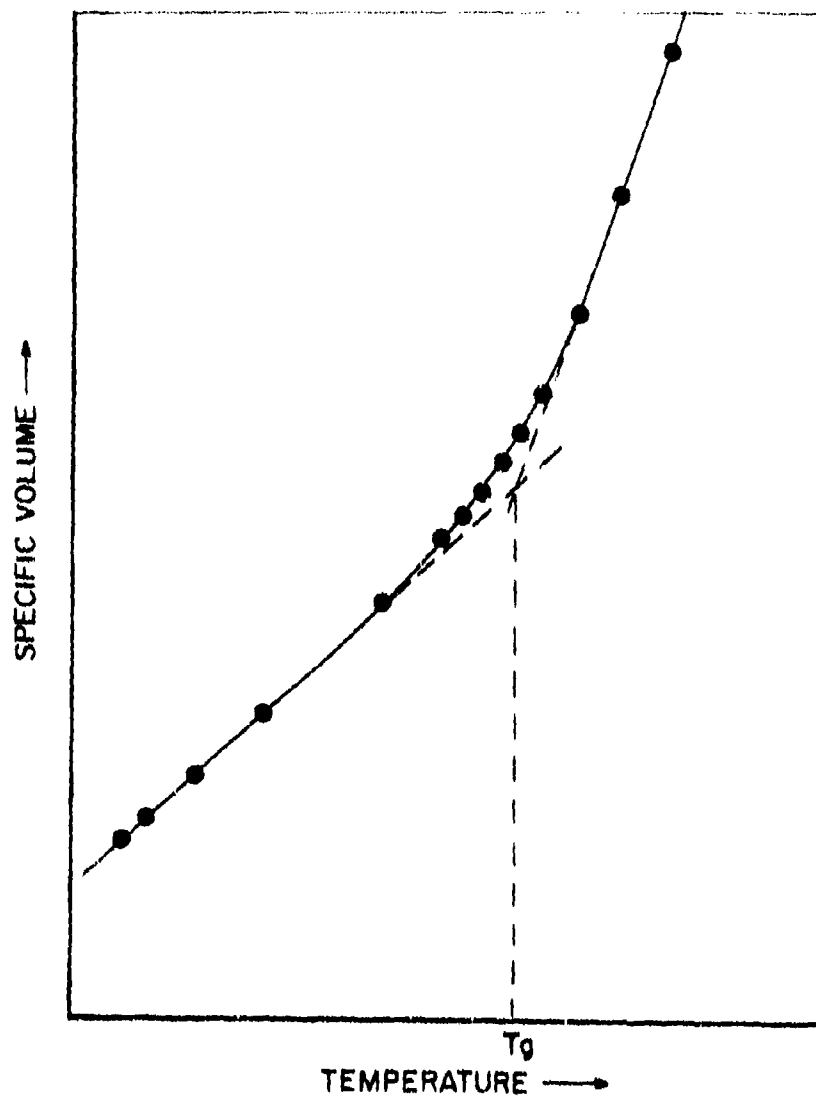


Figure 53. T_g Measurement from Specific Volume vs. Temperature Plot

Based on the above assumptions, Bueche and Kelley (Reference 30) derived the following expression for the T_g of a plasticized system (polymer + diluent):

$$T_g = \frac{\alpha_p V_p T_{gp} + \alpha_d (1 - V_p) T_{gd}}{\alpha_p V_p + \alpha_d (1 - V_p)} \quad (21)$$

where,

T_{gp} = T_g of the polymer

T_{gd} = T_g of the diluent

α_p = polymer expansion coefficient

α_d = diluent expansion coefficient

V_p = volume fraction of polymer

In terms of the percent weight-gain in the polymer, M ,

$$V_p = \frac{1}{1 + \rho_p / \rho_d [(0.01) M]} \quad (22)$$

where ρ_p and ρ_d are the densities of the polymer and diluent, respectively.

b. Experimental

Several experimental techniques were considered for performing the T_g measurements with one of the most important criterion being that those specimens evaluated after moisture absorption not be "dried-out" by the test. For this reason, techniques such as differential scanning calorimetry (DSC) and thermomechanical analysis (TMA) which use very small samples were ruled out. The technique which was selected for making T_g measurements was the heat distortion temperature (HDT) test.

This test is diagrammatically illustrated in Figure 54. A stress of 264 psi is applied to a specimen measuring 5.0 in. long by 0.5 in. thick

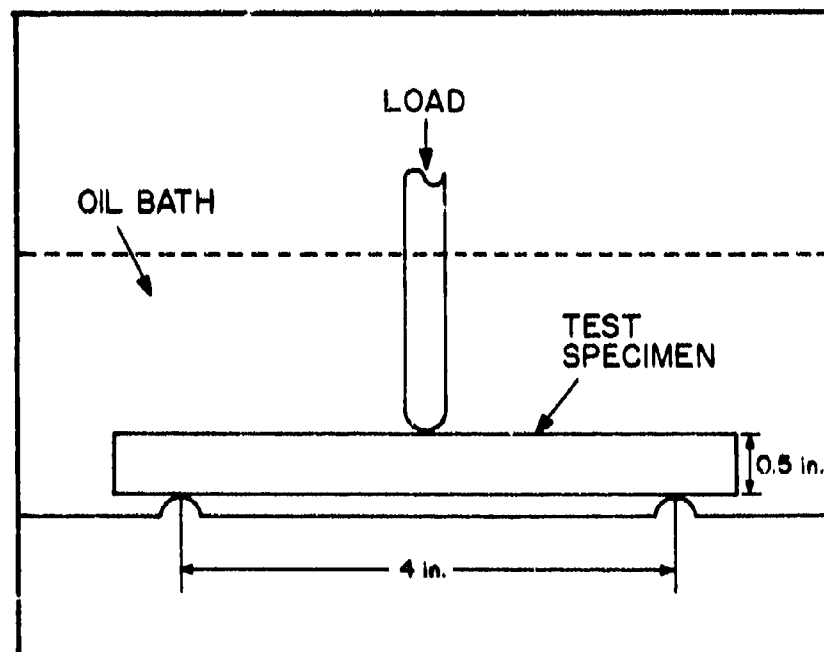


Figure 54. Diagram of HDT Test Apparatus

by 0.125 in. wide. A constant heat-up rate of 2°C per minute is maintained. The large size of the specimen and the presence of the oil bath were expected to minimize water loss during testing. This was confirmed by post-test measurements which yielded weight losses less than 10% of pre-test water weight-gain.

Measurements were made of temperature and specimen deflection for various water weight-gains (W.G.) during this test and these data are plotted to yield the type of plot shown in Figure 55. The curve is analogous to those for \bar{V} vs. T and E_p vs. T . The point at which the extrapolations of the linear portions of the two regions of the curve intersect is taken as the T_g . The HDT procedure yielded T_g 's identical to those obtained using the TMA and DSC technique for "dry" control specimens. Individual HDT curves for the various environmental exposure conditions are shown in Appendix A.

c. Results and Discussion

The effect of moisture on the T_g of this epoxy resin can be seen by referring to the HDT curves in Appendix A. A dry, control T_g of 177°C (350°F) was determined. With increasing moisture absorption there is a proportional shift in T_g to lower values. This behavior is illustrated in Figure 56 for dry, 3% and 5.7% weight-gain specimens after 160°F/100% RH exposures. Figure 57 shows curves for dry, 3.16% and 4.32% weight-gain specimens after 180°F/75% RH exposures. The T_g values from these HDT curves were plotted as a function of weight percent water content for absorption at 100% RH (Figure 58) and 75% RH (Figure 59). There is a gradual lowering of T_g until the equilibrium moisture content associated with the particular humidity condition is reached, whereupon there is no further lowering of the T_g . This is further evidence to support the contention that microcracking is responsible for weight-gains greater than equilibrium values. If the additional water were being physically absorbed there would have been a further decrease in T_g .

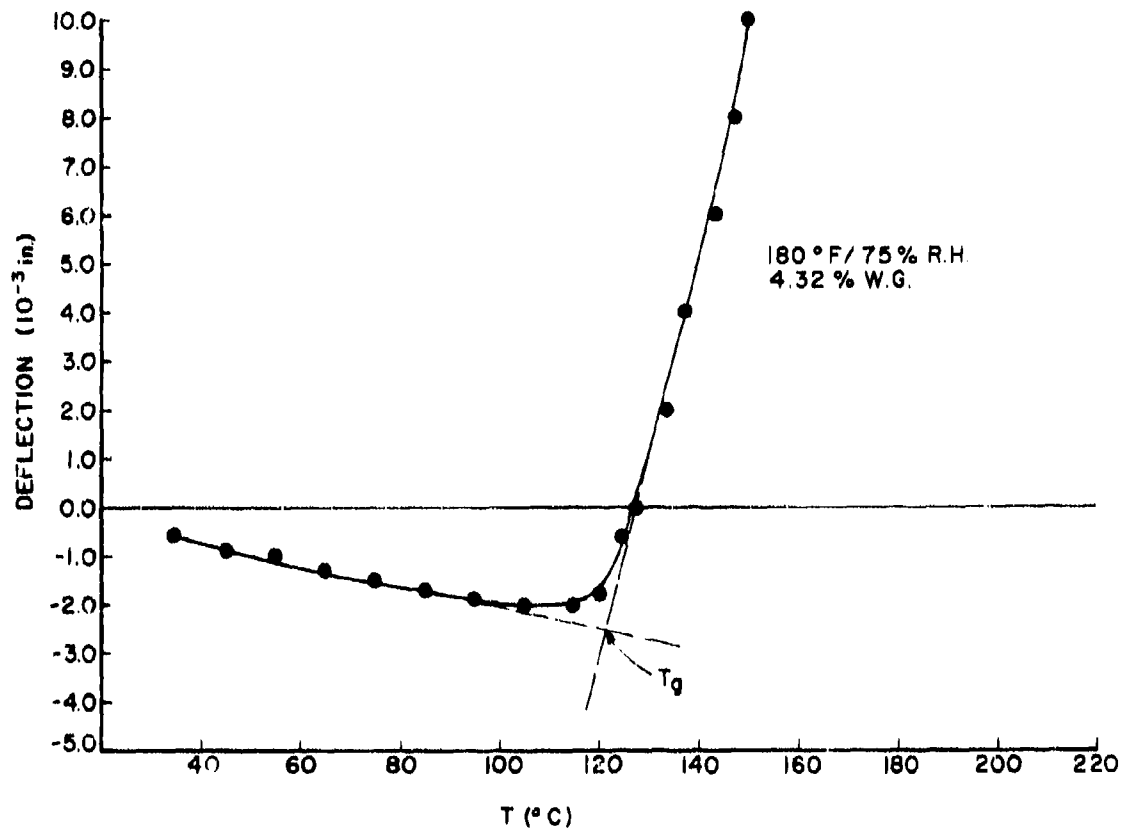


Figure 55. T_g Determination from HDT Test

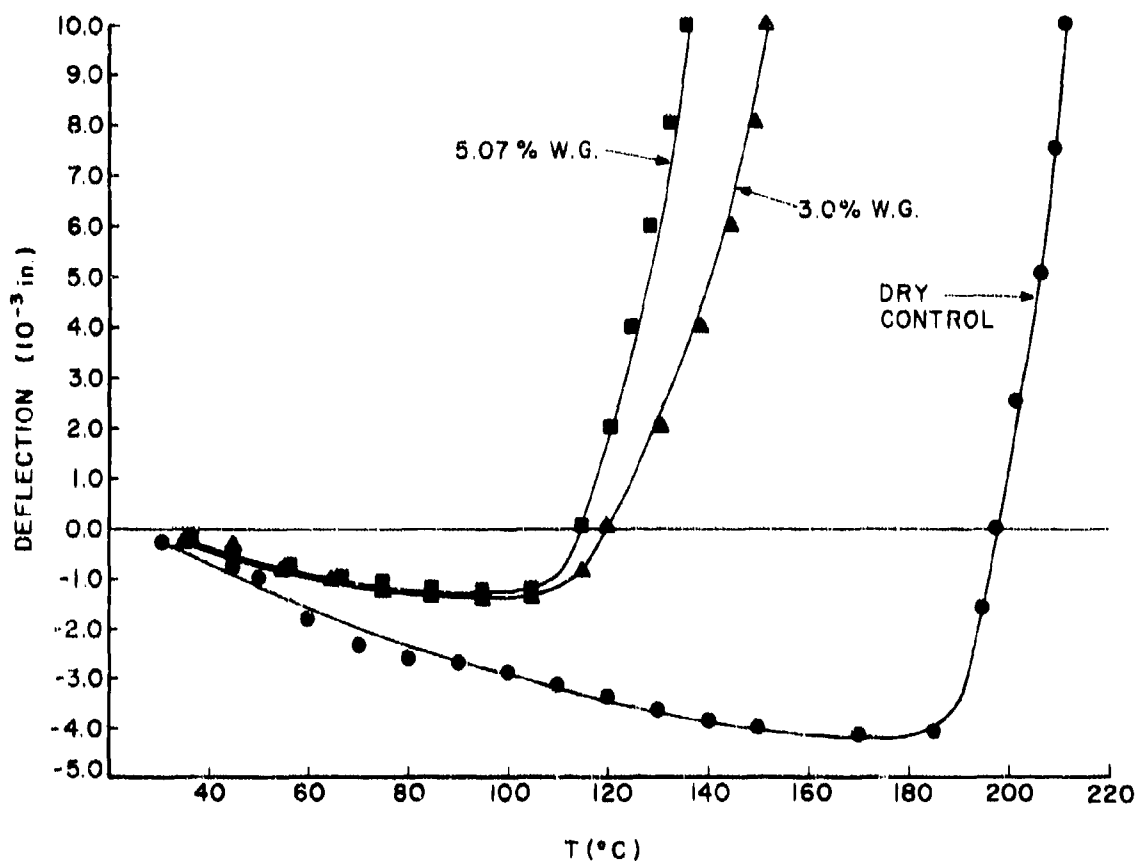


Figure 56. HDT Curves as a Function of Absorbed Moisture -
160°F/100% RH

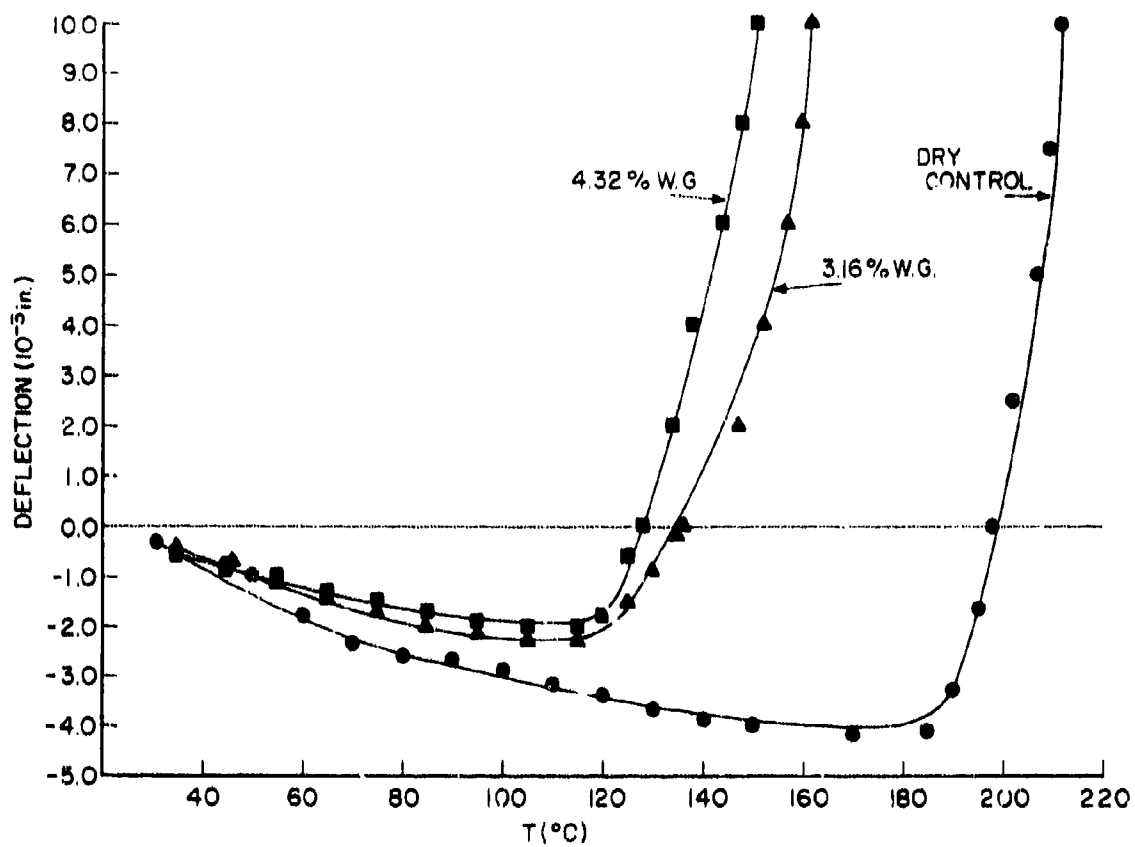


Figure 57. HDT Curves as a Function of Absorbed Moisture for 180°F/75% RH Exposure

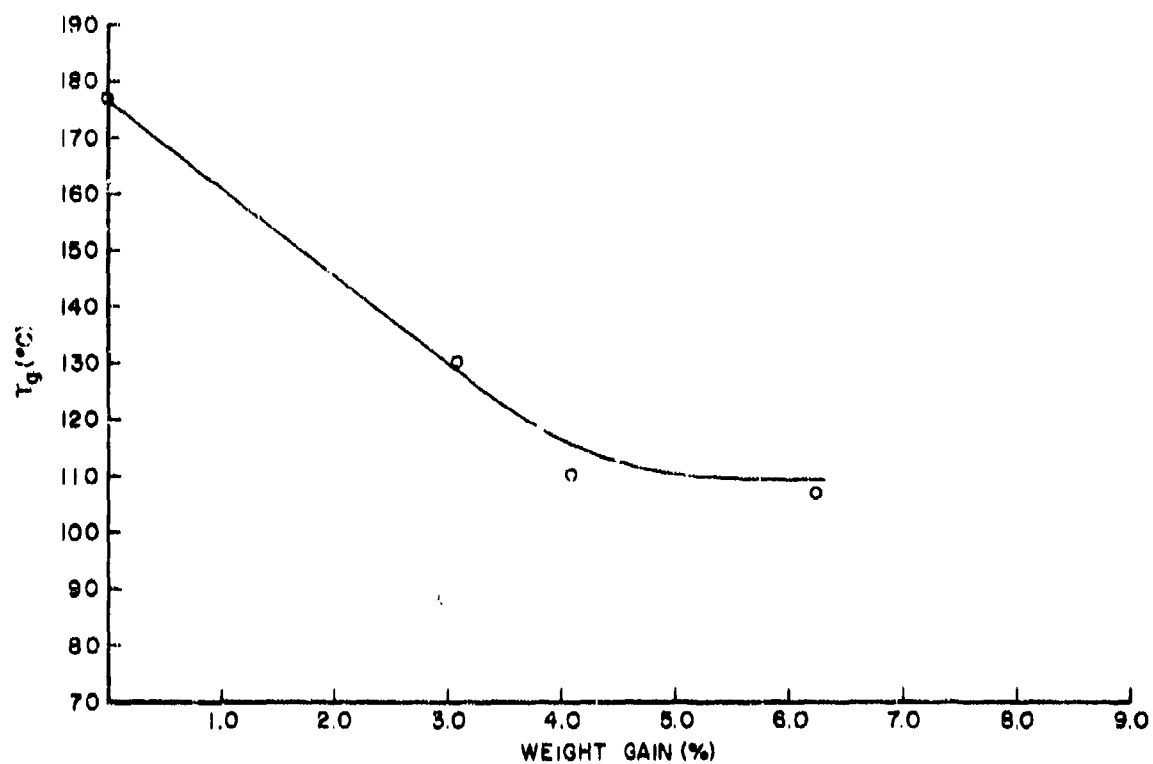


Figure 58. T_g as a Function of Absorbed Moisture for 10% RH Exposure

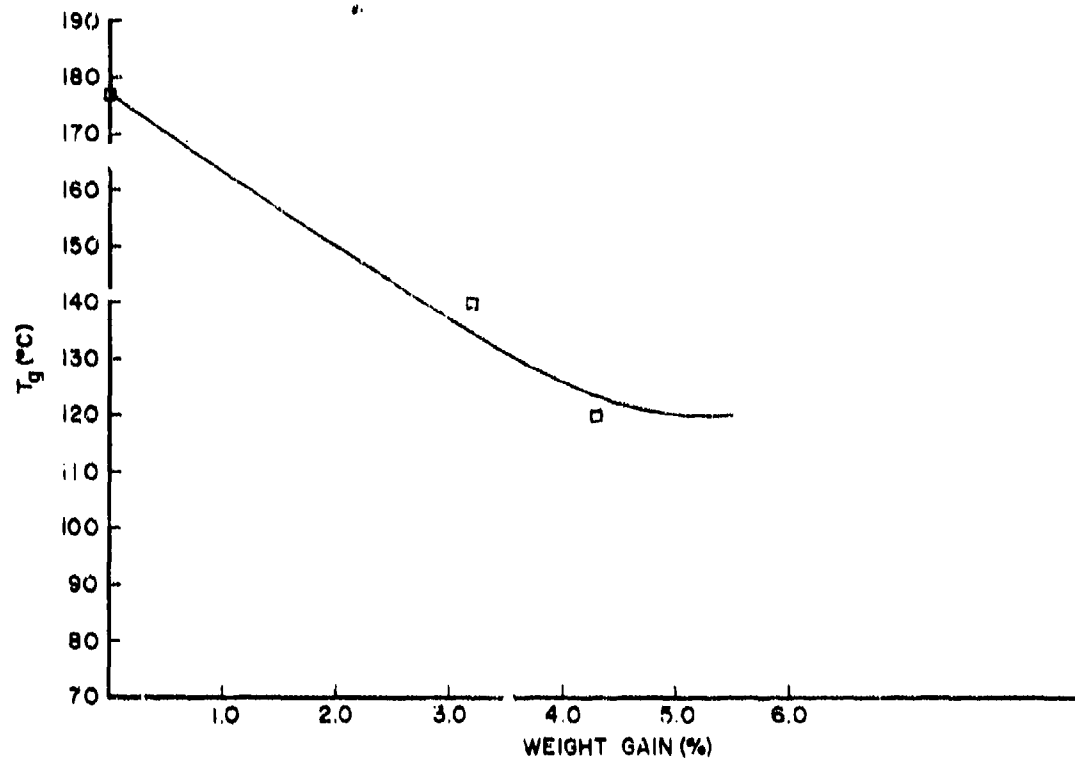


Figure 59. T_g as a Function of Absorbed Moisture for 75% RH Exposure

It is worthwhile to note that when measurements are being made of T_g vs. water weight-gains, nonuniform moisture distributions will be present in the specimens until an equilibrium moisture content is achieved. These nonuniformities would influence the experimental results in a manner dependent on the particular experimental technique being employed. Therefore, to meaningfully apply a quantitative relationship such as that of Bueche and Kelley, it is important to have a uniform, equilibrium distribution of moisture in the test specimens.

The T_g values for equilibrium moisture contents were combined to produce a plot of T_g vs. equilibrium weight percent water (Figure 60). As noted, when the condition of equilibrium distribution of diluent is achieved, one can apply the Bueche-Kelley relationship (Equation 21) to arrive at a theoretical prediction of the effect of absorbed moisture on the T_g of the polymer. The theoretical curve, shown in Figure 60 for comparison with the experimental data points, was derived from the following parameters:

$$\begin{aligned}\alpha_p &= 3.78 \times 10^{-4}/^{\circ}\text{C} \\ \alpha_d &= 4 \times 10^{-3}/^{\circ}\text{C}, T_{gd} = 4^{\circ}\text{C} \\ \rho_p &= 1.28 \text{ g/cm}^3, \rho_d = 1.0 \text{ g/cm}^3\end{aligned}$$

The 75% RH and 100% RH data points for the effect of equilibrium moisture absorption on T_g are in accord with the Bueche-Kelley relationship.

A plot of T_g vs. moisture weight-gain was also made for specimens which had received a daily thermal-spike in addition to exposure to 160°F and 100% RH (Figures 61 and 62). The behavior observed is quite similar to that for the constant 160°F/100% condition. This indicates that the thermal-spike is not generating any effects on the T_g in addition to those observed for the humidity only condition. The exceptionally large weight-gains of these tests can be attributed to microcracking as was previously discussed. The presence of microcracks would not alter the T_g of the resin but could influence the results of the particular test method.

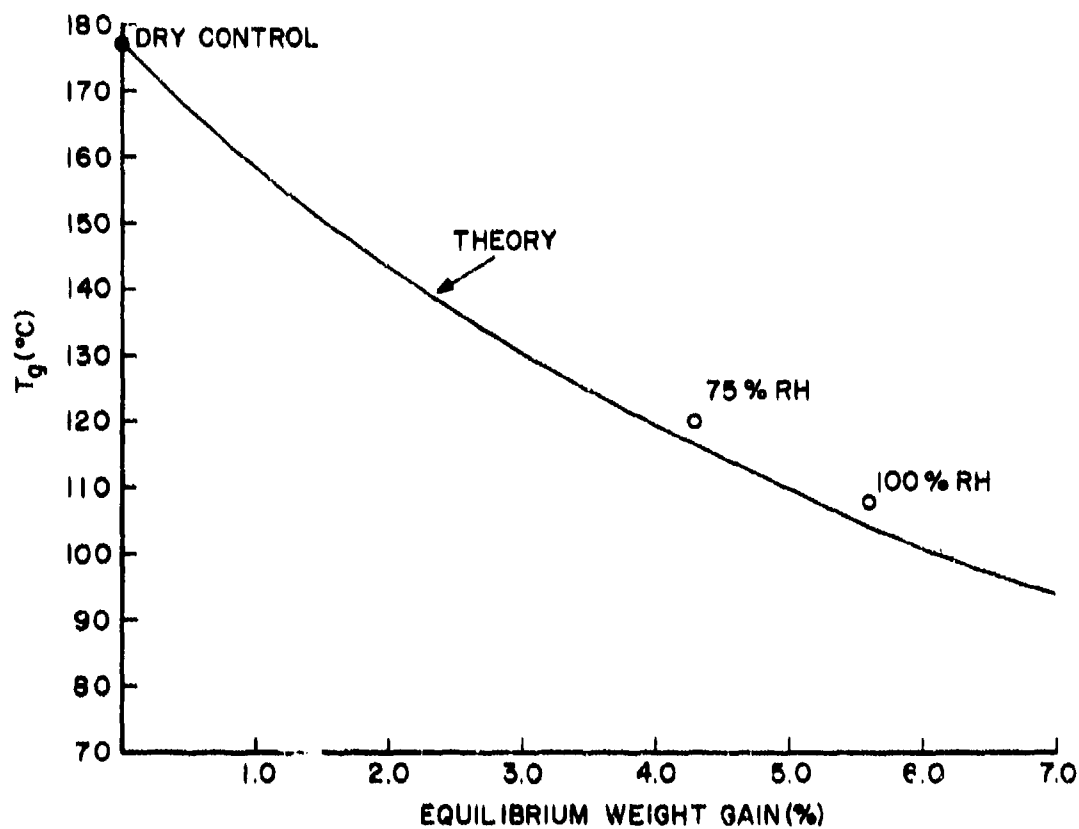


Figure 60. T_g vs. Equilibrium Weight-Gain

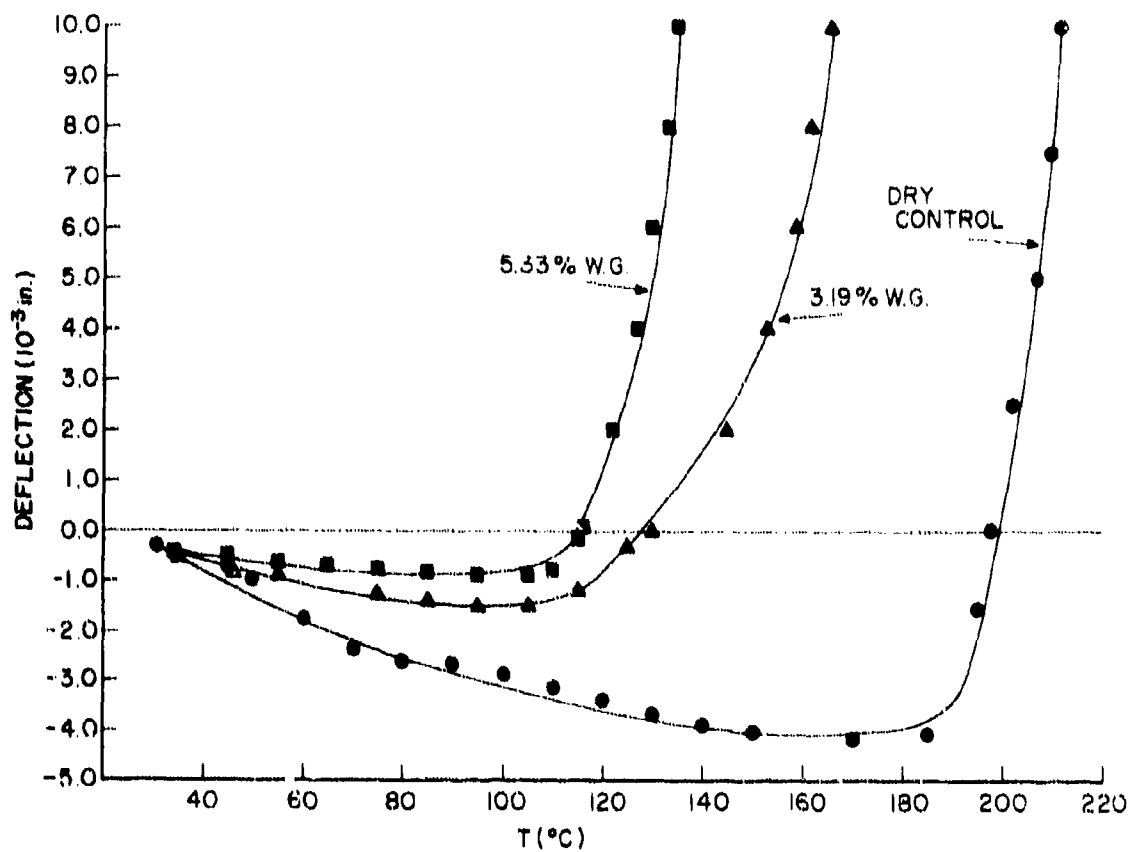


Figure 61. HDT Curves as a Function of Absorbed Moisture for 160°F/100% RH/1 Daily Thermal-Spike Exposure

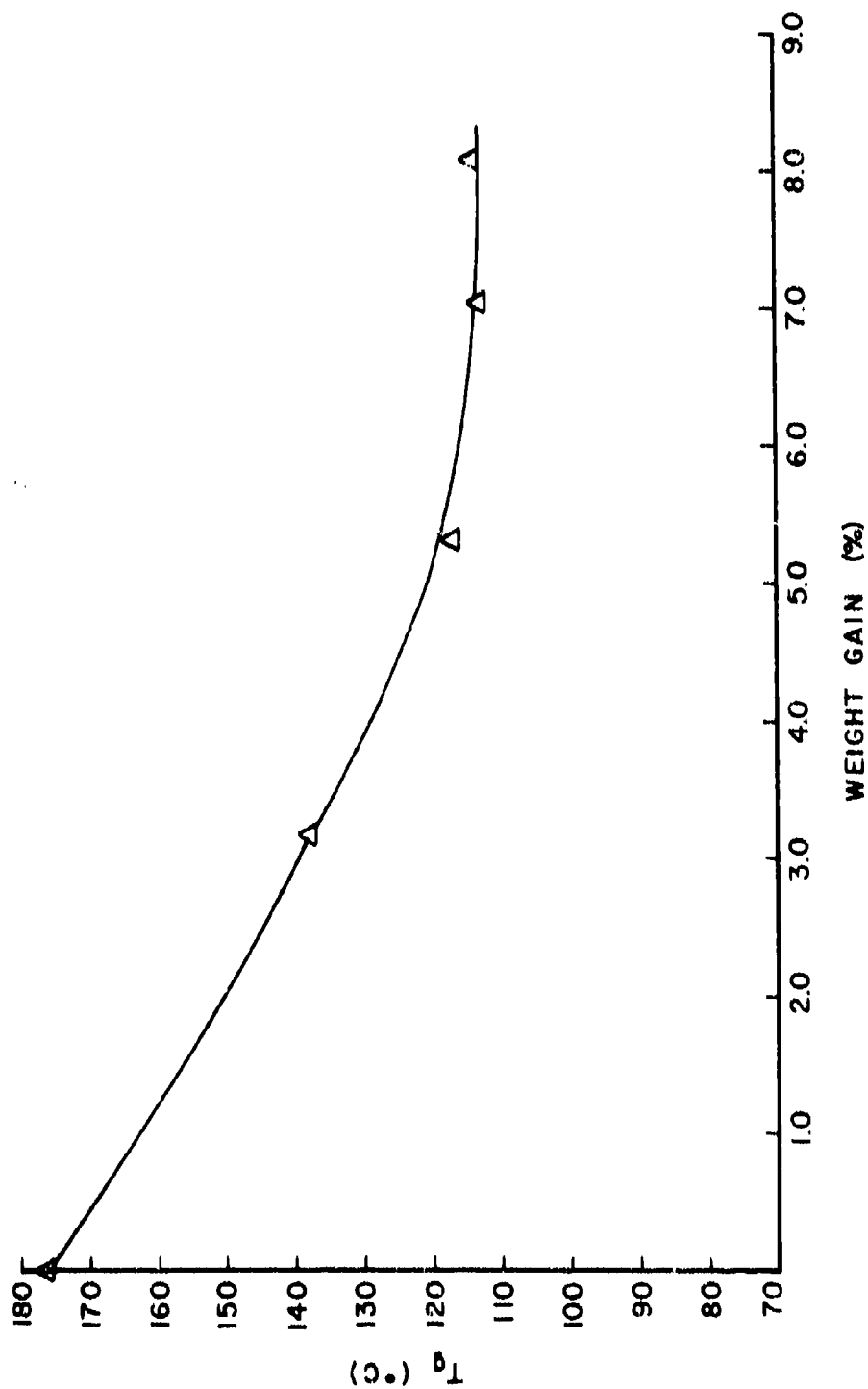


Figure 62. T_g as a Function of Absorbed Moisture for 160°F/100% RH/1 Daily Thermal-Spike Exposure

The results of this phase of the investigation indicate that among its possible deleterious effects, water behaves as a classical plasticizer, i.e., it lowers the T_g of the epoxy as a function of the amount absorbed. This phenomenon would also manifest itself in other concurrent effects such as swelling (see discussion in diffusion section) and shifting the E_r curves to lower temperatures (Figure 52) or, equivalently, to shorter times since the polymer is viscoelastic. Changes in T_g would also result in changes in any other time-temperature dependent mechanical properties such as those determined in constant strain rate tensile testing which will be discussed in the next section.

4. STRESS-STRAIN STUDIES

This section will consider the stress-strain behavior of the resin material under conventional constant strain-rate and dynamic conditions as well as stresses which are induced as a result of moisture gradients, combined moisture-temperature gradients, or further chemical reaction in the resin.

a. Tensile Tests

The first series of tests performed were tensile moduli determinations. These were done to determine the effect of absorbed moisture on the stress-strain behavior of the matrix. Both constant strain-rate and dynamic mechanical measurements were made.

Constant strain-rate tests were performed using "dog-boned" tensile specimens (Figure 63). Tests were run on a conventional Instron Test Machine using a strain-rate of 0.05 inches per minute.

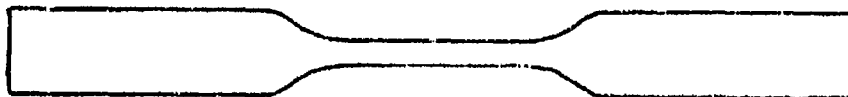


Figure 63. Constant Strain-Rate Tensile Test Coupon

Tests were performed at RT, 200, 250, and 300°F with elongation being measured with a 1-inch gage-length extensometer. The results of the dry control tests are shown in Figure 64. There is a slight decrease in modulus and a concurrent slight increase in elongation as the temperature is raised. The curves shown in Figure 65 were obtained after an equilibrium weight-gain was achieved in a 100% RH environment. The effect of moisture is extremely dramatic. At 300°F the moisture-exposed polymer has become extremely ductile with an elongation of over 20%. This compares to the dry polymer strain of 3.3% at 300°F. This is classical behavior for a plasticized polymer as was shown in Figure 52. The presence of a low molecular weight plasticizer reduces the T_g and results in a softer, more ductile matrix at temperatures lower than those of the dry polymer.

To further illustrate the plasticization phenomenon, stress relaxation curves were prepared from the constant strain rate tensile tests. Figure 66 shows the typical relaxation behavior at various temperatures for the dry polymer. Figure 67 shows the relaxation behavior at the same temperatures for wet (equilibrium weight-gain) specimens. Using linear superpositioning (Reference 18), stress relaxation master curves were prepared for both wet and dry tests as shown in Figure 68. The dramatic plasticization effect of water is clearly evident. The presence of the plasticizer has shifted the curves to smaller times.

Consider a reduced value of a response function at some temperature T and also at a reference temperature T_0 . The ratio of the time to attain the specified value of the response at temperature T to the time required at reference temperature T_0 is the shift factor a_T for any given temperature T (Figure 69). Time and temperature (or equivalently, plasticization) affect the viscoelastic response of the polymer only through the product of a_T and actual time. The relationship

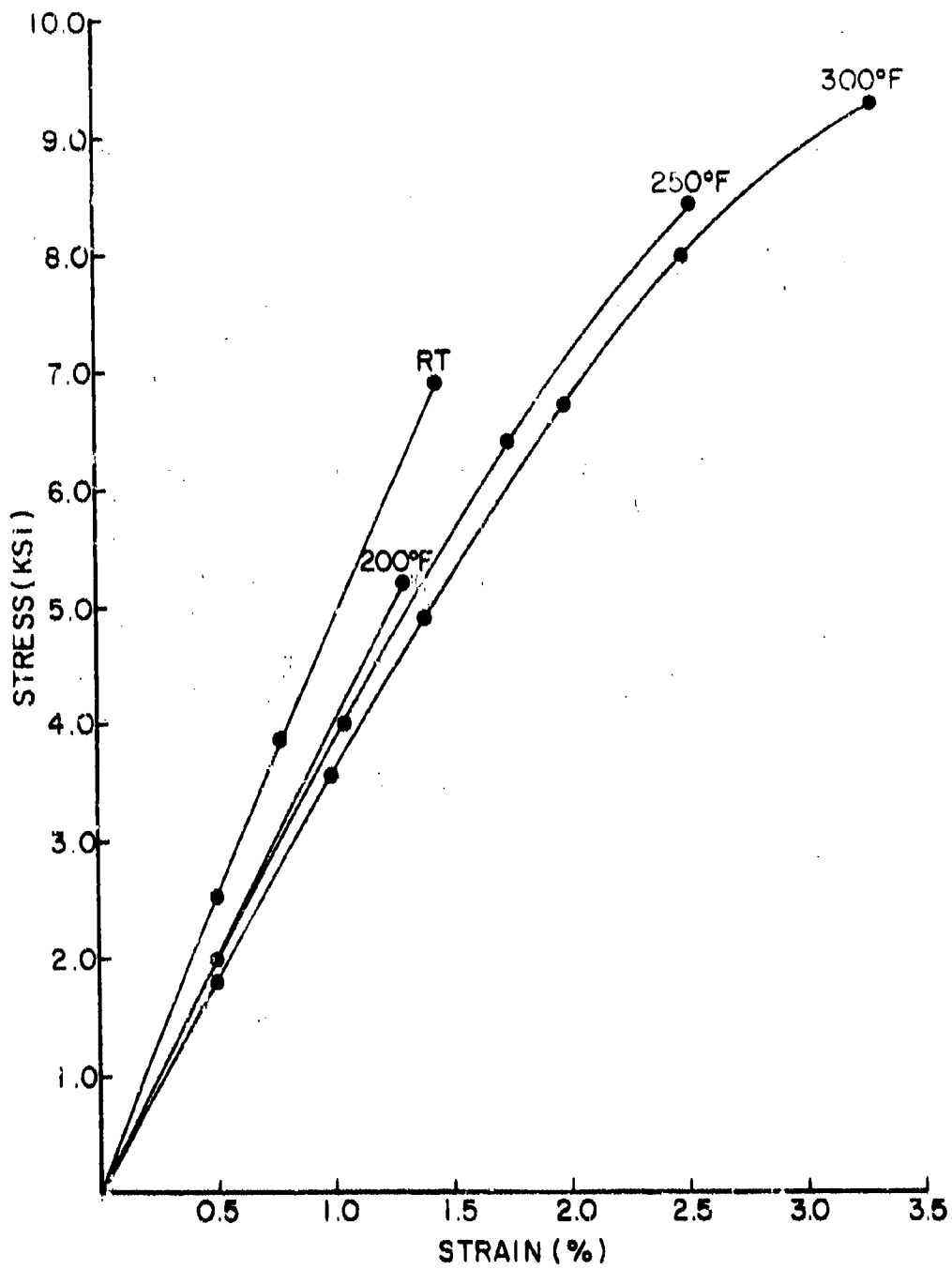


Figure 64. Stress-Strain Behavior of Dry, Control Epoxy Specimens

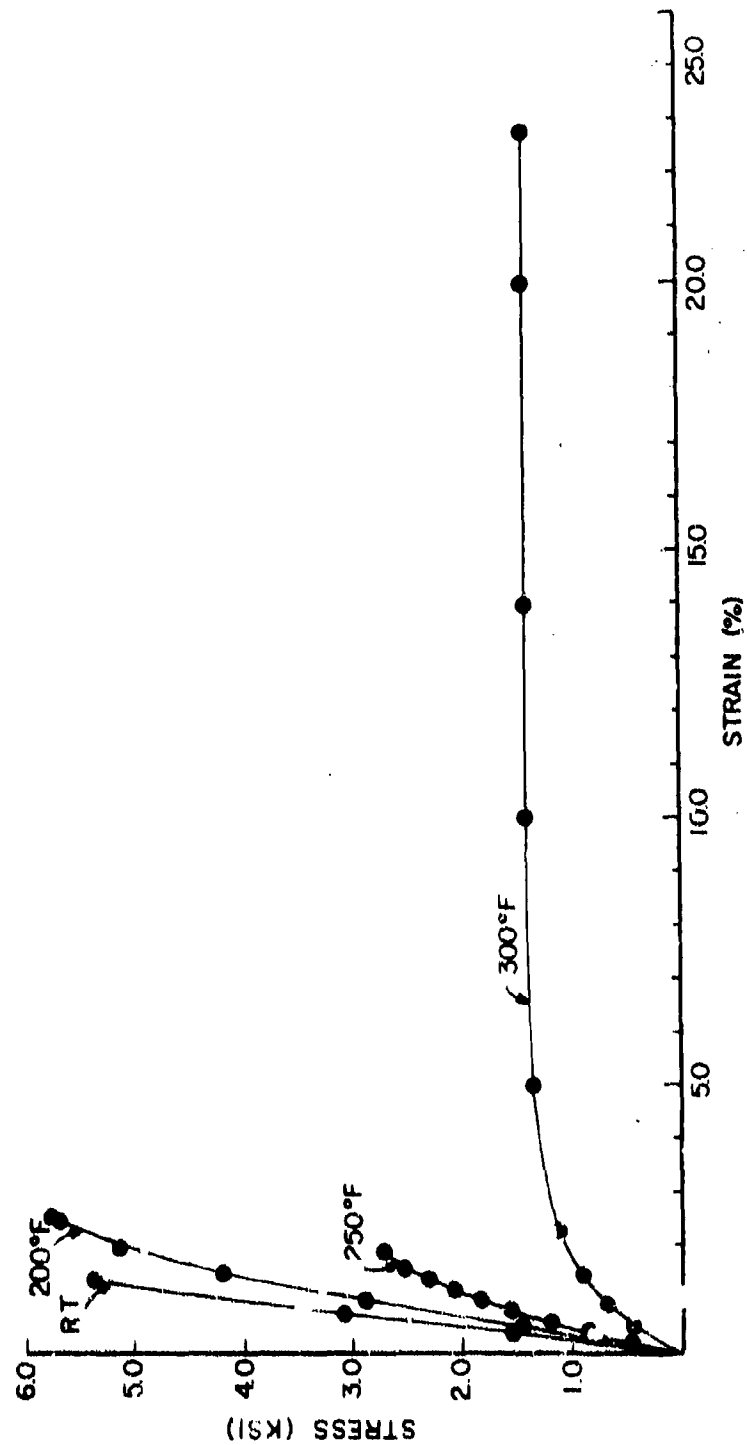


Figure 65. Stress-Strain Behavior of Wet (Equilibrium Weight-Gain) F-oxo Specimens

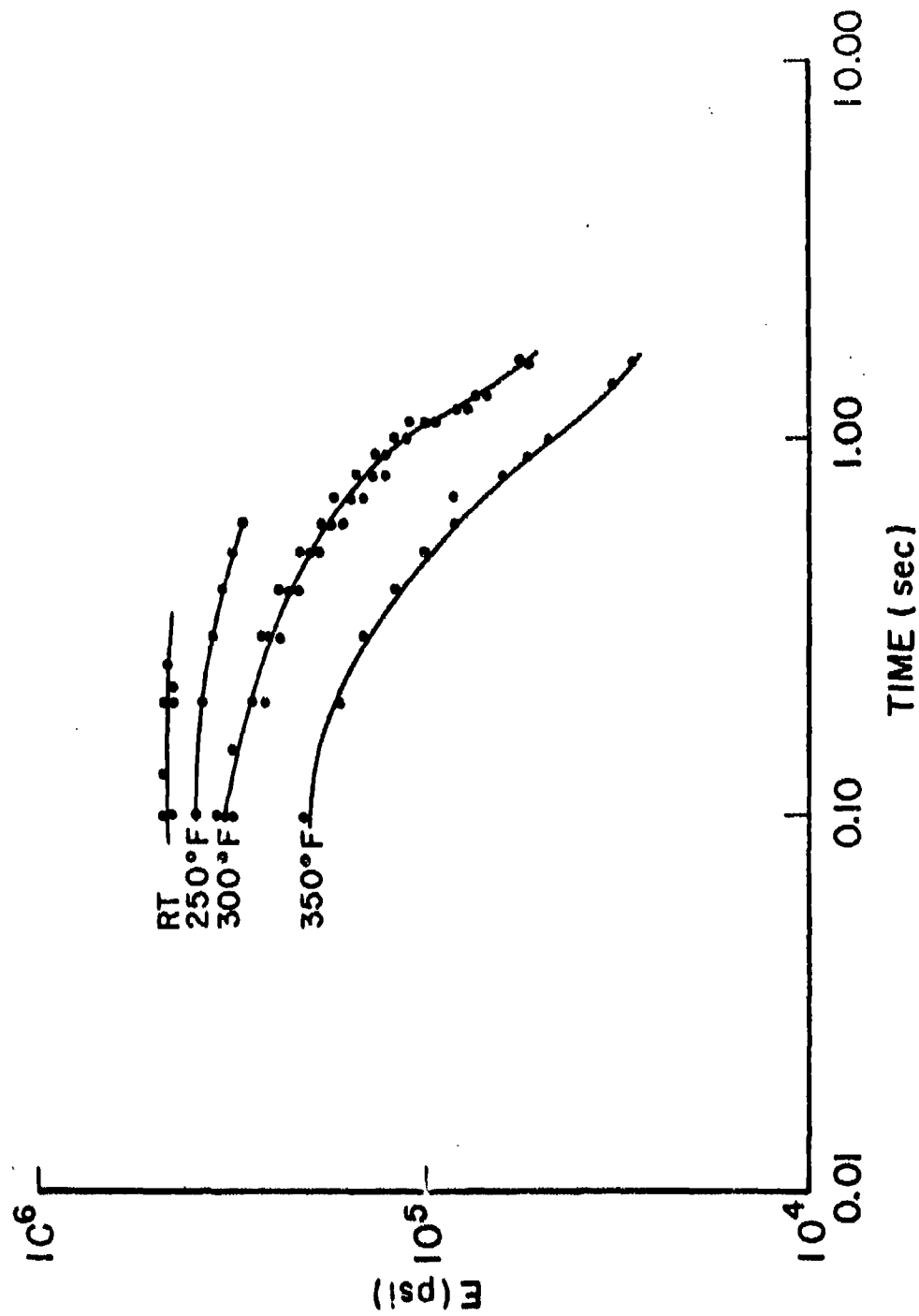


Figure 66. Relaxation Modulus as a Function of Temperature for Dry, Control Specimens

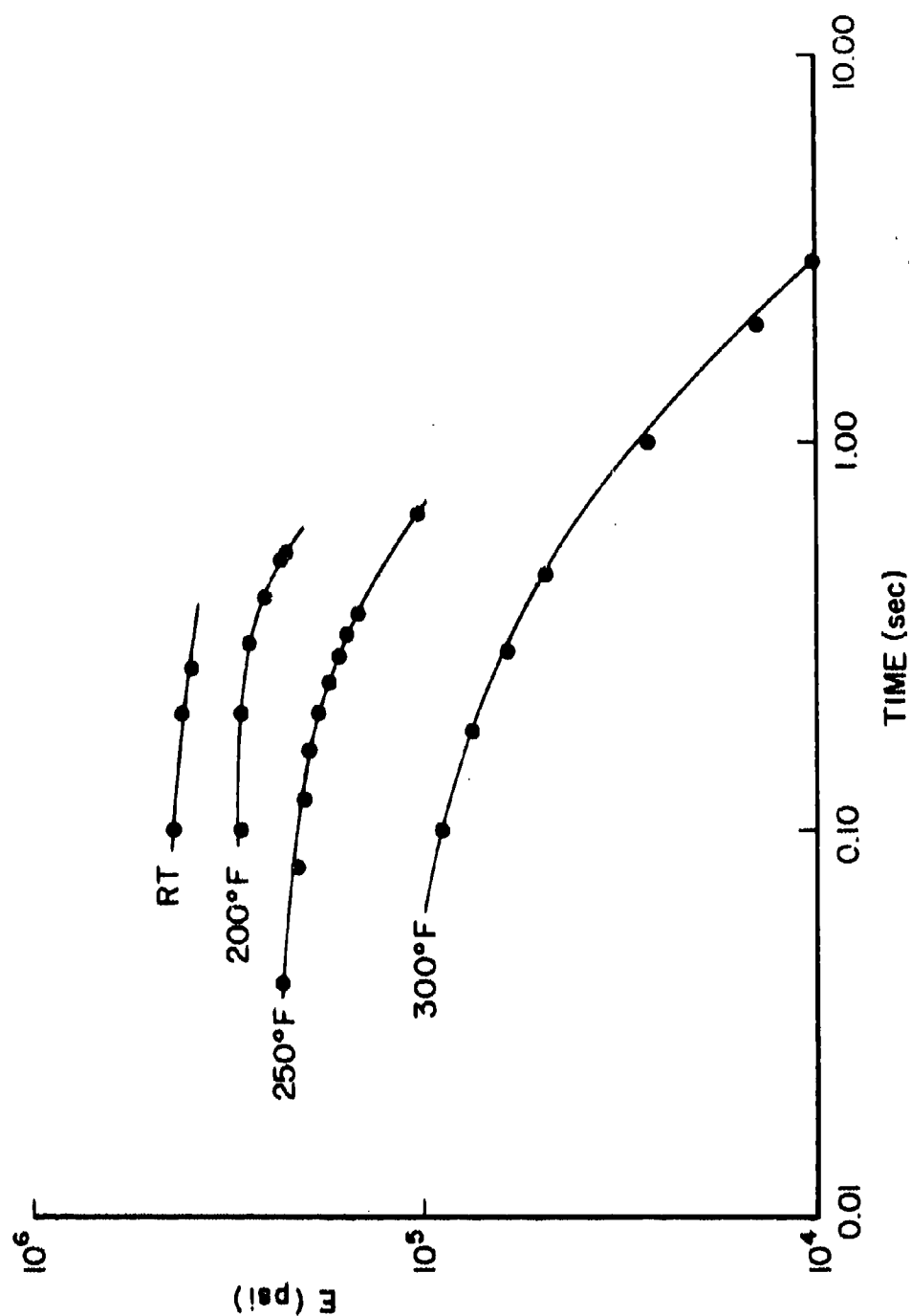


Figure 67. Relaxation Modulus as a Function of Temperature for Wet (Equilibrium Weight-Gain) Specimens

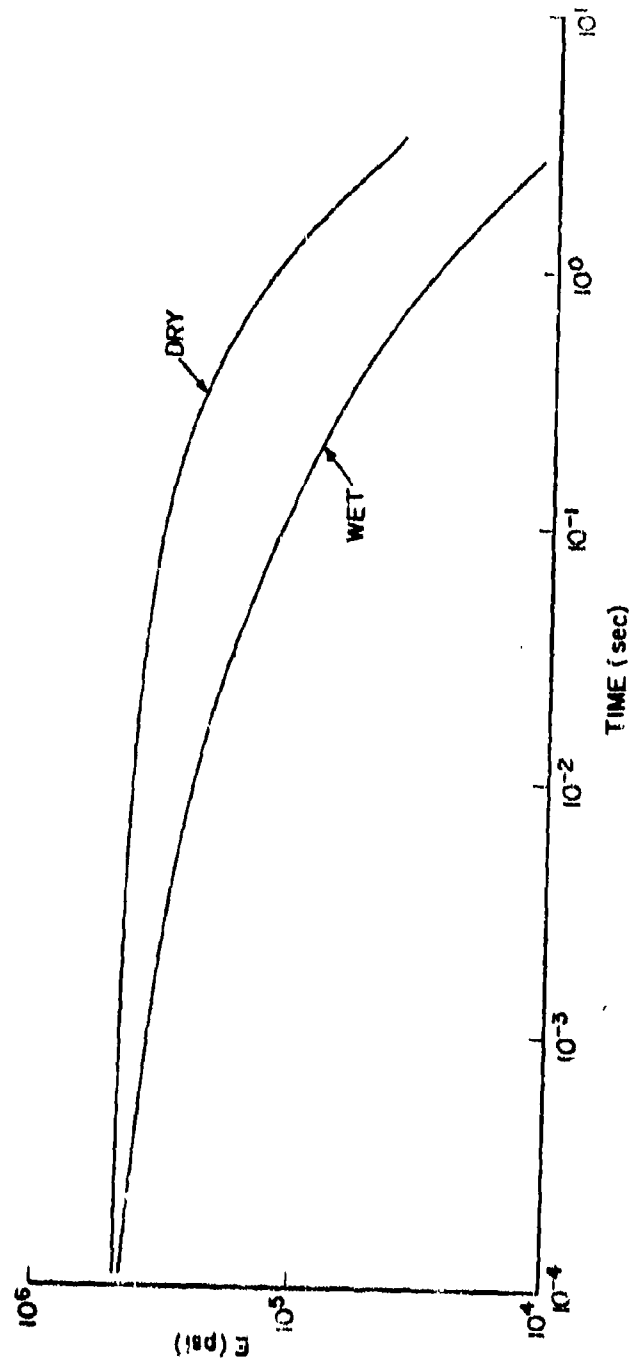


Figure 68. Relaxation Modulus Master Curves, Reference Temperature = 300°F

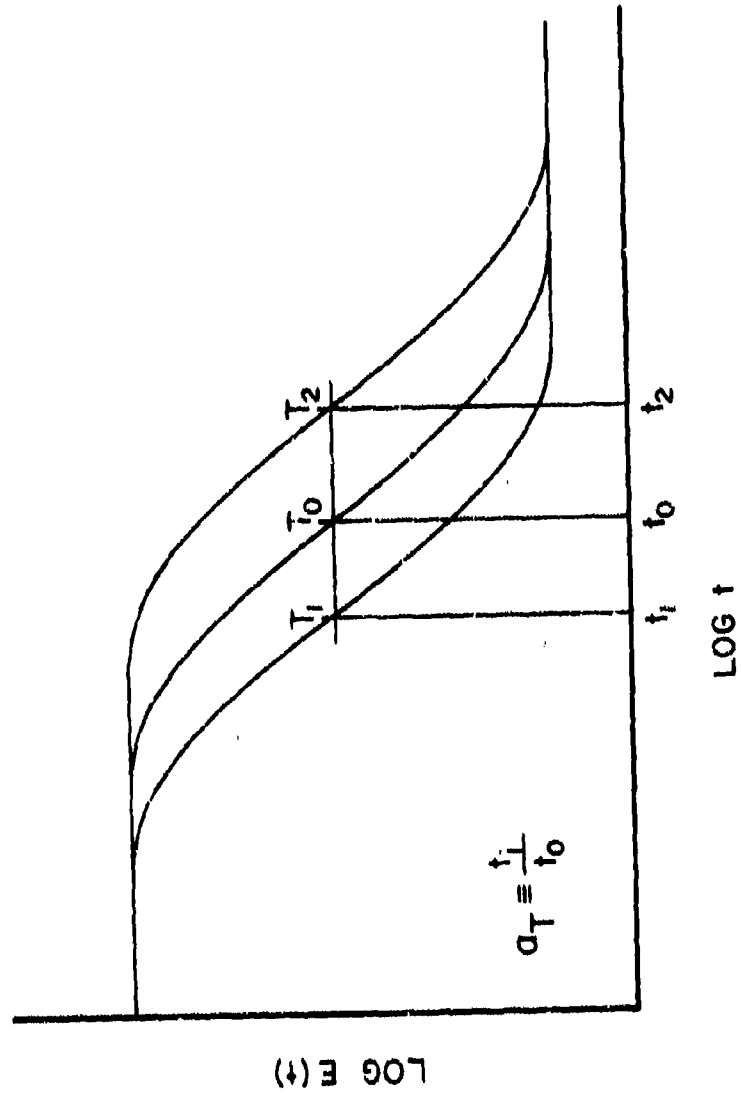


Figure 69. Determination of Shift Factor from Different Modulus - Temperature Curves

between the shift factor and temperature is given by the Williams-Landel-Ferry (WLF) (Equation 31):

$$\text{Log } a_T = \frac{C_1 (T - T_r)}{C_2 + (T - T_r)} \quad (24)$$

where C_1 and C_2 are constants and T_r is a reference temperature specific to a given polymer.

A shift factor, a_T , for the displacement of the modulus curves to lower times due to plasticization by water was determined from the master curves in Figure 68. A value of $\tan \delta$ was thus determined, which means that the same response will be exhibited ten times faster by the "wet" specimen than the "dry" specimen.

Dynamic mechanical measurements were performed on a Rheovibron Dynamic Viscoelastometer. A film sample measuring approximately 0.125 in. x 2.0 in. x 0.008 in. was subjected to an oscillating load (11 cps) while being heated from -150 to +250°C at a constant heating rate of 3°C per minute.

Dynamic (oscillatory) measurements give rise to dynamic moduli which are complex numbers. In this case, the complex modulus E^* is given by

$$E^* = E' + i E'' \quad (24)$$

where E' and E'' are the real (elastic or storage) and imaginary (viscous or loss) parts respectively of the complex modulus, E^* . The mechanical loss tangent, $\tan \delta$, is defined by the equation

$$\tan \delta = E'' / E' \quad (25)$$

The importance of these quantities lies in the fact that $\tan \delta$ reaches a maximum in the vicinity of a transition temperature where important physical changes are taking place in the resin. The real modulus, E' , is important from a design standpoint since it gives an

indication of the temperature range where the material exhibits useful load-bearing capability. In a region of a glass transition, the modulus may change by as much as a factor of a hundred. In addition, the loss modulus, E'' , maximizes in the same range as does $\tan \delta$. Any plasticization effects or other physical effects should be observable by following changes in these parameters.

The results obtained on "dry" control samples are shown in Figures 70 and 71 for the $\tan \delta$ and moduli, respectively. There is a low temperature transition at -60°C and the T_g is at 170°C . The low temperature transition has been attributed (Reference 32) to motions of glycidyl groups in the epoxy molecule. The presence of additional hydrogen bonding or the occurrence of additional cure or reaction in the plasticized state could shift this transition to higher temperatures.

Figures 72 and 73 show the $\tan \delta$ and moduli data respectively for a specimen that was exposed until it reached an equilibrium weight-gain at $160^\circ\text{F}/100\% \text{ RH}$ and was then dried to zero weight loss in a vacuum oven at 200°F . The maximum in the low temperature $\tan \delta$ value was shifted to -30°C while the T_g was raised to about 180°C . There was also a slight increase in the storage modulus. These results indicate that further reaction (cure or cross-linking) had taken place in the wet, plasticized sample. The physical concept for this occurrence is as follows. The T_g of a cross-linked epoxy is proportional to the degree of cross-linking which, in turn, is a function of cure temperature and time. Raising the cure temperature provides the unreacted end groups with sufficient mobility for further reaction to take place resulting in additional cross-linking and, in turn, a higher T_g and storage modulus. In a similar manner, the presence of water in the plasticized resin would exert a solvent or dilution effect that could provide sufficient mobility to the end groups so that further cure or cross-linking could take place at a lower temperature than the cure temperature.

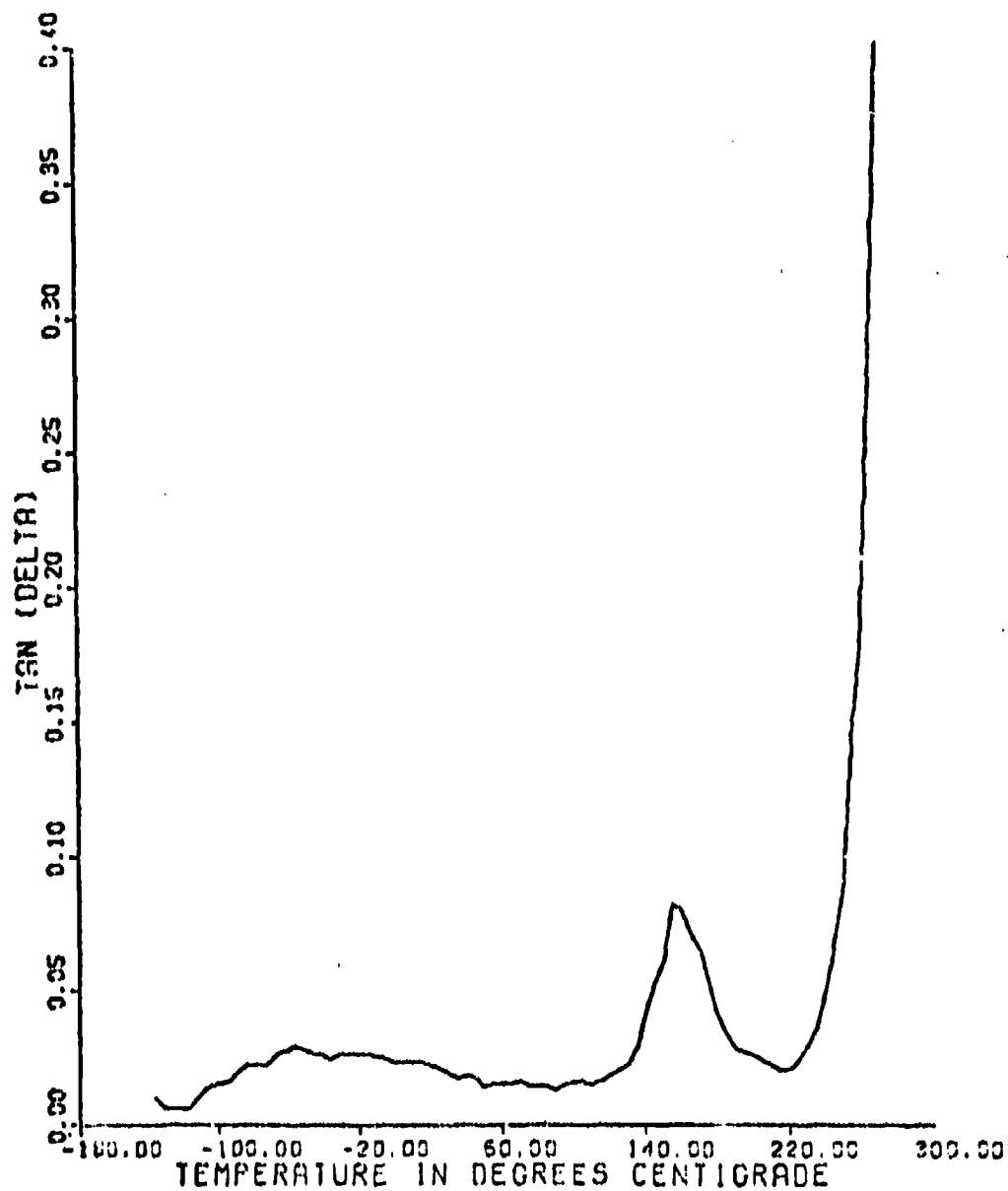


Figure 70. Tan δ vs. Temperature for Dry, Control Sample

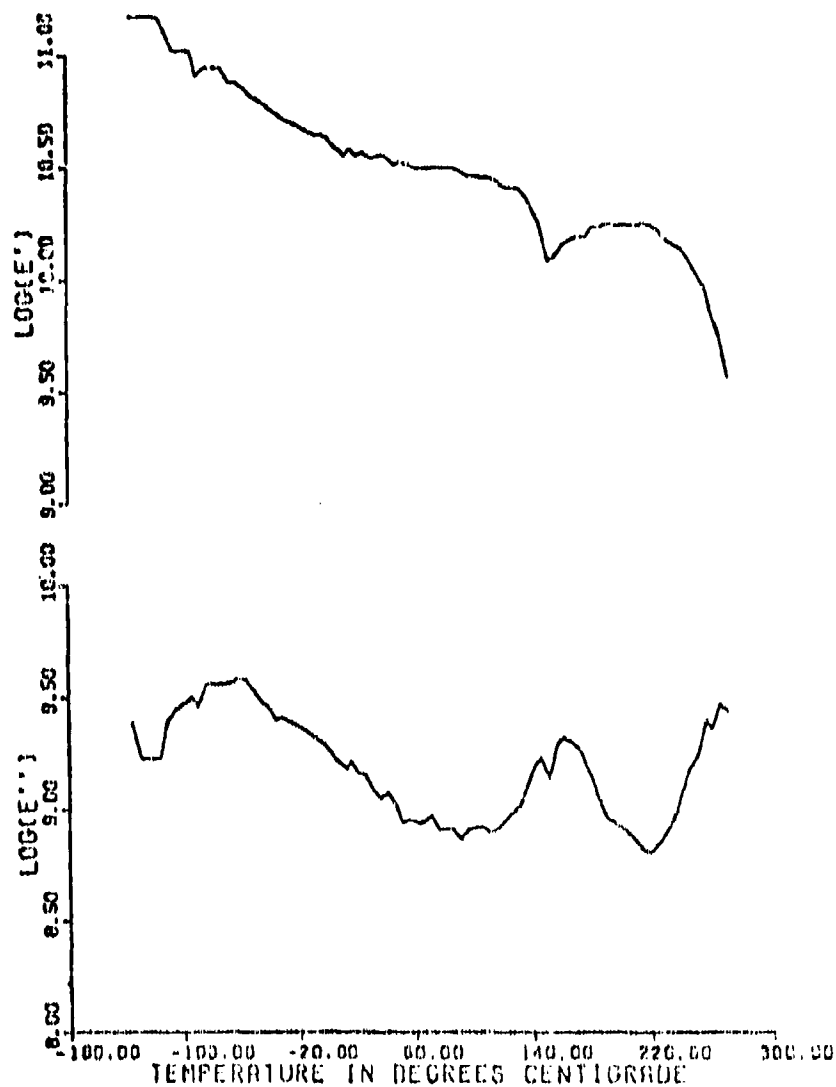


Figure 71. Storage Modulus (E') and Loss Modulus (E'') vs. Temperature for Dry, Control Sample

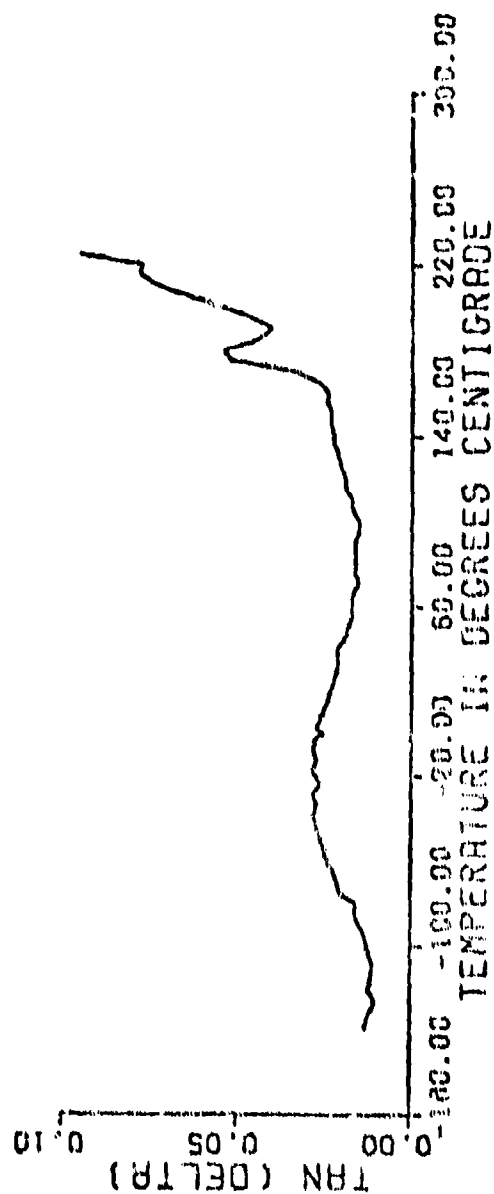


Figure 72. Tan δ vs. Temperature for Specimen Exposed to Equilibrium Weight-Gain and then Dried

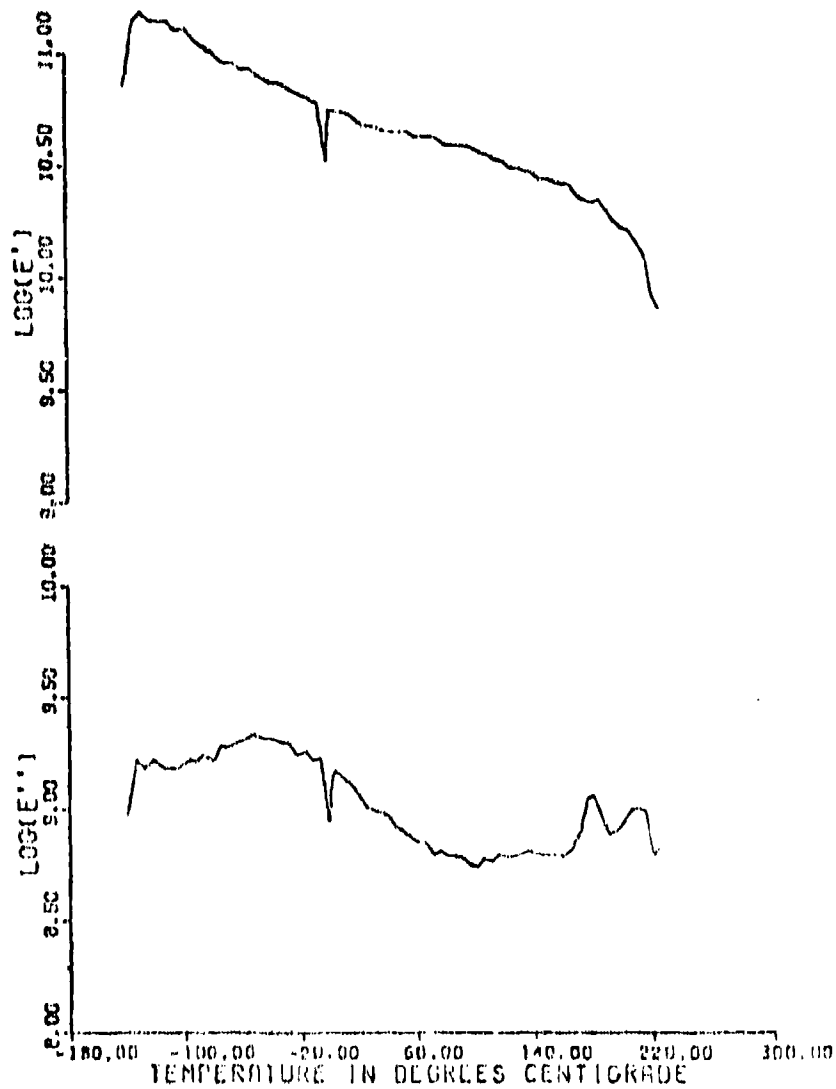


Figure 73. Storage Modulus (E') and Loss Modulus (E'') vs. Temperature for Specimen Exposed to Equilibrium Weight-Gain and then Dried

b. Near Infrared Studies

Additional evidence for this "further reaction concept" was obtained through a study of the near infrared (IR) spectra of epoxy film samples. The near IR region (0.6-2.5 μ) is particularly suitable for studying epoxy films. In the conventional IR region (2-15 μ) it is usually necessary to employ elaborate preparation methods with very thin (<0.5 mil) films to get sufficient transmission of IR radiation to have interpretable spectra. Otherwise, it is necessary to use an internal reflectance technique. In the near IR region one can use specimens varying from 1 to 125 mils in thickness and get very useable spectra.

The major absorption peak for α -epoxides is located at 2.2 μ and was first reported by Goddu and Delker (Reference 33). The applicability of this peak, as well as other peaks in the near IR region, to the study of epoxy resins was subsequently described by Dannenberg (Reference 34).

A typical spectrum for an as-fabricated, control sample is shown in Figure 74. The peaks of major importance are:

1.43 μ	- OH
1.50 μ	- NH
1.91 μ	- OH (Water)
2.20 μ	α - epoxide
2.43 μ	- CH (Aromatic)

No attempt will be made to apply specific assignments to these absorptions. They will be discussed in general terms as regards the chemical changes taking place during the epoxy cure.

Figure 75 shows several spectra for this epoxy as a function of extent of cure. The peak associated with the epoxide functionality progressively decreases in intensity as the epoxide ring is attacked by the amine curing agent. Simultaneously, because of the reaction of the

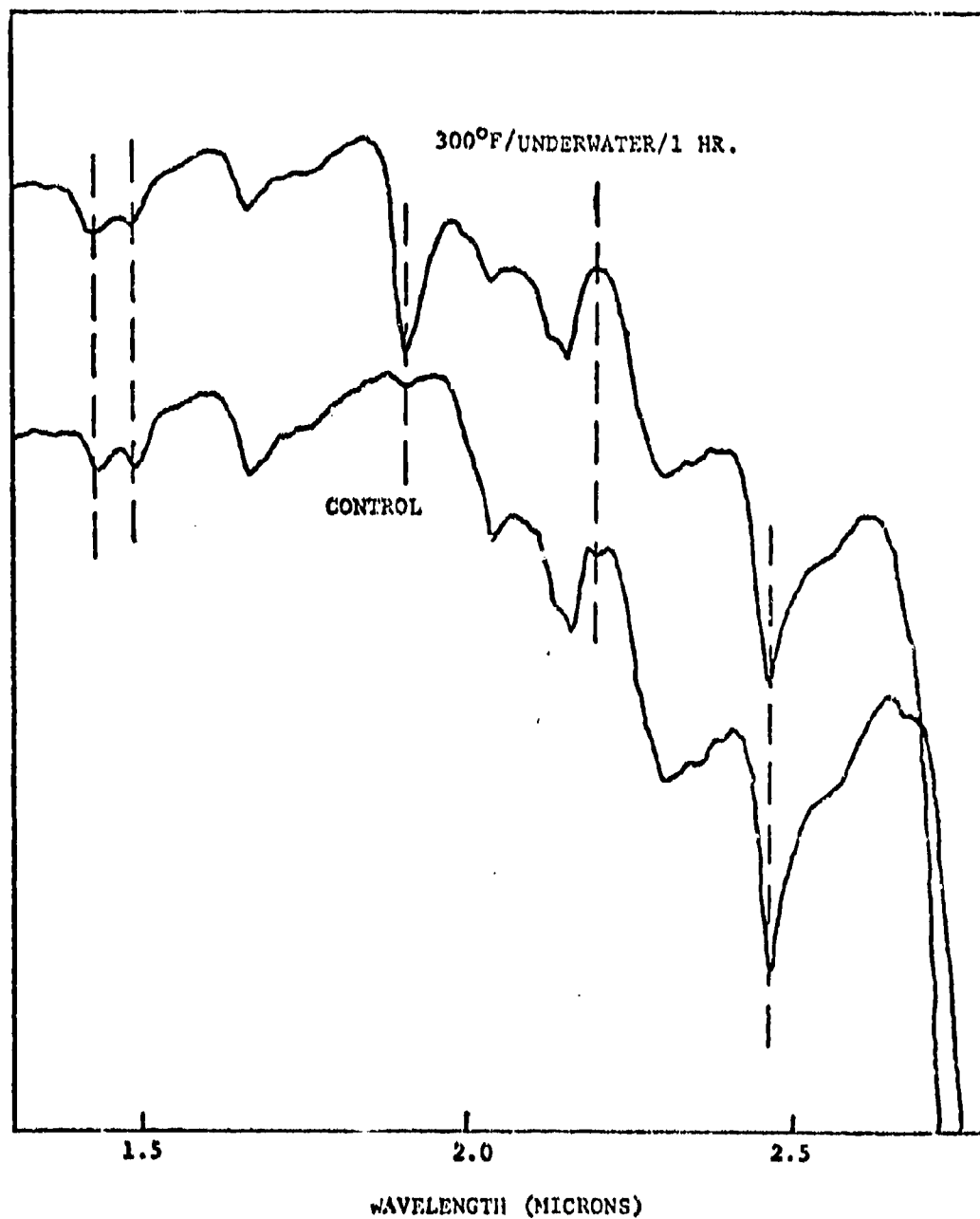


Figure 74. Near IR Spectra of Dry, Control Specimen and Aged (300°F/Underwater/1 HR) Specimen

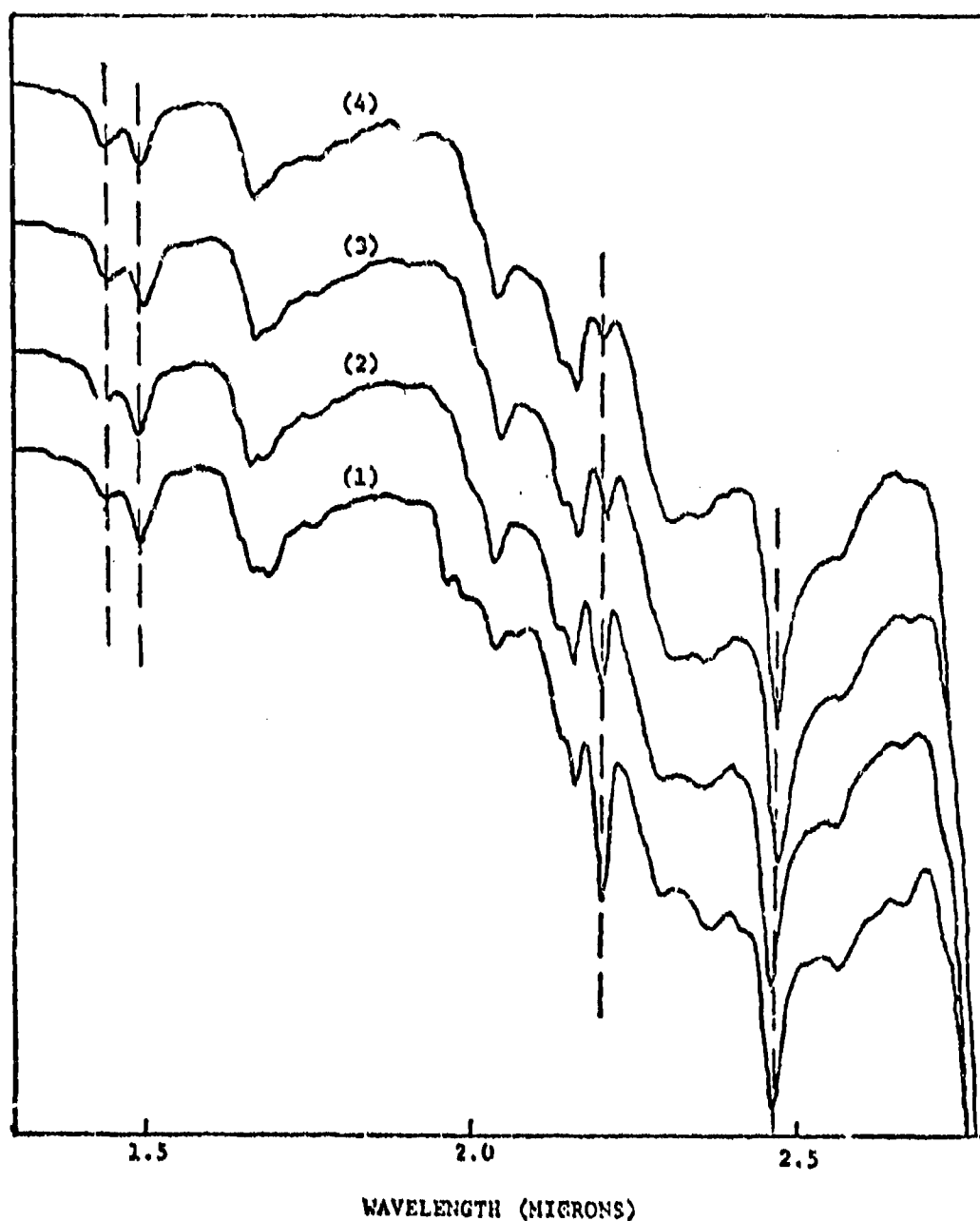


Figure 75. Near IR Spectra of Epoxy Resin as a function of Cure-
 (1) 1 HR at 250°F, (2) 3 HRS at 250°F, (3) 3 HRS at
 250°F + 1 HR at 300°F, (4) 3 HRS at 250°F + 1 HR
 at 300°F + 1/2 HR at 350°F

curing agent, the -NH absorption gradually decreases with increasing extent of cure. The -OH generated by the epoxy ring opening (1.43μ) gradually increases with increasing degree of cure. Therefore, as shown by the spectra, further cure is associated with: a decrease in epoxide; an increase in -OH; and a decrease in -NH.

Also shown in Figure 74 is the spectrum of the same control sample after exposure to a 300°F /underwater environment for one hour. The small epoxide peak has disappeared completely, the -OH peak (1.43μ) increased in intensity, and the -NH peak decreased slightly. Also strikingly evident is the large peak associated with water (1.91μ). It was observed during this study that the absorption at 1.91μ is a very useful indicator for following moisture absorption and desorption and therefore could be used quite easily as a quality assurance tool. IR spectra were also taken over the conventional IR region ($2-15\mu$) for both the control and exposed specimens with no detectable differences being found.

Although the spectra indicate that additional chemical reaction is taking place, it is not clear whether additional cure is taking place or the epoxide is undergoing hydrolysis to a diol. Therefore, a series of tests were performed in which the rubbery modulus was measured on control specimens and specimens exposed to the 300°F /underwater environment for one hour.

It was found that the control specimens had an average rubbery modulus of 2,400 psi while the 300°F /underwater exposed specimens had an average rubbery modulus of 2,950 psi. This increase in rubbery modulus can only occur as a result of increased cross-linking or further cure.

This additional cure phenomenon can have several ramifications. For one, it could alter the absorption-desorption process since the diffusion medium is changing. Secondly, it could lead to localized regions of stress concentration where flaws could form and grow.

This is because most bonds are elongated or stressed in a moisture-temperature-stress environment. Any new bonds forming as a result of additional cure will be in a non-stressed, equilibrium conformation. When the temperature is lowered, humidity reduced, and stress removed, most of the bonds will resume their unstressed, equilibrium conformations with the result that the newly formed bonds are now placed under stress. Because of their low concentration, they will be prime sites for bond breakage which could lead to microcracking.

c. Environmentally Induced Stresses

In a category which might be labeled "environmentally induced stresses" are those stresses generated by the absorption of water and concurrent specimen swelling. The specimen's resistance to this swelling leads to the development of compressive stresses. In the diffusion process, a concentration gradient of moisture in the epoxy plate exists in the manner shown in Figure 76 where M_0 and M_∞ represent the initial (dry) and equilibrium moisture contents, respectively. The surface is at M_∞ while the core is nearly dry early in the diffusion process. Therefore, compressive stresses ($-\sigma$) will be greatest at the surface. These will be balanced by biaxial tensile stresses ($+\sigma$) in the core of the material (Reference 35). For a constant temperature and humidity exposure the moisture gradient and corresponding stress state would have the appearance shown in Figure 76. This condition will change with time as the interior moisture concentration approaches M_∞ . Therefore, in the case of a constant humidity/temperature exposure there will be a stress field associated with the moisture gradient and this stress field will change as the moisture gradient changes.

For the case of the thermal-spike environment (Figure 8), the moisture gradient will now be accompanied by a thermal gradient. Because of this we will have to arrive at some net stress condition resulting from the linear superposition of the stresses for each type of gradient. For simplicity, it is assumed that each phenomenon is acting independently, that thermal diffusion is of greater magnitude

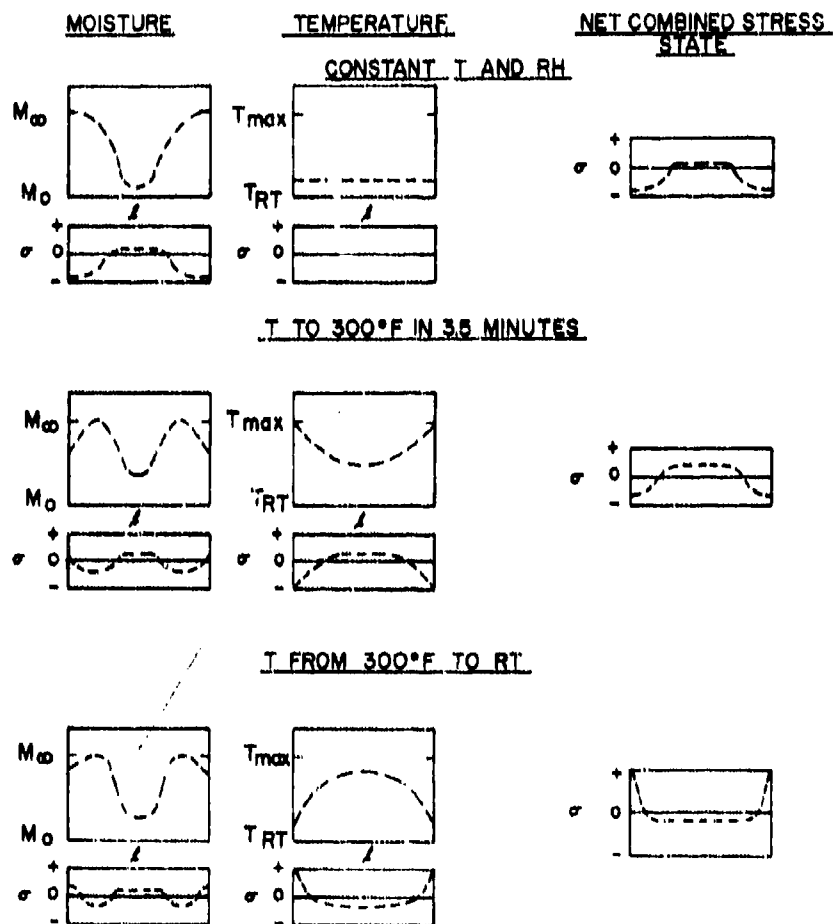


Figure 26. Qualitative Determination of Gradients and Stress States for Thermal-Spike/Humidity Environment

than moisture diffusion, and the magnitudes of the moisture-induced and temperature-induced stresses are of the same order.

The different gradients, corresponding stress states, and net, combined stress states are shown in Figure 76 for the thermal-spike/humidity environment. As can be seen, the specimen at room temperature in the humidity only condition has compressive stresses at the surface and tensile stresses in the core. The thermal-spike then produces a combined stress state wherein the surface compressive stresses are reduced and the remaining stress field has the same profile but is of different magnitude than the room temperature condition. The rapid cool down to room temperature results in a large tensile stress localized near the surface, balanced by a compressive stress through the center of the specimen. Therefore, the humidity/thermal-spike environment causes the specimen to be cycled compression to tension. No attempt is made here to place actual values on the stresses or to specify actual gradients. The purpose is to point out that gradients do exist (both moisture and thermal) and as a result corresponding stress states are imposed on the specimen. Whether or not microcracks could be formed and propagated as a result of these stresses will depend on both the magnitude of the stresses and number of times imposed.

5. CREEP STUDIES

a. Background

The creep behavior of a polymeric material is studied by subjecting a sample to a constant stress and recording the resultant time-dependent strain over a given period of time. A typical creep curve for a cross-linked rubber is shown in Figure 77 (Reference 18). The creep behavior of a viscoelastic polymeric material is very analogous to its relaxation behavior which was illustrated with the relaxation modulus vs. temperature plot shown in Figure 52.

When a cross-linked rubber is subjected to a tensile stress, it will progressively elongate until an equilibrium extension is reached.

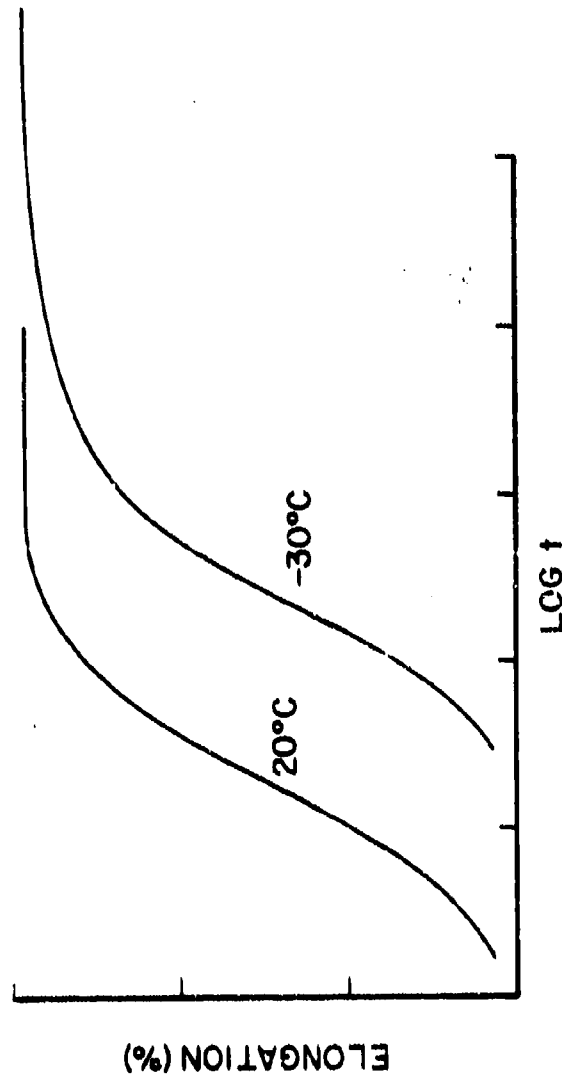


Figure 77. Typical Creep Curves for a Cross-Linked Rubber
(Reference 18)

For the rubber to elongate it is necessary for the various polymer chains between cross-links to elongate by displacement of their segments through a matrix of surrounding chain segments. Therefore, each segment will experience frictional retardation forces from other segments. Because of this, the attainment of the equilibrium elongation is a time-dependent phenomenon. However, various external forces can alter this time dependency. Increasing the temperature will lower the retardation forces and shorten the elongation time (Figure 77). Similarly, the addition of a plasticizer will allow the elongation rate to be increased. This type of time-temperature behavior typifies viscoelastic materials.

If the polymer is undergoing creep at a temperature above its T_g , the equilibrium elongation will be reached at the so-called rubbery plateau which was previously discussed. For a cross-linked system such as the epoxy resin or a rubber, no further elongation should be observed once the rubbery plateau is achieved because the load bearing polymer chains between cross-links are fully extended. Because of this characteristic behavior of cross-linked systems during creep, this type of test is capable of yielding considerable insight as to the mechanisms of property loss.

Consider Tobolsky's work (Reference 19) on chemical stress relaxation in cross-linked rubber networks. Stress relaxation tests performed at temperatures where the material was in its rubbery state showed that these rubbers exhibit a fairly rapid decay to zero stress at constant extension (Figure 78). Since in principle, a cross-linked rubber network in the rubbery region should show little stress relaxation, the behavior was attributed to a chemical rupture of the cross-linked network. Specifically, the chemical rupture was found to be due to the attack of the polymer chains by molecular oxygen. A series of tests were performed in both air and inert atmospheres to illustrate this phenomenon (Figure 79). Using this type of testing it was also possible to demonstrate the effect of temperature on the chemical stress decay as shown in Figure 80. In short, these types of tests such as creep extension tests where one is operating in the rubbery region give

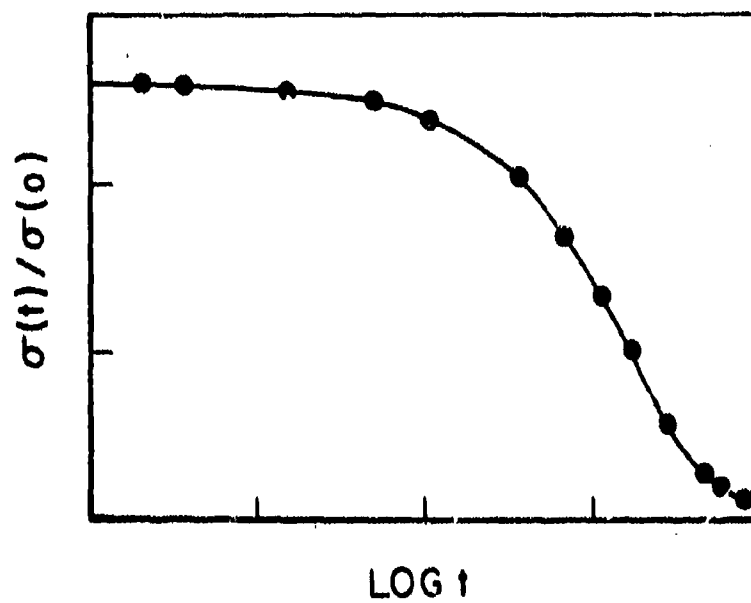


Figure 78. Stress-Relaxation Behavior of a Cross-Linked Rubber at 100°C (Reference 19)

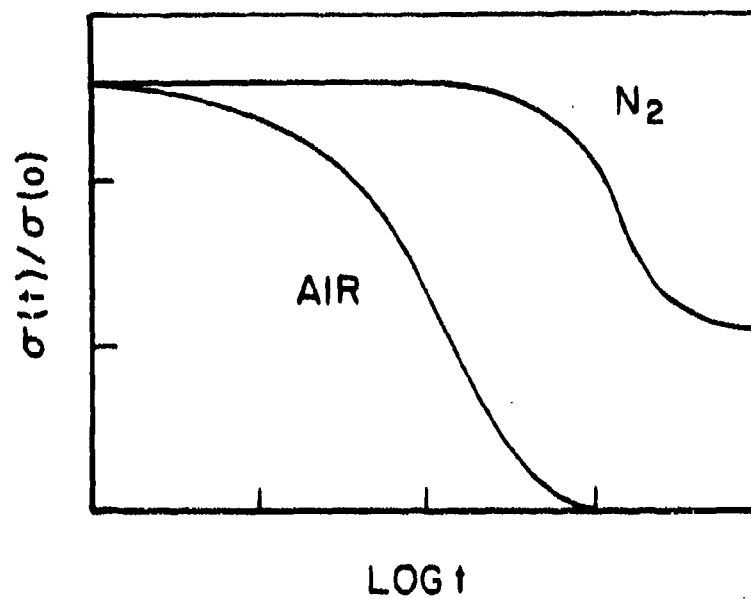


Figure 79. Stress-Relaxation Behavior of a Cross-Linked Rubber at 120°C in Air and Purified Nitrogen (Reference 19)

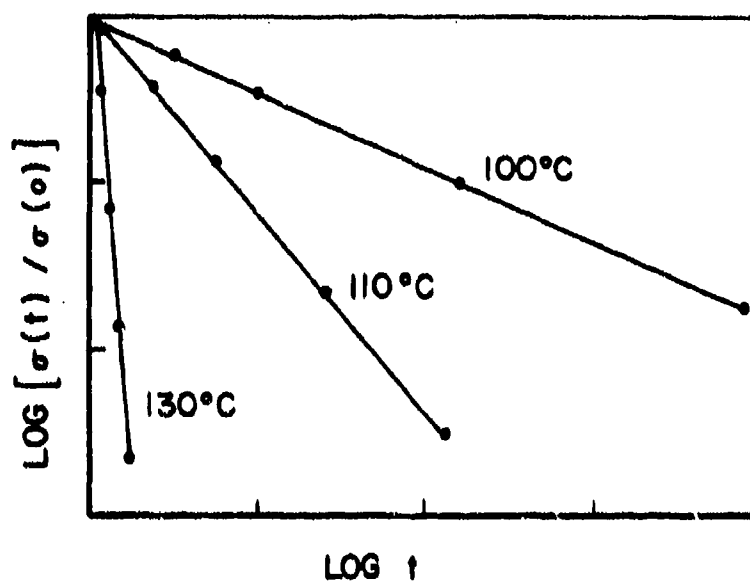


Figure 80. Stress-Relaxation Behavior of a Cross-Linked Rubber as a Function of Temperature (Reference 19)

very meaningful mechanistic information. In the case of a cross-linked rubber where a truly homogeneous, infinite, cross-linked network is present, the continued elongation of a sample beyond its rubbery extension can only be due to chain scission processes and vice versa, i.e., chain scission processes will result in additional elongation beyond that of the rubbery plateau.

These types of tests (creep or stress relaxation) can also yield information as to other possible failure mechanisms. In the case of a creep test, once the rubbery elongation is reached, in principle the specimen should be capable of remaining in that condition indefinitely if no chain scission is taking place. However, because of the formation and growth of microcracks, cavities, or other flaws or imperfections while in this stressed/elongated state, rupture takes place as a function of time, and therefore, time-to-rupture becomes a very meaningful parameter.

Consider the rupture process itself. The first phase of the rupture process involves the development of cracks which can be either stress-induced or possibly pre-existent. All materials contain, or develop under stress, inhomogeneities that give regions of stress concentration. These regions of stress concentration are prime sites for the formation of cracks or cavities.

In considering the growth of a crack in a material which exhibits Griffith flaw behavior the Griffith Crack Theory is employed. When the stress near a crack tip reaches the cohesive strength of the material, the crack will begin to propagate, quickly reaching a limiting velocity. In terms of the Griffith criterion, the crack will begin to grow when the decrease in stored elastic energy resulting from an increase in crack length becomes equal to the surface energy, i.e.,

$$c^{1/2} \sigma = \left(\frac{2}{\pi} E \gamma \right)^{1/2} = K_c \quad (26)$$

where,

σ = Stress

c = Crack Length

E = Tensile Modulus

γ = Surface Energy

K_C = Fracture Toughness

It is generally found that a crack grows slowly, but at a progressively increasing rate, until a constant, high velocity results (Reference 36). However, in the case of a cross-linked rubber, the slow growth phase may take place over a relatively long period of time and the transition to high-speed growth which precedes rupture occurs very rapidly (Reference 37). The fracture surface formed during slow growth generally develops a fibrous structure near the crack tip (Reference 38) similar to what was observed in the SEM studies discussed in a previous section.

For the case of cross-linked rubbers, a semi-quantitative relationship has been provided by the Bueche-Halpin theory of rupture (References 39, 40). This theory assumes that the crack growth rate during the slow growth phase is controlled by the viscoelastic response of the material in the region of the crack tip. The crack in a specimen under a constant load (creep) grows at some constant rate until a high-speed growth criterion is satisfied. The dependency of the rupture process on the viscoelastic properties of the material have been illustrated as follows.

The effect of temperature on the rupture stress σ_b as a function of the best temperature T minus the glass transition temperature T_g has been shown to produce the behavior illustrated in Figure 81 for several different cross-linked rubber systems (Reference 40). This type of behavior illustrates that changes in T_g will produce changes in the rupture stress, σ_b . Specifically, if we are testing the material above T_g and the T_g were lowered by plasticization the result should be a reduction of the rupture stress.

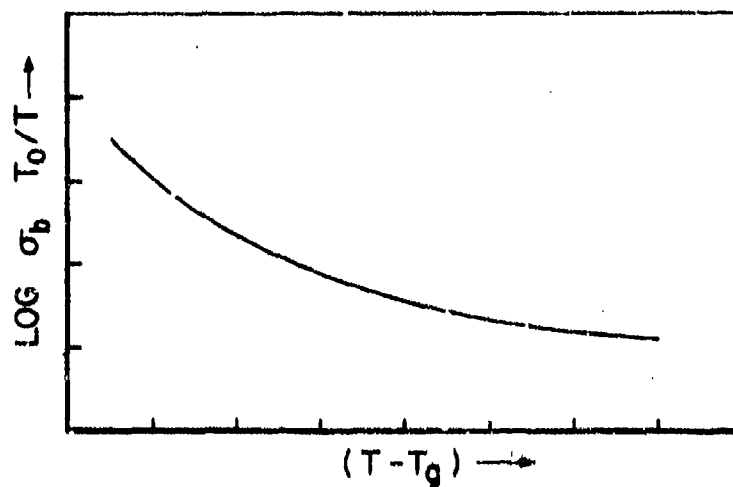


Figure 81. Effect of Temperature on the Rupture Stress of Cross-Linked Rubbers (Reference 40)

Time effects have been illustrated by a series of tests in which a specimen is subjected to constant load (creep) until rupture at time t_b takes place (Reference 40). Variations in load or test temperature cause variations in t_b as shown in Figure 82(a). Curves for various temperatures exhibit a natural order, the higher the temperature the lower the curve (Figure 82(a)). They can be superpositioned as previously described for relaxation moduli by shifting along the $\log t$ axis until all points fall on a single continuous master curve as shown in Figure 82(b). The shift required at each temperature is given by the shift factor a_T which was described in a previous section. Equivalence of time and temperature on a_b was first introduced by Bueche (Reference 41) and Smith (Reference 42) and now is experimentally accepted. The important observations to be made from this plot are that the lower the applied stress the longer the time-to-break and the higher the temperature the lower the stress required for rupture. If the shift factor is applied to the master curve as shown in Figure 83, to give the dotted curve, it can be seen that for an equivalent stress level the time-to-break has been reduced. This type of shift is what would be observed if the T_g were lowered by plasticization as shown in Figure 52.

This type of response can be incorporated into the Griffith theory for crack growth, where the stress is related to the crack length by

$$K_{Ic} = \sigma \sqrt{c} \quad (27)$$

Typical behavior for a material's critical stress as a function of crack length is shown in Figure 84. As the crack gets larger, the stress required for spontaneous growth of the crack gets lower. Combining the Bueche-Halpin theory with the Griffith crack growth theory involves consideration of the material's viscoelastic response in the vicinity of the crack tip in relationship to its crack growth behavior. Increasing the test temperature, lowering the T_g at a fixed test temperature, or increasing plasticizer content will result in a shift of the original σ vs c curve (solid line) to a new position (dotted line). As a result of the viscoelastic behavior of the material, the altered material is

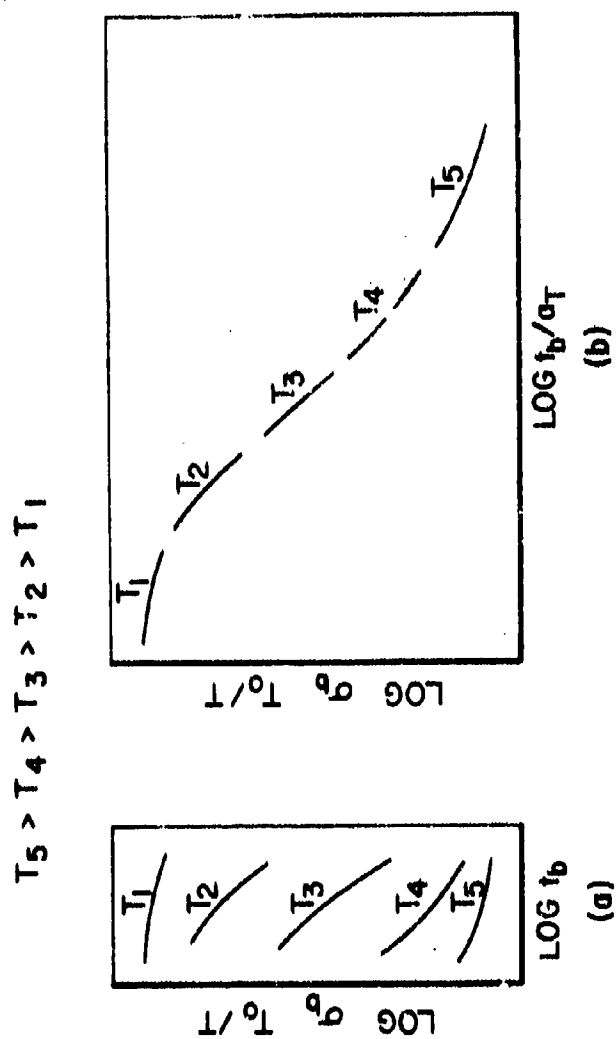


Figure 82. Creep-Rupture Stress vs. Time for Different Test Temperatures (Reference 40)

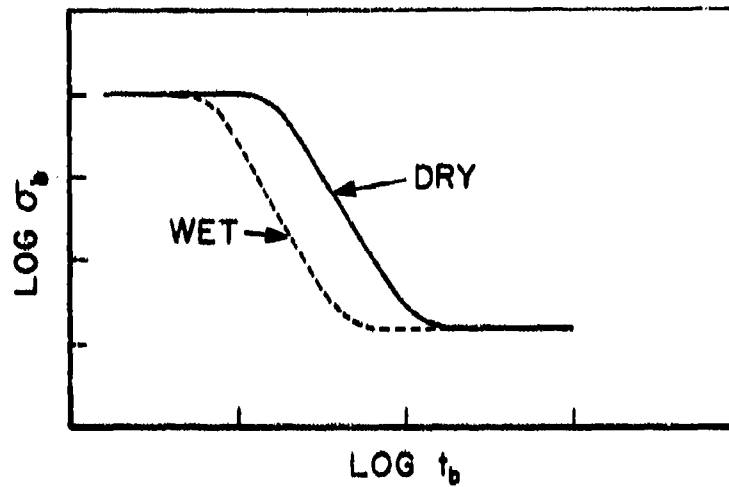


Figure 83. Hypothetical Rupture Stress vs. Time Curves at a Constant Temperature

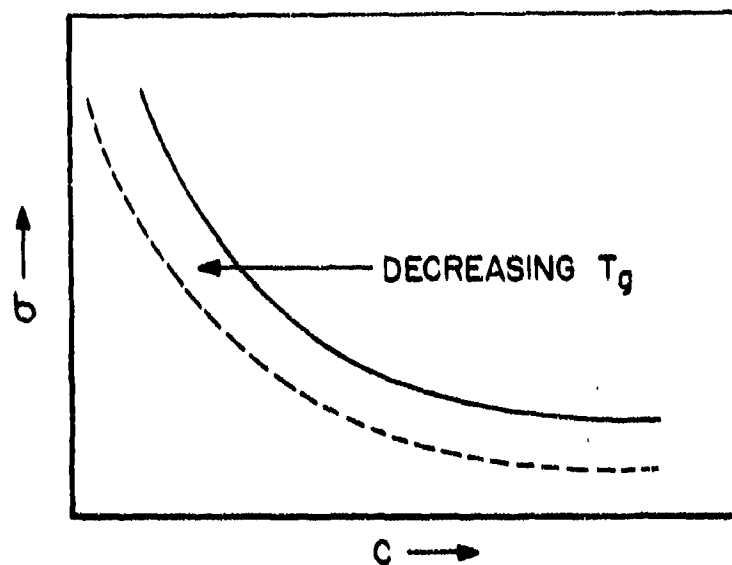


Figure 84. Hypothetical Critical Fracture Stress vs. Crack Length Curves

unable to store as much energy and therefore the critical stress for spontaneous crack growth is reduced. Equivalently, the crack length necessary for an applied stress to initiate spontaneous crack growth is decreased.

This type of behavior was further demonstrated by Braden and Gent (Reference 43) in a study of the formation and propagation of cracks on the surface of stressed rubber specimens exposed to ozone. Cracks did not develop in unstressed specimens because of the apparent reaction of ozone with rubber to form a protective surface film. However, when applied tensile strains exceeded 5%, cracks formed on the surface and grew perpendicular to the direction of the applied stress. Increased stress or strain resulted in an increased number of cracks. This implied that ozone attack and subsequent crack formation took place at sites of high stress concentration. Braden and Gent showed that for a crack to propagate in the presence of ozone, a minimum characteristic stress must be exceeded. Therefore, at a given strain, the condition for crack growth would be exceeded only for a certain fraction of flaw sites, the number of such sites increasing with increased strain. This was demonstrated using rubber strips coated with a protective grease film except for a given amount of exposed surface area. By measuring the tensile stress required for appearance of cracks, it was found that the critical cracking stress increased as the size of the exposed area decreased. These results imply that a distribution of flaw sizes must exist and as the exposed area was reduced, the probability of exposing critically sized flaws for a given applied stress was correspondingly reduced.

The critical stress required for cracks to form in surfaces of different smoothness was demonstrated by leaving an edge of a test specimen exposed and measuring the critical stress required for crack formation. Surfaces of different smoothness were prepared by testing die-cut specimens having variable length flaws and specimens whose edges contained numerous small razor cuts. These results (Figure 85)

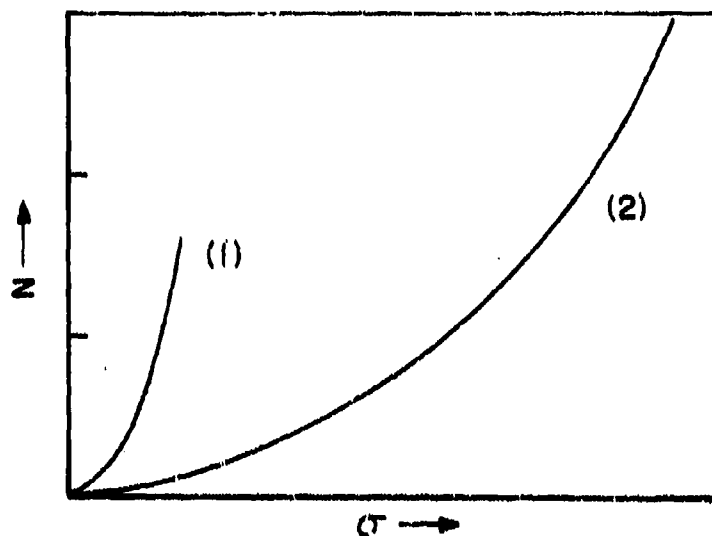


Figure 85. Number of Cracks per cm vs. Applied Stress for Rubbers Having Pre-Existent Flaws-(1) = RAZOR-CUT, (2) = DIE-CUT (Reference 43)

provide evidence for the view that all real materials contain heterogeneities which act as stress concentrators, thereby reducing the strength of a bulk material.

At any point on a curve of σ vs. c there will exist at least one crack having a critical crack length relative to the applied stress. Braden and Gent's work implies that for the case of the shifted curve there will be a greater probability of the existence of at least one crack having the critical length for growth because the formation and growth of cracks has been facilitated by the viscoelastic response of the material. Similarly, the critical stress for crack growth to occur has been reduced.

In relation to the creep test, the quantity of cracks formed should be proportional to the applied stress and, in turn, the greater the crack quantity the greater the probability of having cracks of sufficient size for crack growth to take place, thereby resulting in decreased time-to-break or lower rupture stresses. Alterations in the viscoelastic properties of the polymer (e.g., plasticization or changes in test temperature) should result in modifications of the time-to-rupture and crack growth process.

In summary, the creep test can give very meaningful information as to the mechanisms of property losses. When the tests are performed in the rubbery region, an examination of further extension or time-to-failure can give a good insight into the processes taking place.

b. Experimental

The creep test performed in this study consisted of optically measuring the elongation as a function of time of an epoxy test specimen in a given environment under a constant load. Test specimens were "dog-boned", film samples, approximately 6 mils thick, having the shape shown in Figure 86. This shape was chosen to ensure failures in the gage section. The specimen was tabbed with 10 mil aluminum foil which

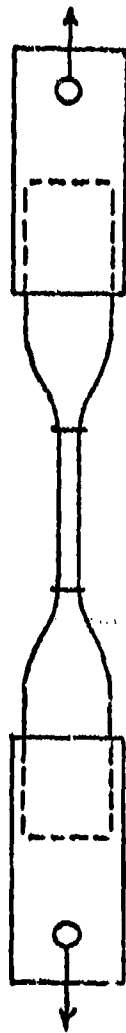


Figure 86. Bomb Creep Test Specimen Configuration

had holes punched in the ends for mounting and weight attachment. An anaerobic adhesive was used to bond the tabs to the specimens. Spring steel clips were also used over the tabbing area to prevent specimen slippage. A special alignment jig was used for tabbing the specimens to ensure axial alignment of the holes and gage section. The gage length was marked with fiducial marks consisting of boron filament bonded to the specimen with the anaerobic adhesive.

To study the elevated temperature behavior of the epoxy as a function of moisture it is necessary to choose the test conditions so that the cross-linked epoxy is in its rubbery state where the behavior of well-characterized, analogous systems such as the cross-linked rubbers can be used for reference (the fact that cross-linked epoxies exhibit mechanical behavior equivalent to cross-linked rubbers has been well documented (Reference 44)). Another requirement is that the test temperature be lower than the cure temperature in order to avoid the complicating factor of additional cure. Further, it would be desirable that the test temperature be reasonably close to the use temperature of the material. All of these requirements are satisfied by the chosen test temperature of 300°F.

In the presence of moisture the effective T_g of the plasticized system is below 300°F (Figure 60) which satisfies the above requirement. However, since the boiling point of water is 212°F, it is necessary to perform the test in a bomb (under pressure). Performing the test in a bomb ensures that steady-state conditions are present so that the results of the test are not diffusion-controlled. A bomb was designed and built to achieve these test conditions (Figure 87). It consisted of a thick-wall pyrex glass tube specimen chamber and stainless-steel end caps having O-ring seals. Metal tie-rods were used to prevent the steam pressure from forcing off the end caps. One end cap was fitted with pressure fittings for evacuating the chamber and passing through inert gases. The use of the glass tubing allowed the strain measurements to be made optically.

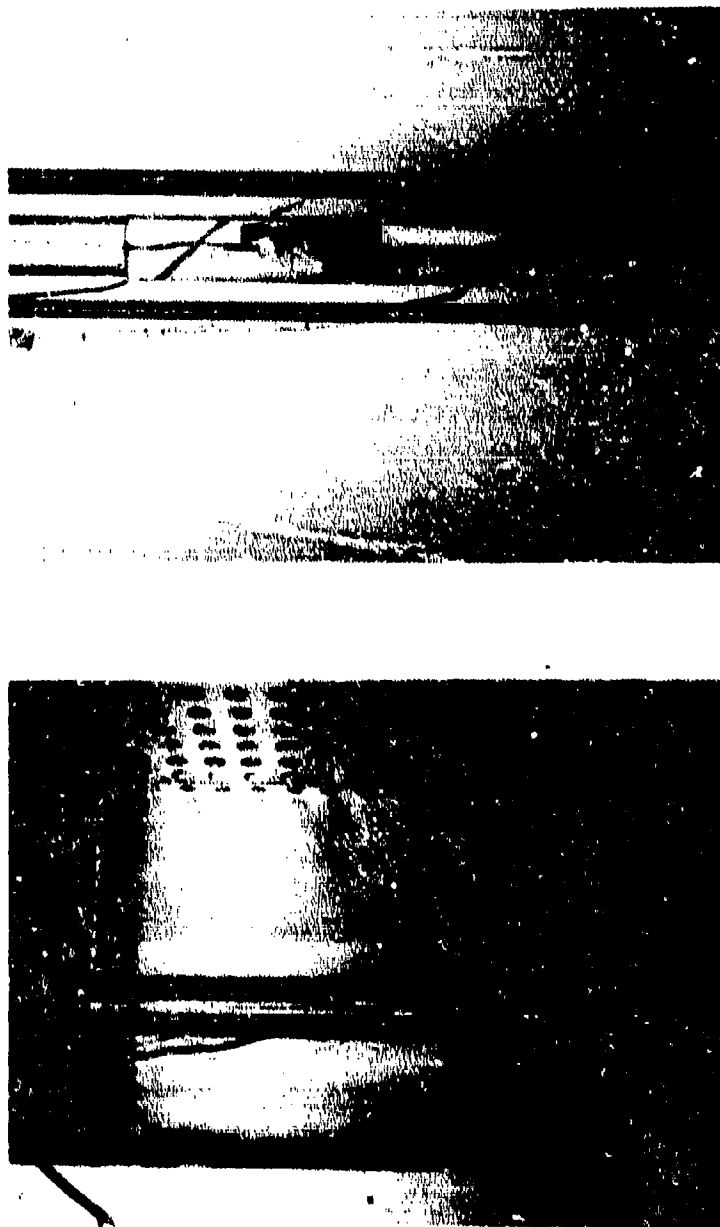


Figure 87. Bomb Creep Test Apparatus Mounted in an Oven

The whole test set-up was mounted in a furnace for testing at 300°F (Figure 87). After adding double distilled water, the chamber was evacuated and purged with nitrogen three times. The test was performed at 300°F using a cathetometer to monitor movement of the boron fiducial marks as a function of time. The ultimate stress, σ_u , used in guiding the tests (1400 psi) was taken from the values found in the constant strain rate tensile tests performed at 300°F after equilibrium exposure at 160°F/100% RH.

Because of a slight temperature gradient in the test furnace, the upper part of the test chamber was at a slightly higher temperature than the 300°F temperature maintained just below the surface of the water. Therefore, there was a lower moisture concentration at substantial distances above the water's surface than at and below the surface. This experimental condition was used as a means for testing specimens at two different moisture absorption contents. As previously discussed, the amount of moisture absorbed is directly proportional to the relative humidity or moisture concentration, therefore, performing the creep test underwater and substantially above the water would correspond to testing specimens of two different moisture contents. The underwater test was a "worst" condition that achieved maximum moisture content and is defined herein as saturation. The above water test achieved a lower moisture content, defined as less than saturation.

c. Results and Discussion

The results of the creep tests performed underwater at 300°F are shown in Figure 88 where percent elongation is plotted vs. log time for stresses of 10, 20, 25, 30, and 50% of ultimate. With increasing stress there is a proportionate increase in elongation and decreased time-to-break. The shapes of the curves are quite similar to the creep curves and relaxation modulus curves previously presented. Within about 30 minutes all of the specimens had passed through the transition region and had reached the rubbery plateau.

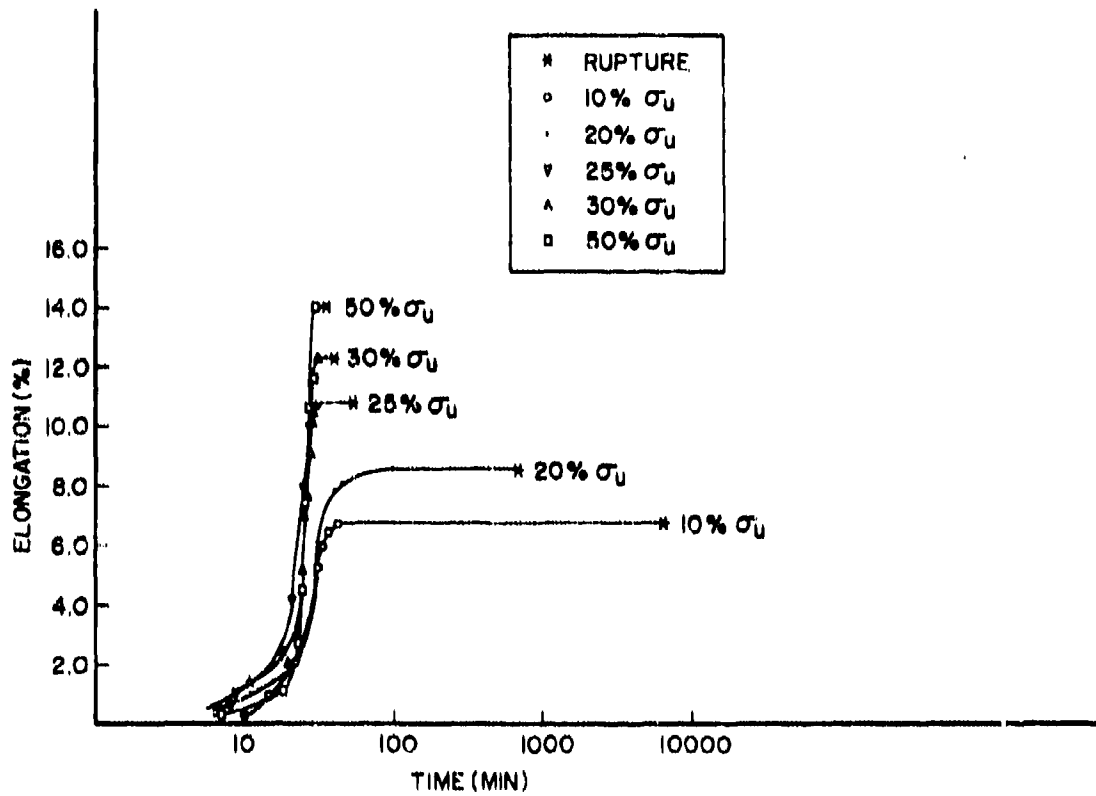


Figure 88. Elongation vs. Time for Bomb Creep Tests at 300°F and Underwater (Saturation)

A plot (Figure 89) was prepared of log stress and log elongation vs. log time-to-break in the rubbery region. As can be seen, linear relationships were obtained for both stress and strain. This agrees with the results of Bueche (Reference 41) and Bartenev (Reference 45). Polarized-light photomicrographs (20x) were taken after each creep test and these are shown in Figures 90-92. For reference, Figure 93 shows polarized-light photomicrographs of an as-fabricated dry control specimen and a dry control specimen which had been subjected to a creep test in a dry nitrogen environment under a 50% of ultimate stress for one week. Figure 94 shows the elongation vs. time for this specimen. Several interesting observations can be made from the photographs of the saturated, underwater exposed specimens. The quantity of cracks appears to be greater for the higher stress level specimens. However, the most striking observation is that the crack size appears to increase with increased exposure time or time-to-break. The cracks grow perpendicular to the direction of applied stress. The photomicrographs for the 10% of ultimate specimen shows the unusual feature of microcracks growing across the width of the specimen in a manner that would obviously lead to rupture.

Another series of 300°F creep tests were performed in the bomb at a height of eight inches above the water level. This was done to achieve another moisture concentration although it was impossible to experimentally measure it. The effect of this lower moisture concentration (<saturation) condition can be seen in Figure 95 where percent elongation is plotted as a function of log time. Compared with the underwater, saturation results, the lower moisture concentration (<saturation) exposure yielded lower strains and increased exposure times at equivalent stress levels. Based on the results of the diffusion and T_g studies it is to be expected that lower moisture contents would result in less plasticization and, in turn, a smaller decrease in T_g . Figures 96 and 97 show polarized-light photomicrographs for stress levels of 10, 30, and 50% of ultimate. A gradual increase in crack density with increasing stress is evident. The crack size appears to be larger for the longer-term exposures.

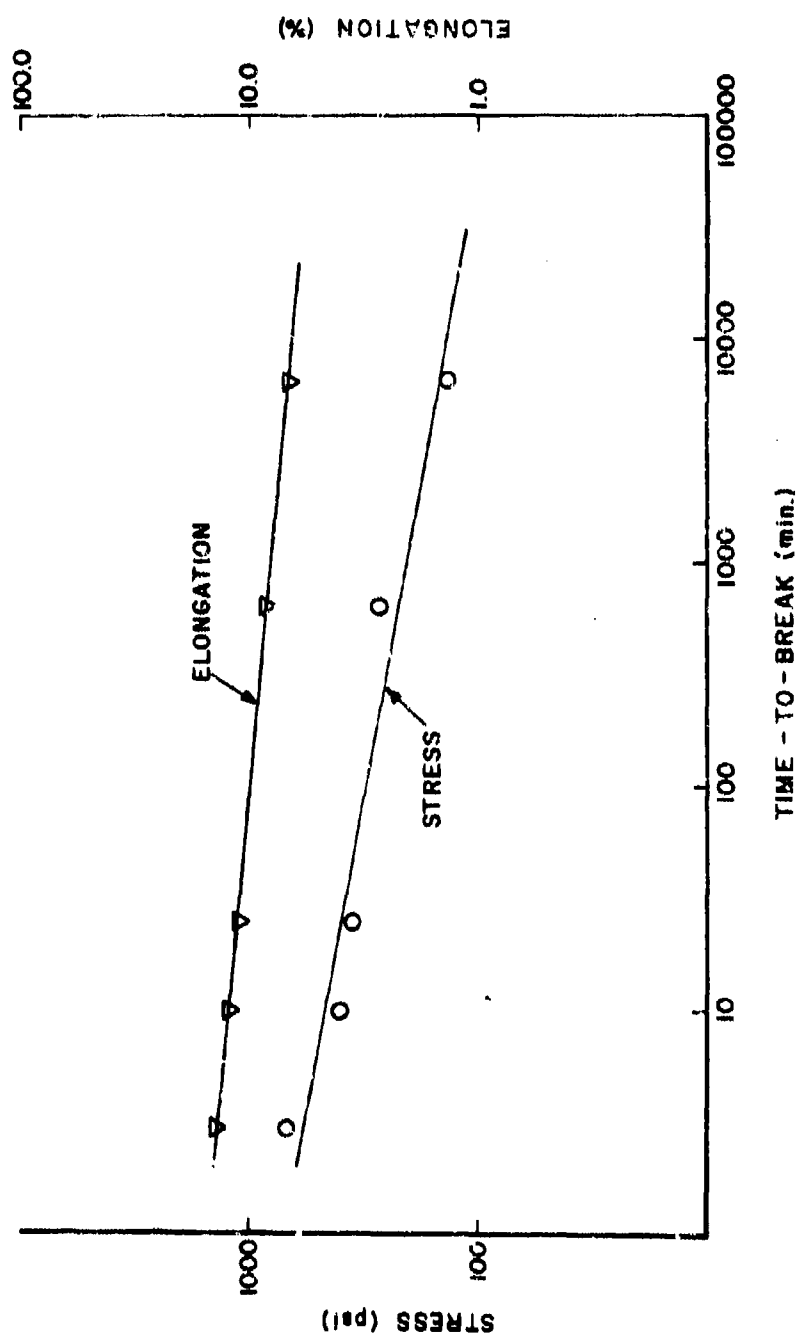
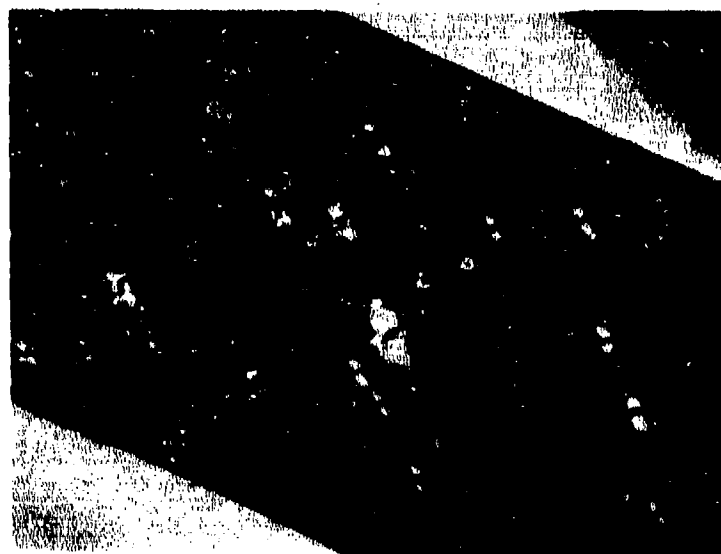


Figure 89. Stress and Elongation vs. Time-To-Break for 300°F/Underwater (Saturation) Creep Tests

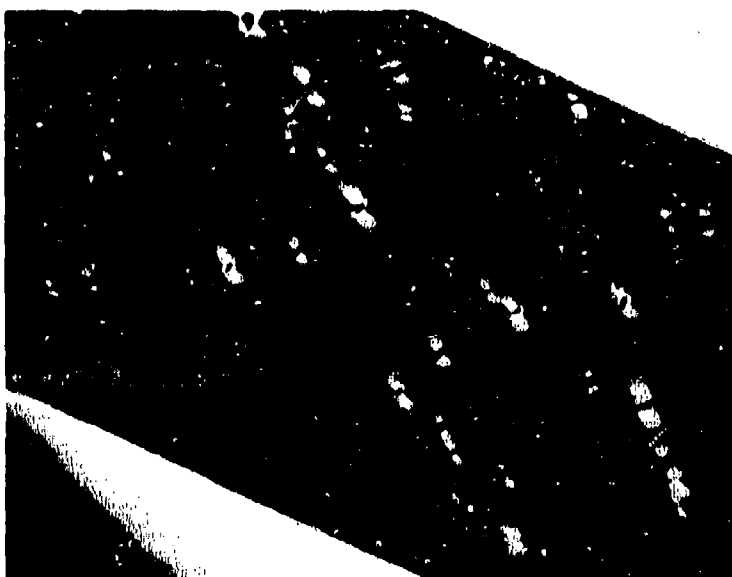


10% OF ULTIMATE

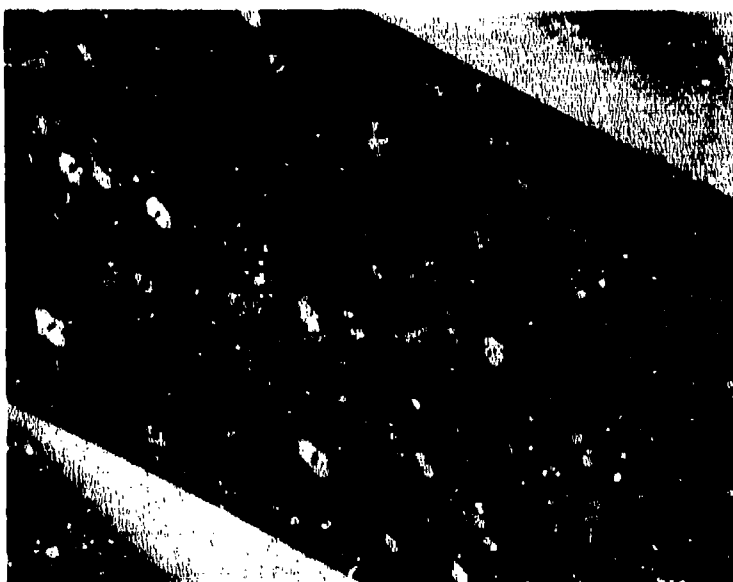


20% OF ULTIMATE

Figure 90. Polarized-Light Photomicrographs (20X) of 300°F/Underwater (Saturation) Creep Test Specimens

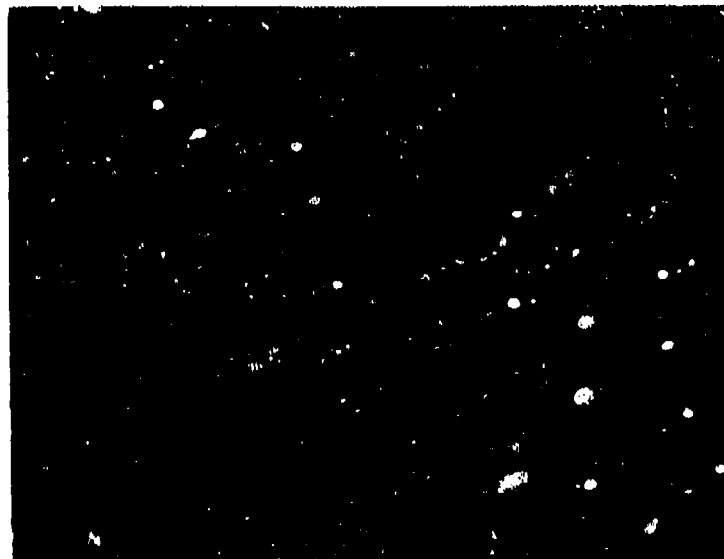


25% OF ULTIMATE



30% OF ULTIMATE

Figure 91. Polarized-Light Photomicrographs (20X) of 300°F/Underwater (Saturation) Creep Test Specimens

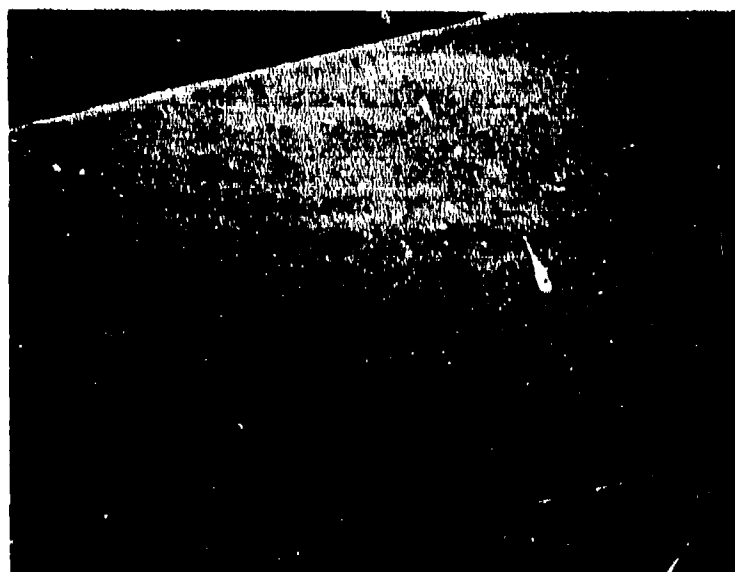


50% OF ULTIMATE

Figure 92. Polarized-Light Photomicrographs (20X) of 300°F/Underwater (Saturation) Creep Test Specimen



AS-FABRICATED



50% OF ULTIMATE/DRY N_2 /1 WEEK

Figure 93. Polarized-Light Photomicrographs (20X) of Dry, Control Specimens

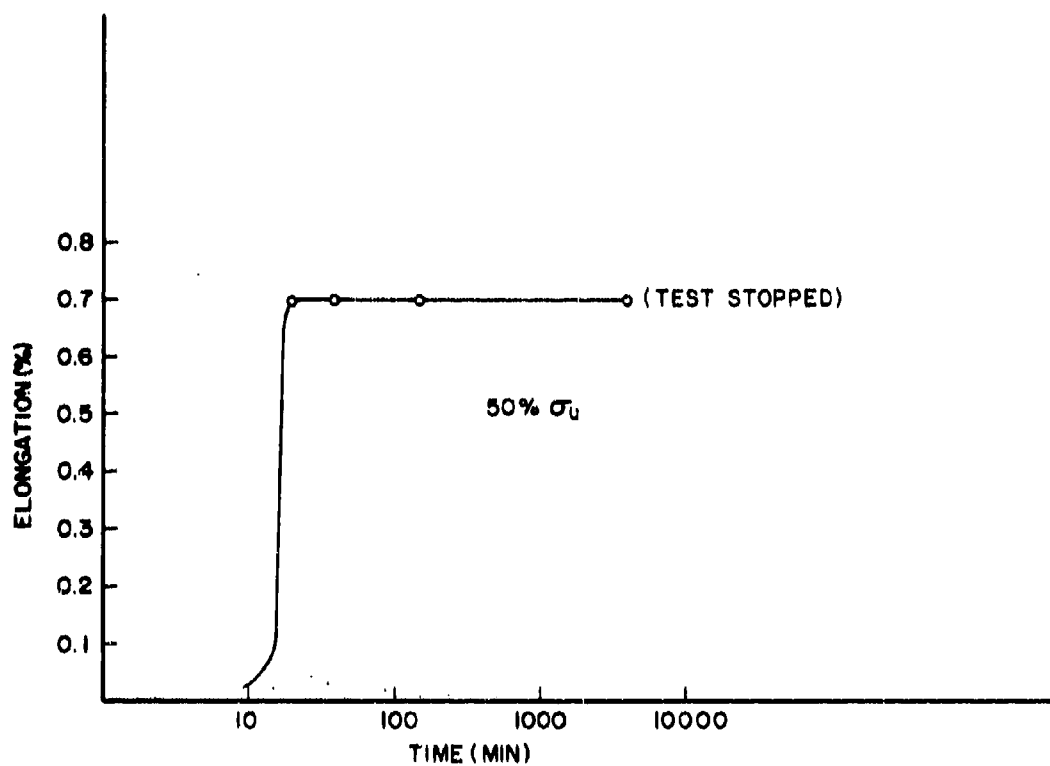


Figure 94. Elongation vs. Time for Bomb Creep Test in Dry Nitrogen

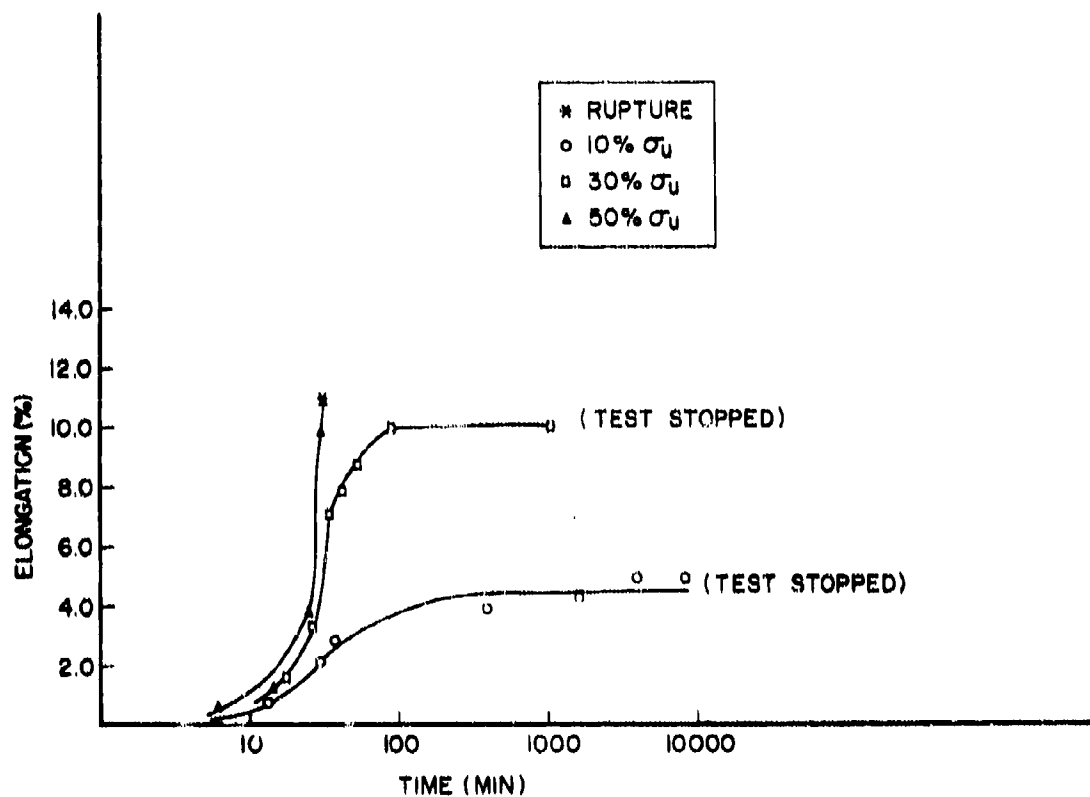
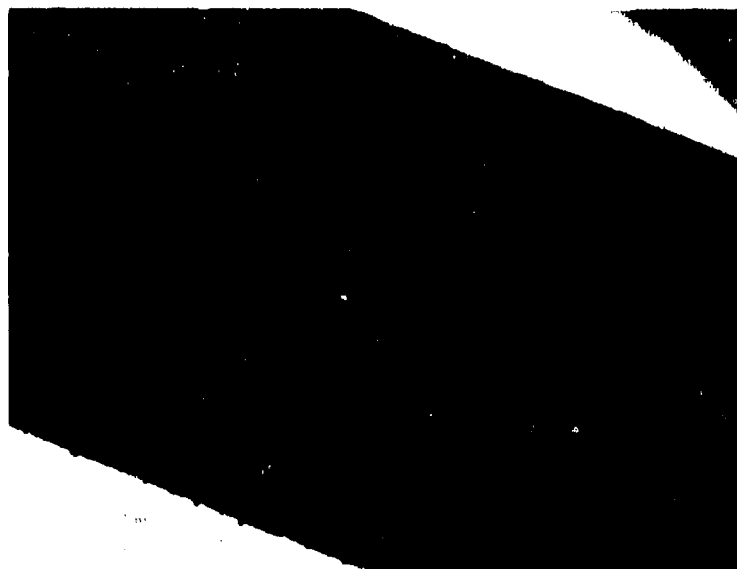


Figure 95. Elongation vs. Time for Bomb Creep Tests at 300°F and Above Water (<Saturation)



10% OF ULTIMATE



30% OF ULTIMATE

Figure 96. Polarized-Light Photomicrographs (20X) of 300°F Above Water (Saturation) Creep Test Specimens



50% OF ULTIMATE

Figure 97. Polarized-Light Photomicrographs (20X) of 300°F Above Water (<Saturation) Creep Test Specimen

The dramatic effect of increased moisture concentration exposures can be seen by comparing the underwater exposure photomicrographs with those of the lower moisture concentration exposure. In particular, comparison of the different moisture levels for the 10% of ultimate stress level shows the striking effect of moisture concentration on crack density and size. Both of these tests were for nearly equivalent exposure times with the saturated, underwater specimens (five-day exposure) rupturing and the above water, less than saturation specimens (six-day exposure) being removed without experiencing failure.

In another series of creep tests, specimens were tested underwater at 200°F. The elongation as a function of time for stresses of 10 and 30% of ultimate are shown in Figure 98. Because of this low temperature, decreased elongations and increased exposure times were observed relative to the 300°F test for equivalent stress levels. In this case the tests were terminated after five days exposure with no failures. The polarized-light photomicrographs (Figure 99), as well as the equivalent exposure times, show that there is little observable difference at various stress levels at these test conditions. The dramatic effect of temperature can be seen by comparing photomicrographs of the 300°F tests with these of the 200°F tests.

An attempt was made using ESCA (electron spectroscopy for chemical analysis) to detect any localized chemical reactions that may be taking place on the surface of the specimens. This analysis was performed on an AEI ES-100 X-ray photoelectron spectrometer; a technique which involves the interaction of impinging photons with the bound electrons of a sample. Different atoms have characteristic electron binding energies which will vary in a distinctive fashion as the atom's environment varies.

This technique was applied to two different epoxy samples to determine if changes of chemistry occurring on the surface could be detected. One sample was a dry control while the other had been subjected to 160°F/100% RH plus one daily thermal-spike until a weight-gain of 7.5% had been attained.

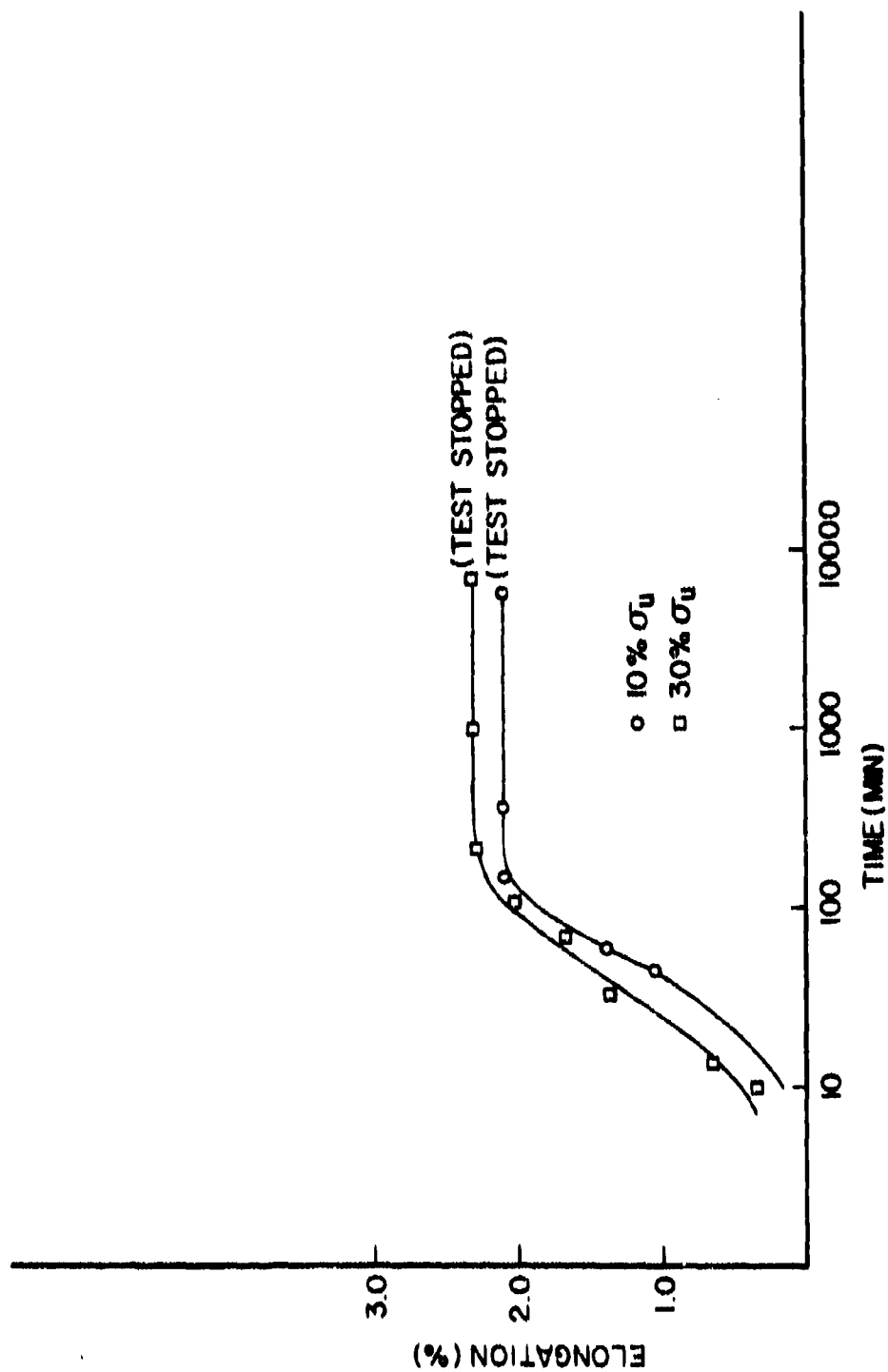
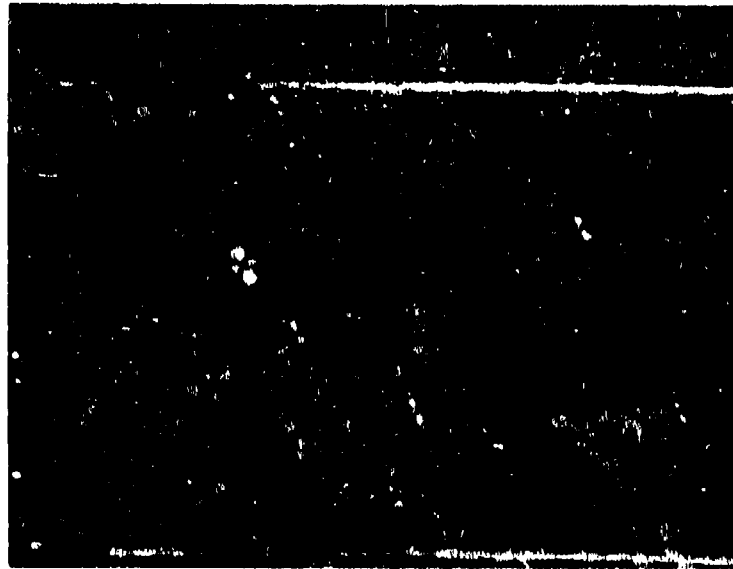
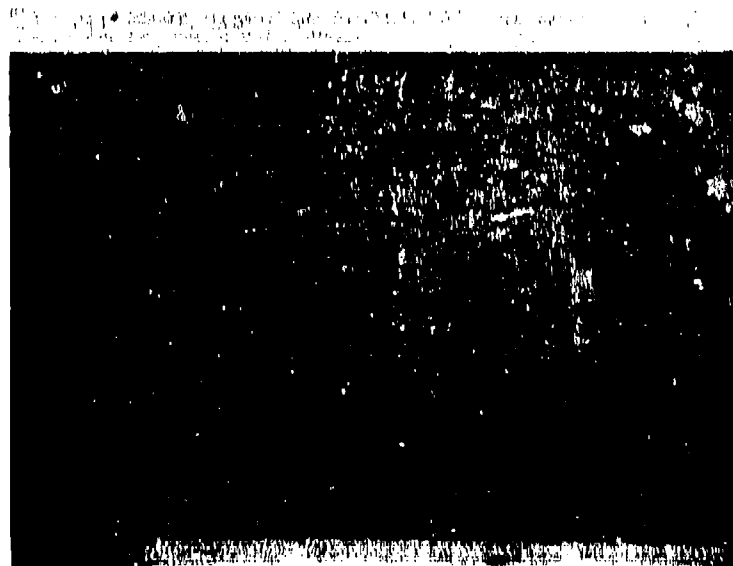


Figure 98. Elongation vs. Time for Bomb Creep Tests at 200°F and Underwater



10% OF ULTIMATE



30% OF ULTIMATE

Figure 99. Polarized-Light Photomicrographs (20X) of 200°F/Underwater Creep Test Specimens

Table 5 summarizes the qualitative and quantitative information extracted from the "overall" ESCA spectrum of the two samples. As would be expected, the major elements found were carbon, oxygen, nitrogen, and sulfur. The concentrations shown are based on carbon as a reference. The most notable change in the aged vs. control was an increase in oxygen. This could be speculated as being due in part to the absorbed moisture.

Table 6 summarizes the carbon, sulfur, nitrogen, and oxygen spectra. In examining each element, different peaks were obtained as a function of the different oxidation states present. The quantitative results presented are based on percent of main element. In general, as an element becomes associated with more electronegative elements (e.g., increased oxidation of carbon), the binding energy increases (Reference 46). The most striking observation is the increased quantity of "oxidized" nitrogen in the aged specimen vs. the control. This could conceivably be the result of some localized chemical reaction such as hydrolysis which could lead to localized chain scission.

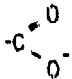
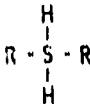

Based on previous work with the analogous polymer systems of cross-linked rubbers, the mechanism by which moisture degrades the elevated temperature properties of the epoxy resin system can be postulated.

Since there is no further elongation once the rubbery plateau is reached, chemical chain scission of any substantial magnitude can be eliminated (although very localized chemical chain scission in such areas as crack tips cannot be ruled out). Experimental results indicate that the failure processes can be described by the Bueche-Halpin theory for rupture of cross-linked rubbers. The times-to-rupture are proportional to the stress, plasticizer content, and test temperature; the quantity of cracks are time-temperature-stress dependent; and the crack growth is time-temperature dependent. Thus, the rupture process (fracture-times and crack growth) are governed by the viscoelastic

TABLE 5
 QUALITATIVE AND QUANTITATIVE ESCA
 RESULTS ON DRY CONTROL AND END ENVIRONMENTALLY
 AGED EPOXY SAMPLES

PEAK BINDING ENERGY (ev)	IDENTIFICATION	ATOMS PER 1000 ATOMS OF CARBON	
		DRY	AGED
536	OXYGEN 1s	243	338
483	NITROGEN 1s	57	87
285	CARBON 2p	1000	1000
198	CHLORINE 2p	9.3	5.5
166	SULFUR 2p	12	17
99	SILICON 2p	11	8.1

TABLE 6
CHEMICAL ESCA RESULTS ON DRY AND
AGED EPOXY SAMPLES

PEAK IDENTIFICATION	PEAK BINDING ENERGY (ev)	CONCENTRATION (% OF MAIN ELEMENT)	
		DRY	AGED
CARBON 1s			
a. C-C, C-H	285.0	100	100
b. C-OH, C=O	286.6	39	31
c. 	288.9	5.8	10.0
OXYGEN 1s	529.4	100	100
SULFUR 2p			
a. 	162.8	26	22.7
b. 	164.7	100	:
NITROGEN 1s			
a. R ₃ N	402.9	100	100
b. R ₃ NO ⁺	404.3	18.6	41

behavior of the material. This is clearly evident from the effect of different plasticizer content (i.e., different T_g 's) and temperature on the rupture behavior of the material.

Hence, as determined in this study one significant mechanism for the loss of elevated temperature properties in a moisture environment is the formation and growth of cracks in the material. This process is governed by the combined effect of stress, temperature, and moisture. Moisture changes the viscoelastic properties of the polymer so that stress-induced formation and growth of microcracks is facilitated. Further, it could be speculated that the crack growth process is aided by localized chemical chain scission at the crack tip.

SECTION V
CONCLUSIONS

The objective of this research program was to determine the mechanisms by which epoxy resins, utilized in high performance composites and adhesives, exhibit losses of their elevated temperature properties as a result of exposure to a humid environment. Studies were conducted relative to the absorption and diffusion processes involved and these were followed by investigations of the mechanical behavior of the epoxy resin as a function of absorbed moisture for various environmental exposures. A variety of experimental techniques were utilized - constant strain rate and dynamic tensile measurements, infrared spectroscopy, heat distortion tests, bomb creep tests, scanning electron microscopy, polarized-light photomicroscopy, and ESCA.

The results of this work confirmed for this specific resin system that:

1. Moisture absorption and transmission can be treated according to Fick's Second Law.
2. Thermal spikes (rapid thermal excursions to high temperatures) accelerate moisture pick-up.
3. Moisture plasticizes the epoxy resin causing a lowering of the T_g which in turn affects mechanical response such as by shifting the relaxation moduli to shorter times.

But more significantly, this work established the following which heretofore had not been observed:

1. Moisture concentration gradients will induce significant stress gradients within a polymer.
2. Thermal-spikes contribute to microcracking in the resin.

3. When the "wet" T_g of the resin drops below the thermal-spike temperature, there is a substantial increase in moisture pick-up.

4. Weight-gains greater than equilibrium absorption levels are due to microcracking in the resin which results in an increase in moisture pick-up.

5. The lowering of a resin's T_g as a consequence of moisture plasticization can be explained in terms of free volume theory and can be quantified in terms of existing free volume theory relationships.

6. Near infrared spectroscopy can be used to determine the degree of cross-linking in an epoxy resin and the amount of moisture it has absorbed. It shows that the epoxy as-fabricated is not completely cured and undergoes further cross-linking in the swollen, wet state at elevated temperatures - a process which can lead to localized regions of high stress concentrations which in turn can lead to microcracking.

7. Creep studies showed that one mechanism for the loss of elevated temperature properties is the formation and growth of cracks. The failure process can be described by the Bueche-Halpin theory for rupture of cross-linked rubbers. The process is governed by the related effects of moisture, temperature, and stress. Moisture changes the viscoelastic response of the material so that stress-induced crack formation and growth is facilitated.

8. It can be inferred from the creep studies that no significant chemically-induced chain scission is taking place, however, this does not completely rule out very localized chemical scission at such areas as the crack tips.

As a result of this investigation the following facts have been substantiated:

1. Epoxy-based structures will absorb moisture from high humidity environments and this absorption process (rates, amounts, times, and distribution) can be predicted using appropriate solutions to Fick's Law.

2. The use temperatures of epoxy composites and adhesives will be governed by the "wet" T_g of the epoxy matrix material.

3. A minimum T_g can be defined based on the equilibrium value of moisture absorption. This will be specific to a particular epoxy resin system. This observation does not preclude the fact that the epoxy sample may pick-up moisture beyond the equilibrium amount. This can happen, but it will be the result of moisture entrapment during microcracking, a phenomenon that would have less effect on the so-called static properties such as tensile modulus, but would significantly influence dynamic properties such as fatigue resistance. This work points out the necessity for further investigations in this area. In particular, the area of structure "lift-cycle" needs to be addressed.

4. Near infrared spectroscopy would serve as a highly effective quality assurance tool, capable of determining the degree of cure or cross-linking and detecting the amount of water in precursor materials.

5. Internal stresses can exist in a polymer structure as a result of moisture gradients.

6. The heat-up rates and temperature extremes of any thermal excursion (thermal-spike) should be taken into consideration in a structural design in such a manner as to preclude the occurrence of significant microcracking in the structure.

7. Irreversible chemically-induced chain scission processes resulting from moisture/temperature exposures should be of no major concern with epoxy-based structures.

8. The effect of absorbed moisture on the formation and growth of microcracks at elevated temperatures should be investigated for composites and adhesives. Those processes most sensitive to the presence of cracks, such as fatigue, must be evaluated. In particular, the structure's fatigue behavior at temperature in a "wet" condition should be characterized. These results should relate directly to the viscoelastic properties of a reinforced resin matrix material.

9. Further studies in this area must be undertaken to account for the effects of other environmental variables such as oxidative atmospheres, fluids, and lubricants.

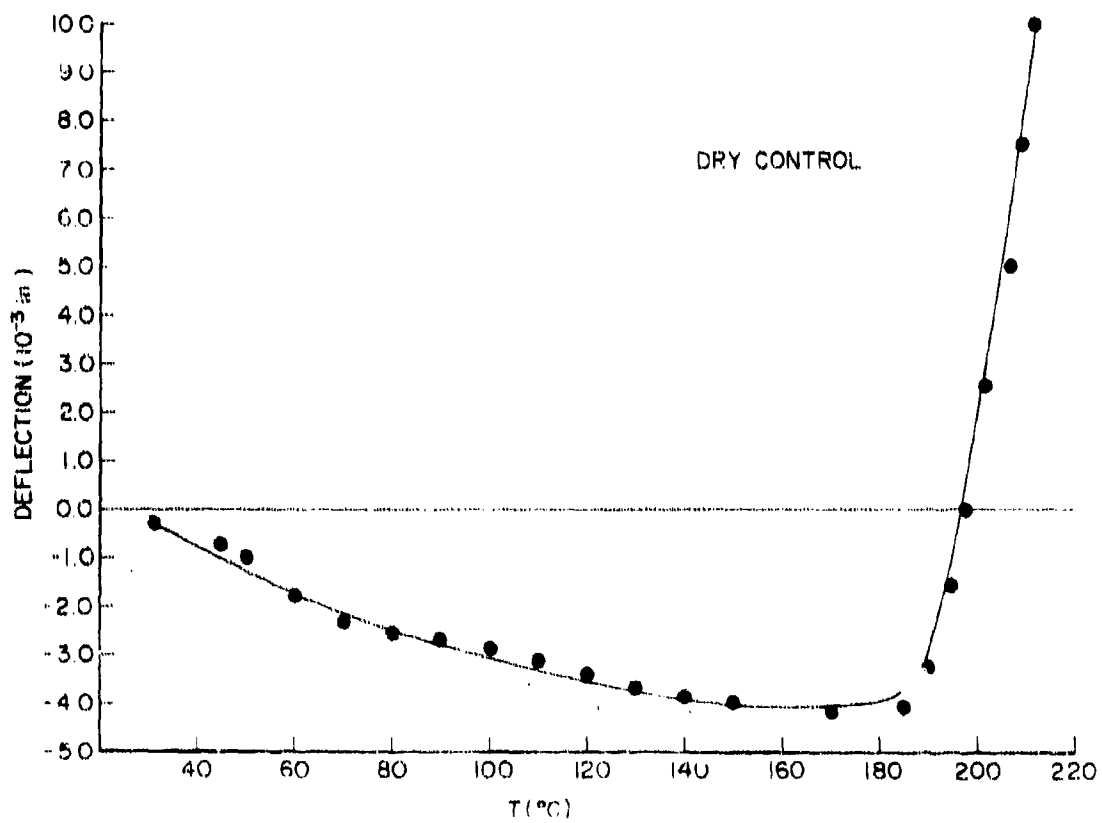
10. Finally, it must be pointed out that this study concerned itself with one particular resin formulation and it can be reasonably anticipated that other factors such as changes in resin chemistry or modifications of viscoelastic properties will influence any given resin's response to humidity and temperature exposures.

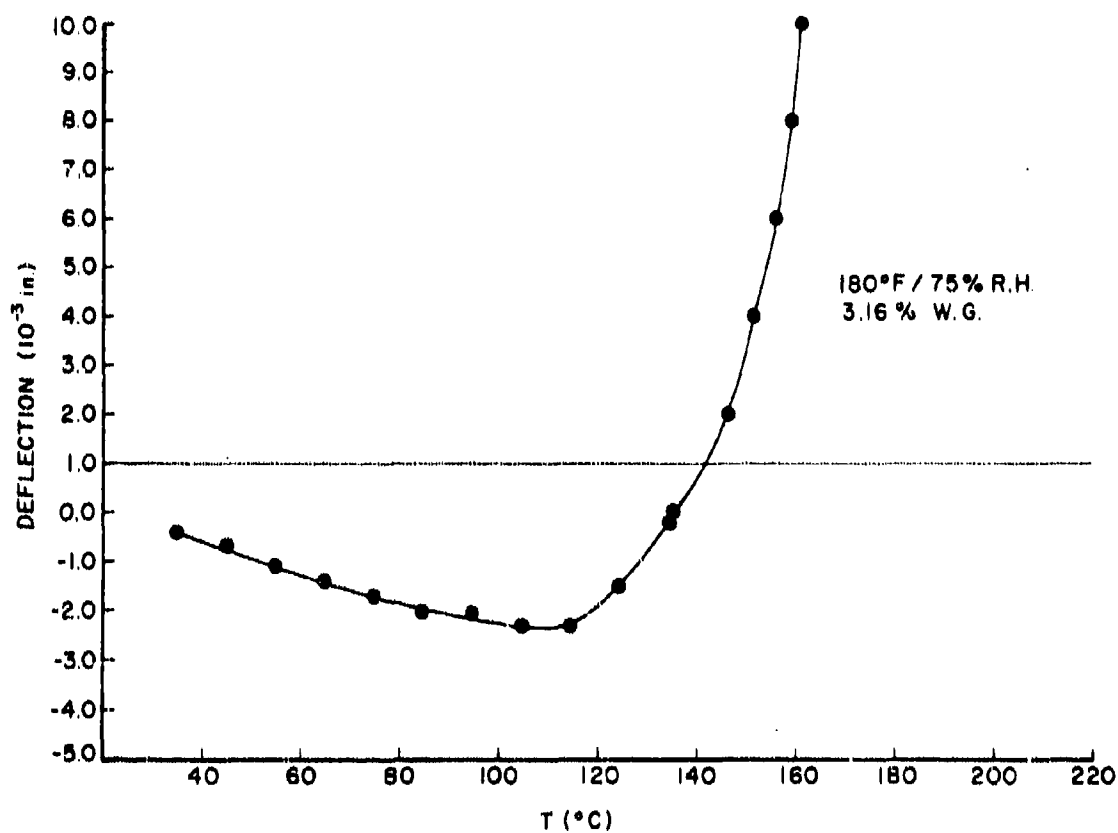
AFML-TR-76-153

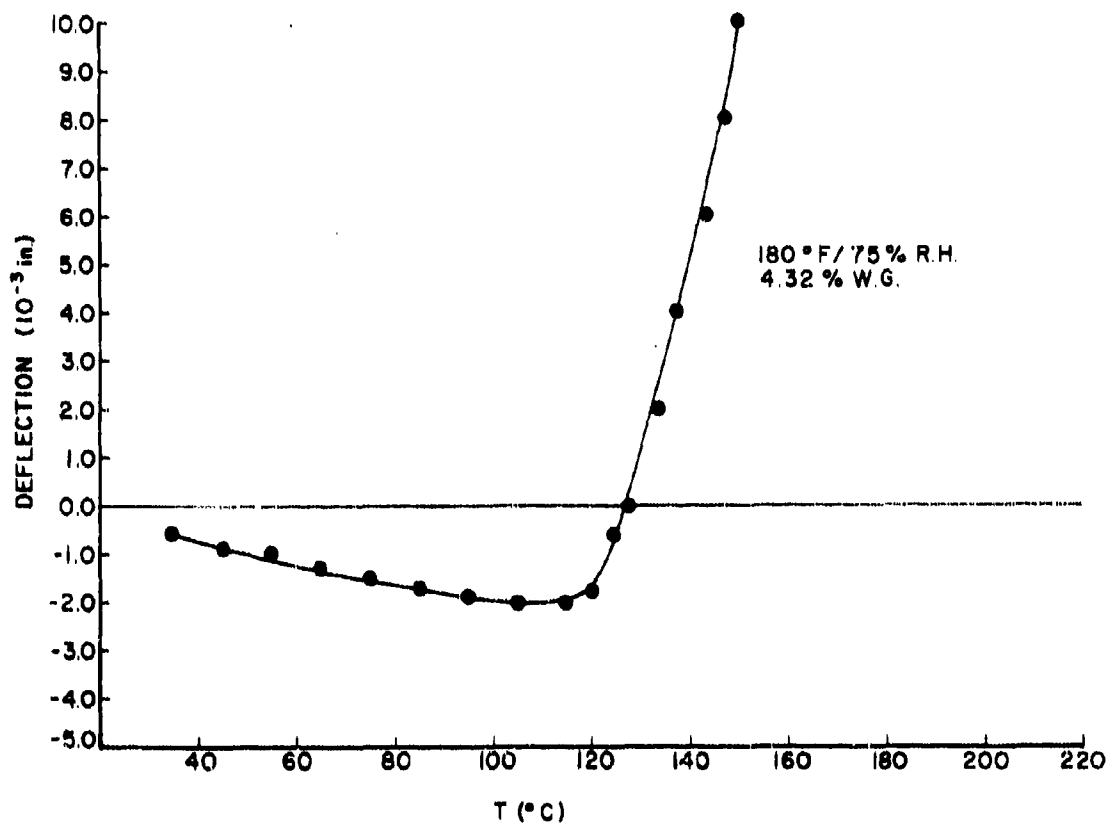
APPENDIX

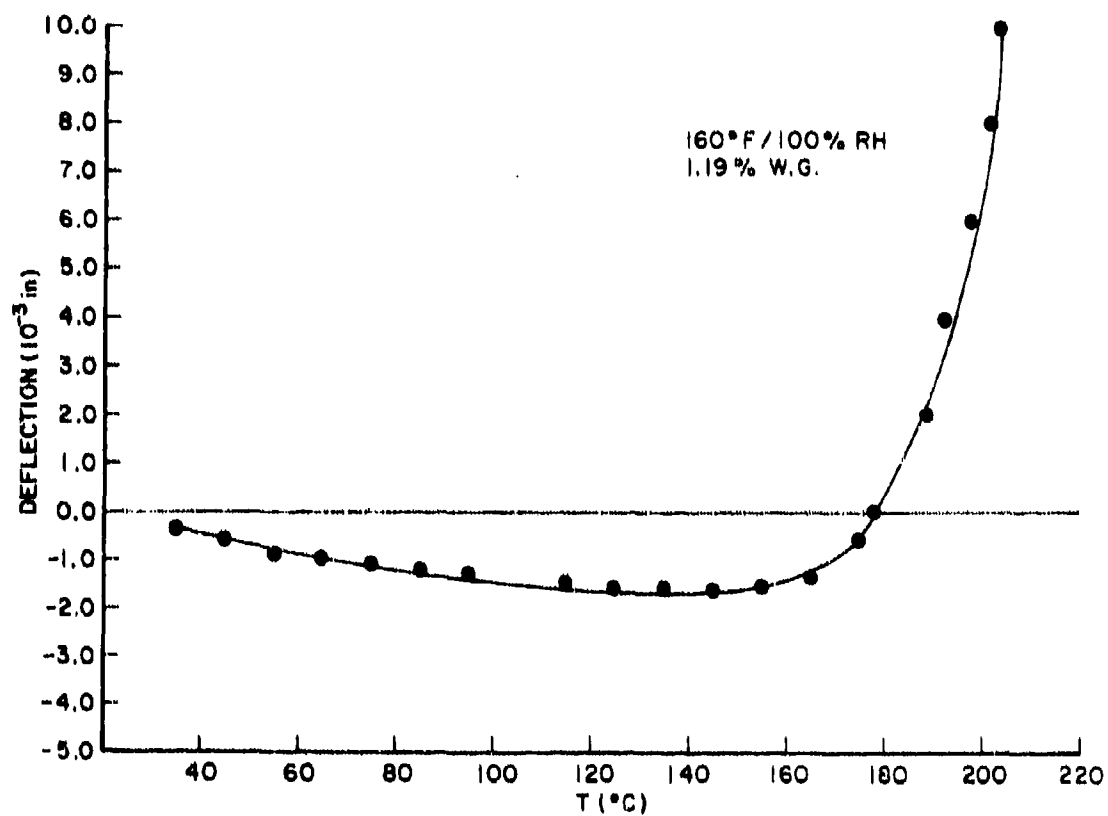
HOT CURVES

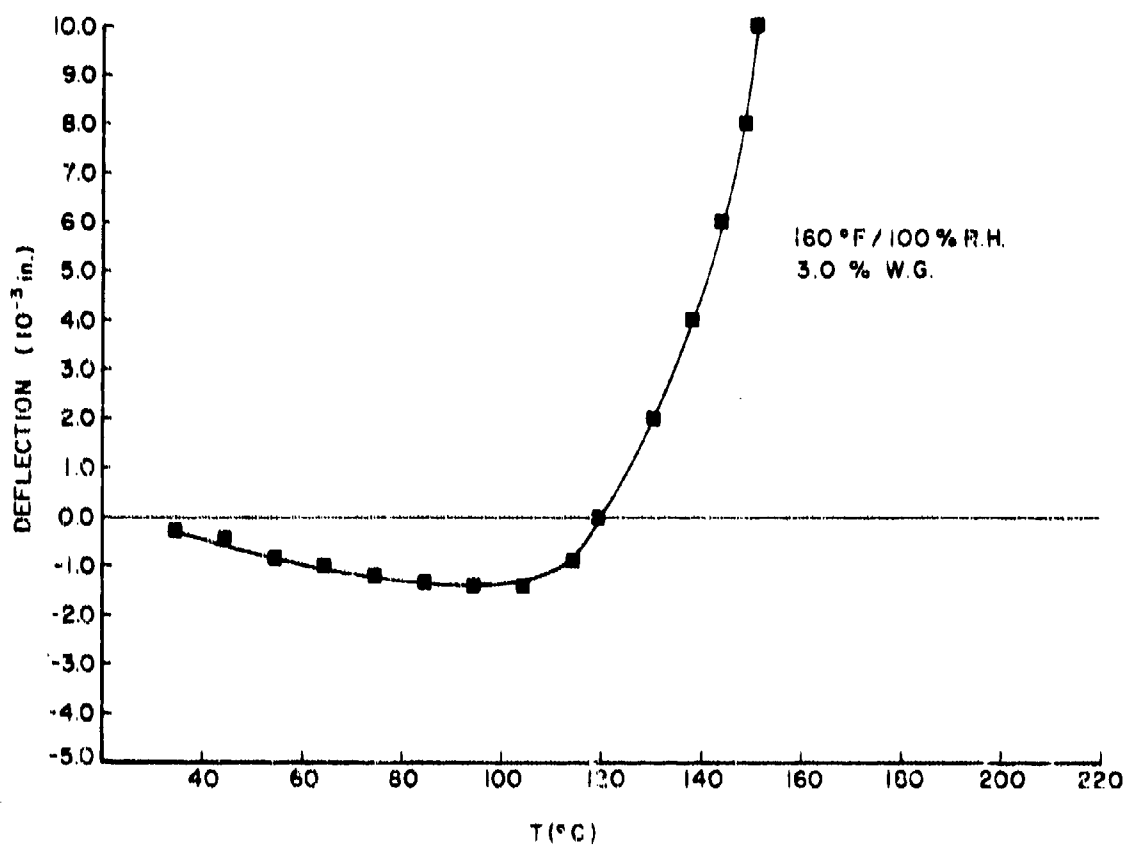
PRECEDING PAGE BLANK NOT FILMED

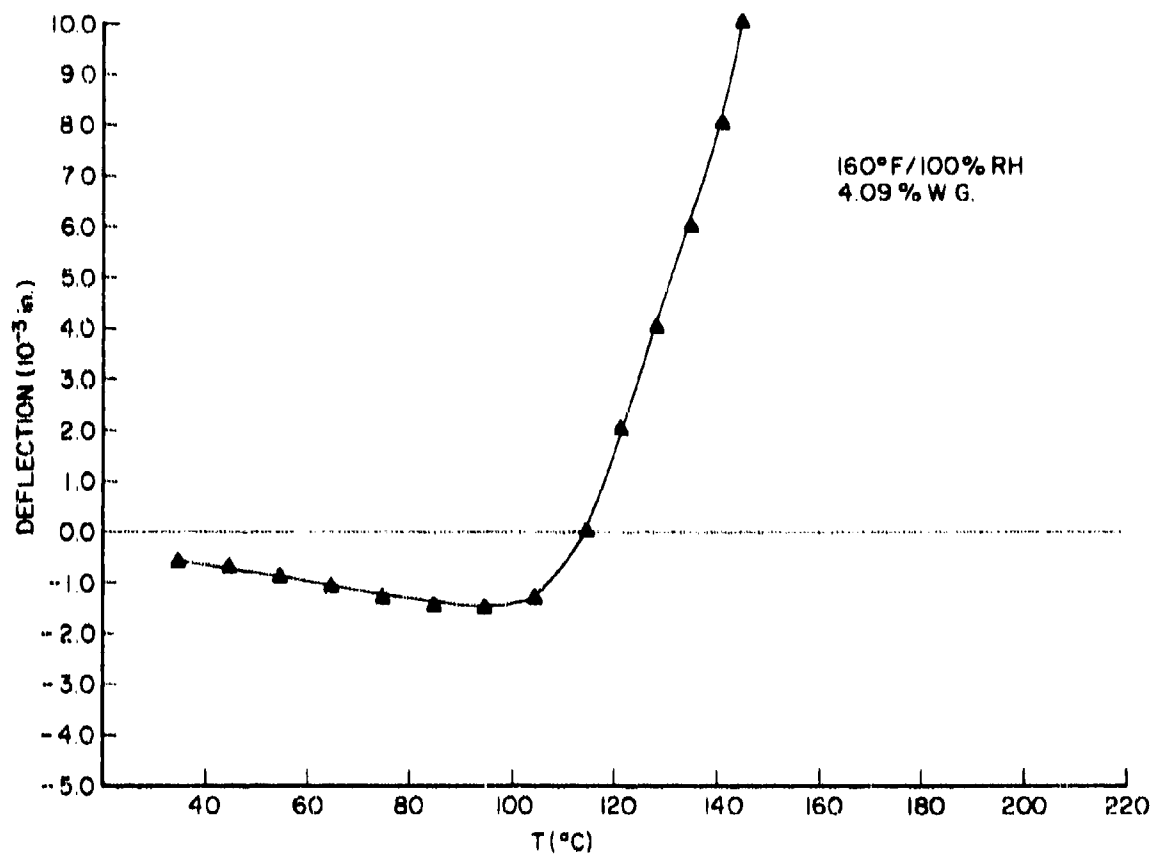


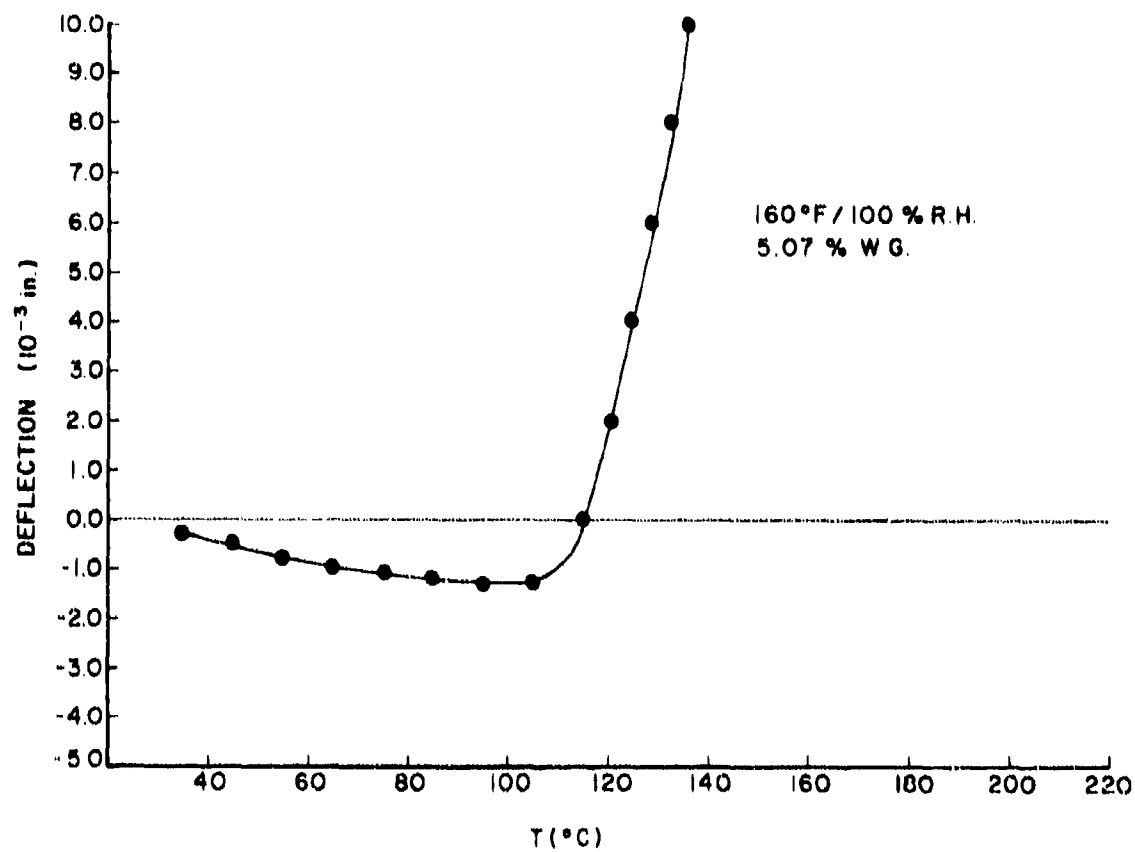


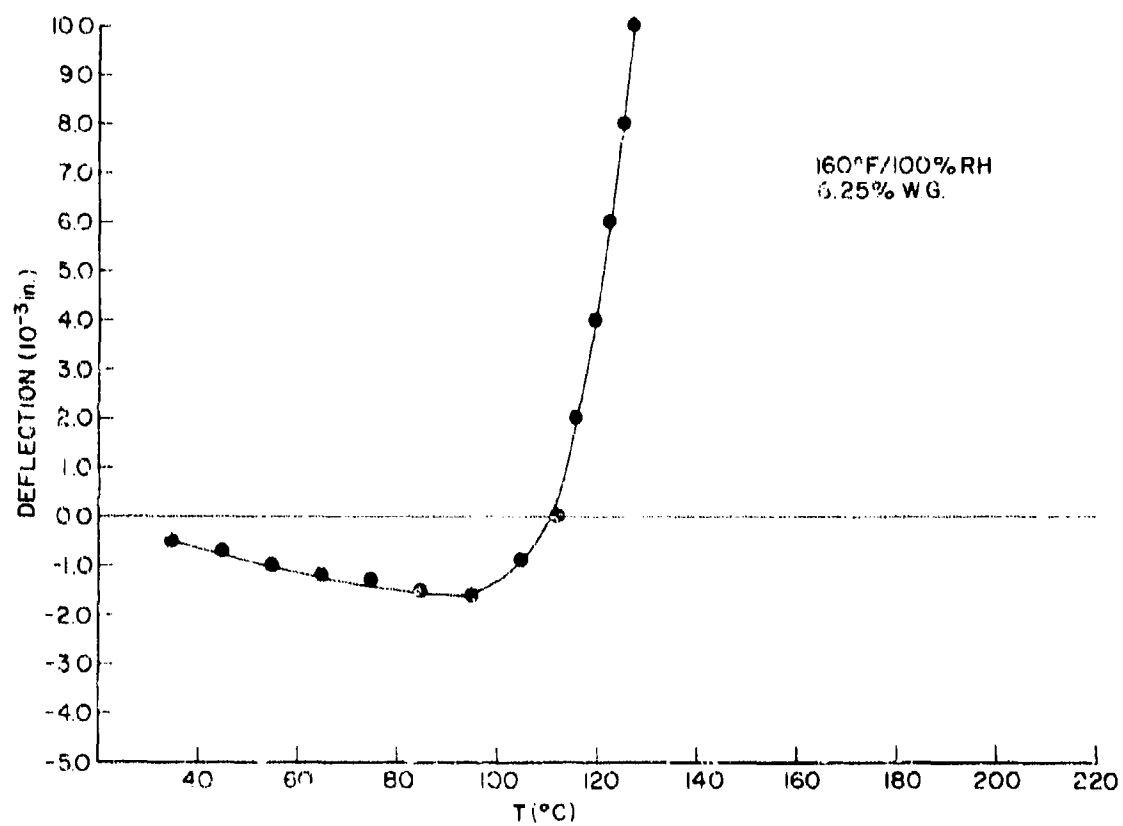


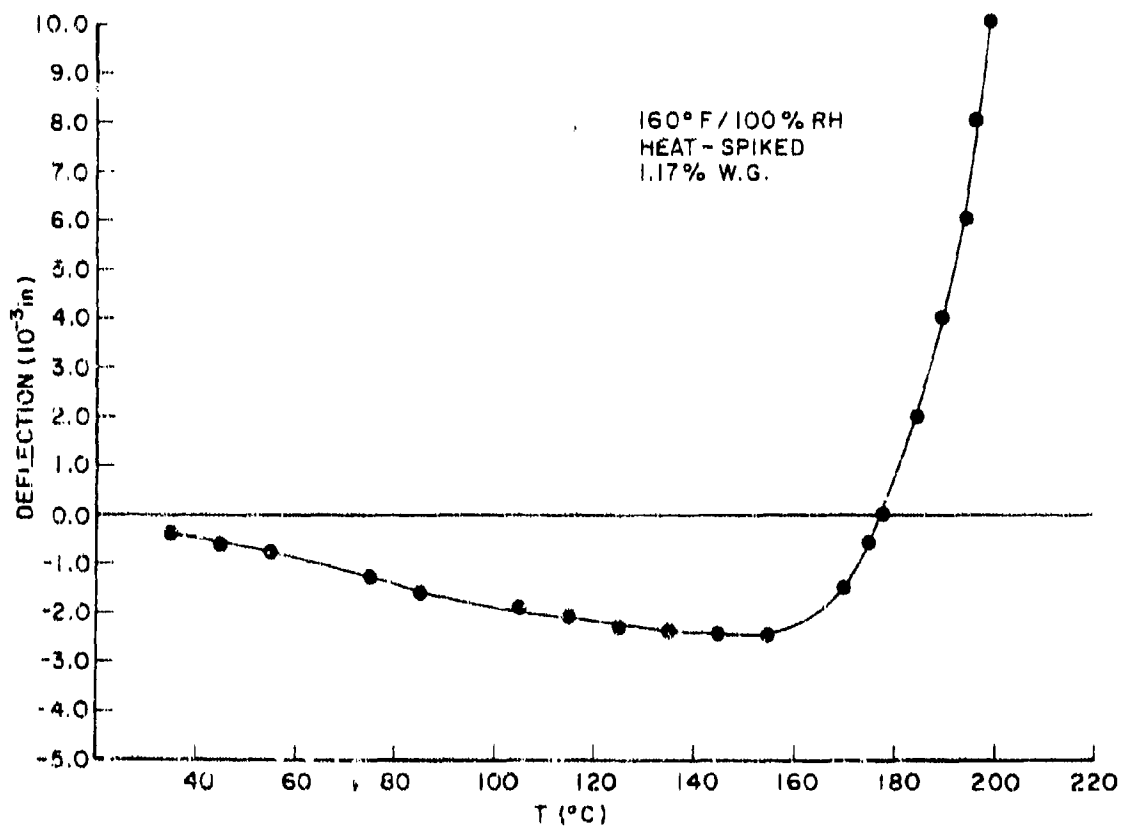


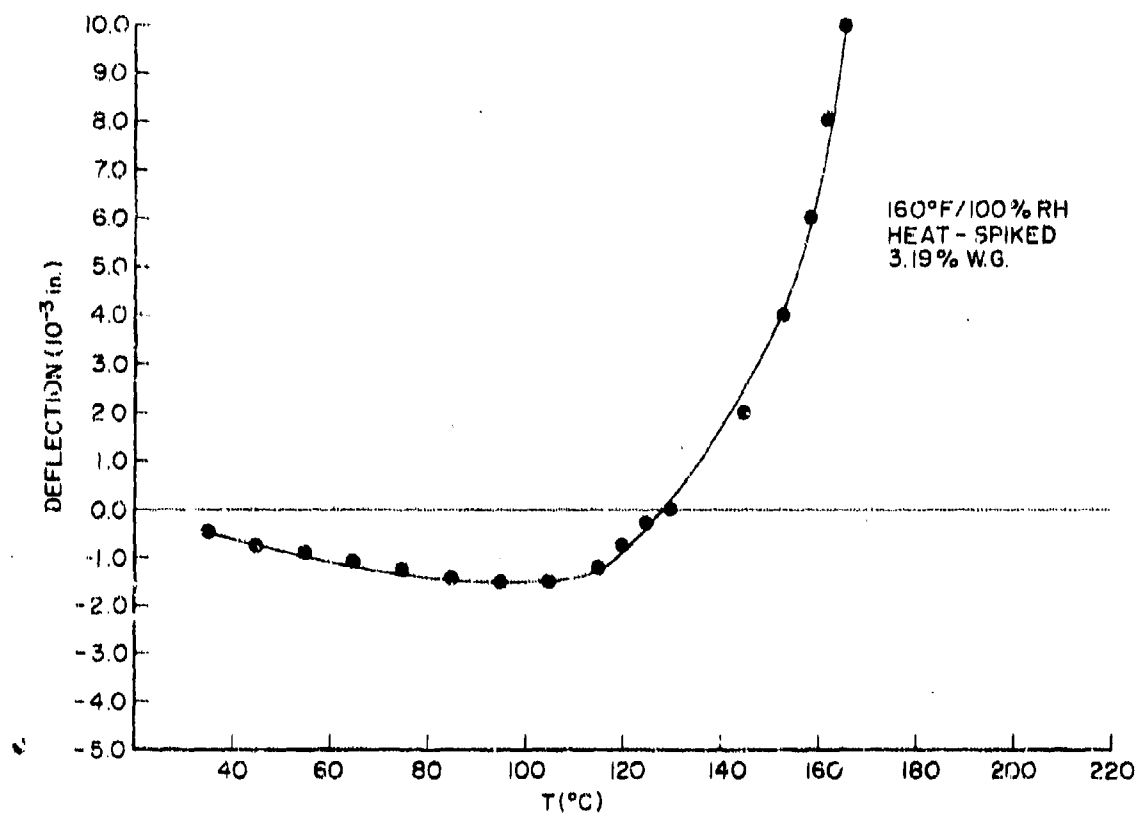


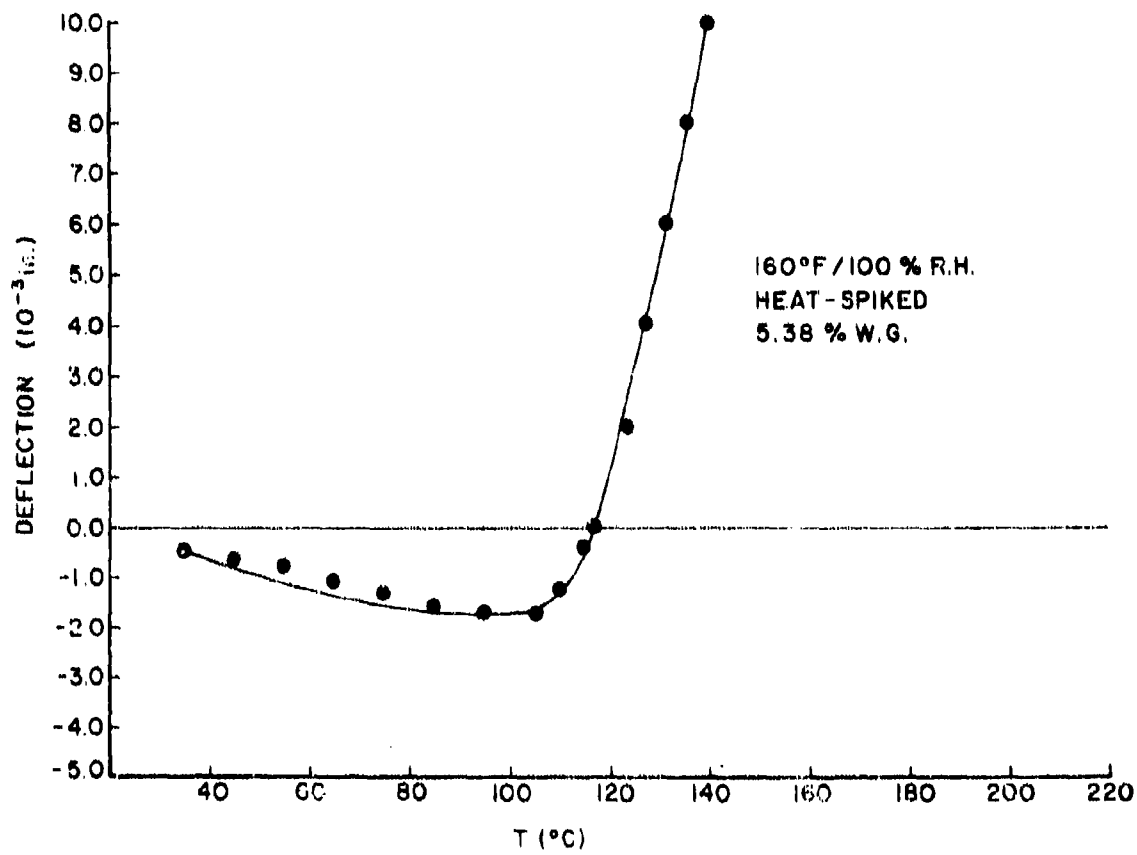


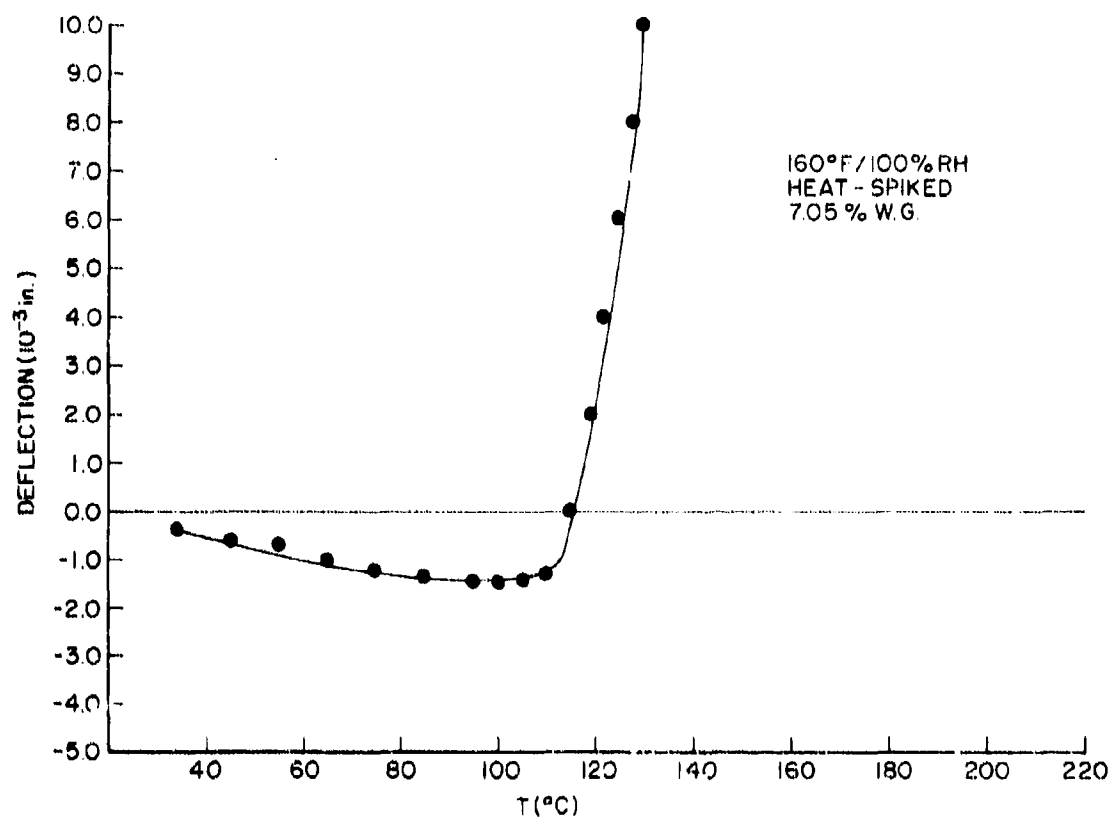


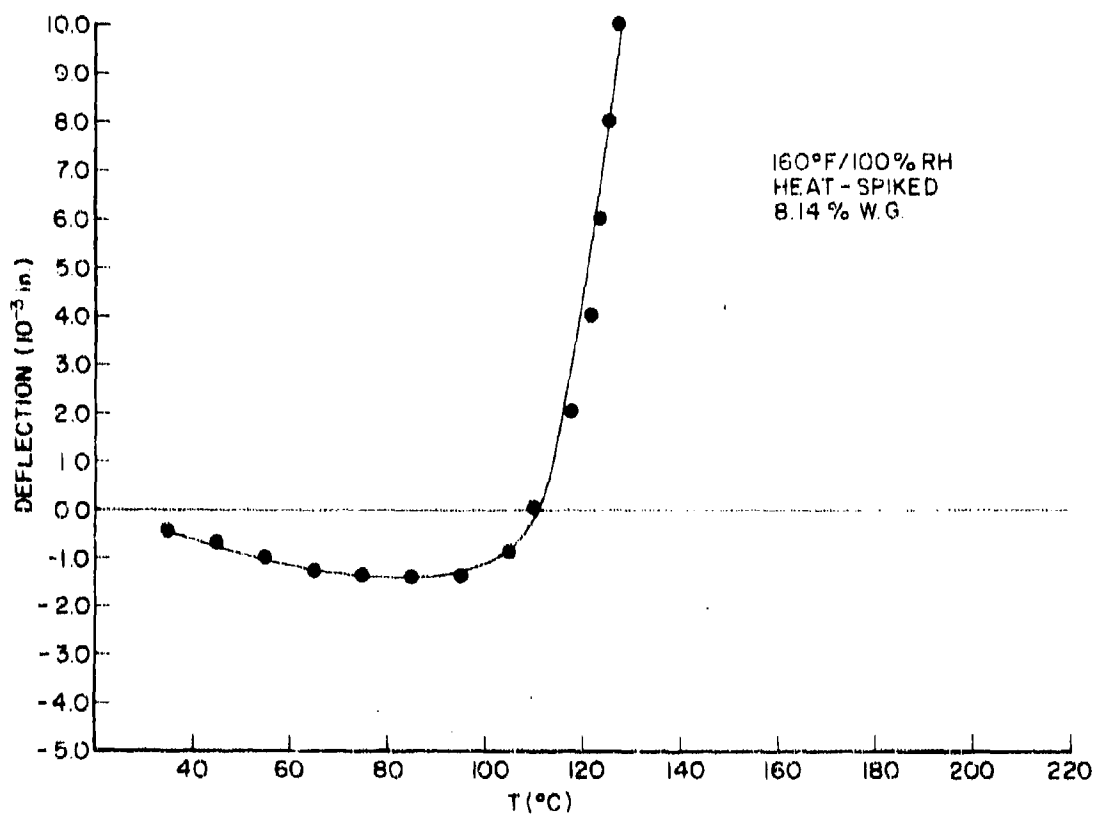












REFERENCES

1. C. E. Browning, The Effects of Moisture on the Properties of High Performance Epoxy Resins and Composites, Technical Report AFML-TR-72-94, 1972.
2. C. E. Browning, "Effects of Moisture on the Properties of High Performance Structural Resins and Composites", Composite Materials: Testing and Design (Third Conference), ASTM STP 546, American Society for Testing and Materials, 1974, p. 284-302.
3. J. Hertz, Investigation into the High-Temperature Strength Degradation of Fiber-Reinforced Resin Composites During Ambient Aging, Report No. GDCA-DGB73-005, Contract NAS 8-27435, June 1973.
4. H. L. Young and W. L. Greever, "High-Temperature Strength Degradation of Composites During Aging in Ambient Atmosphere", Sixth St. Louis Symposium on Composite Materials in Engineering Design, 12 May 1972.
5. D. A. Scolia, "A Study to Determine the Mechanisms of S-Glass/Epoxy Resin Composite Degradation Due to Moisture and Solvent Environments", The Society of the Plastics Industry, 30th Annual Technical Conference, Reinforced Plastics/Composites Institute, February, 1975.
6. W. Scheck, letter report to NASA/MSFC, November 1970.
7. H. W. Eickner, Environmental Exposure of Adhesive-Bonded Metal Lap Joints, Technical Report WADC-TR-59-564, 1960.
8. C. J. Russo, H. A. Newey, and H. V. Holler, New and Improved Laminating Resins for Fiber Reinforced Composites, AFML-TR-69-328, January 1970.
9. I. L. Finar, Organic Chemistry, John Wiley & Sons, Inc., New York, 1963.
10. E. L. McKague, Life Assurance of Composite Structures, Technical Report AFML-TR-75-51, Vol. 1, May 1975.
11. J. F. Carpenter, Moisture Sensitivity of Epoxy Composites and Structural Adhesives, McDonnell Aircraft Company Report MDC A2640, 7 December 1973.
12. G. J. Van Amerongen, "Diffusion in Elastomers", Rubber Chemistry and Technology, Vol. 37, No. 5.
13. R. V. Artamonova, et. al., Vy sokomol. Soedin., Ser. A 1970, pp. 336-342.

REFERENCES (Contd)

14. A. S. Glowacki and D. C. MacDonald, U. S. Rubber Company Report No. SR007-03-04, March 1965.
15. C. Shen and G. S. Springer, Journal of Composite Materials, Vol. 10, 2 (1976).
16. R. S. Stein and A. V. Tobolsky, Textile Research J., 18, 201 (1948).
17. H. Lee and K. Neville, Handbook of Epoxy Resins, McGraw-Hill, New York, 1967.
18. F. Bueche, Physical Properties of Polymers, Interscience, New York, 1962.
19. A. V. Tobolsky, Properties and Structures of Polymers, John Wiley, New York, 1960.
20. J. C. Leslie, et. al., Hercules Analysis of the Composite Aging Problem, Hercules Report H400-12-1-6, March 1970.
21. R. D. Ezell, The Effects of Moisture Absorption on Epoxies, Technical Report NOL-TR-72-108, May 1972.
22. J. M. Augl, "Environmental Degradation Studies on Carbon Fiber Reinforced Epoxies", Air Force Workshop on Durability Characteristics of Resin Matrix Composites, September 1975.
23. C. E. Browning, G. E. Husman, J. M. Whitney, "Moisture Effect in Epoxy Matrix Composites". Composite Materials: Testing and Design (Fourth Conference), ASTM STP, American Society for Testing and Materials, 1976.
24. E. S. Freeman and A. J. Becker, J. Polymer Sci., A-1, 6, 2829 (1968).
25. E. C. Leisegang, A. M. Stephen, and J. C. Patterson Jones, J. Appl. Polymer Sci., 14, 1961 (1970).
26. R. J. Conley, ed., Thermal Stability of Polymers, Marcel Dekker, Inc., N. Y., 1970.
27. R. L. Levy, "Mechanism of Epoxy Moisture Effects", Monthly Report No. 6, Air Force Contract F33615-76-C-5071, July 1976.
28. C. A. May, Exploratory Development of Chemical Quality Assurance and Composition of Epoxy Formulations, Technical Report AFML-TR-76-112, May 1976.
29. B. Rosen, ed., Fracture Processes in Polymeric Solids, Interscience, N. Y., 1964.

REFERENCES (Contd)

30. F. N. Kelley and F. Bueche, J. Polymer Sci., 50, pp. 549-556 (1961).
31. M. L. Williams, R. F. Landel, and J. D. Ferry, J. Am. Chem. Soc., 77, 3701 (1955).
32. C. A. May and F. E. Weir, SPE Transactions, July 1962.
33. R. F. Goddu and D. A. Delker, Anal. Chem., 30, 2013 (1958).
34. H. Dannenberg, SPE Transactions, January 1963.
35. B. Rosen, J. Polymer Sci., 49, pp. 177-188 (1961).
36. B. L. Averbach, et. al., ed., Fracture, Wiley, N. Y., 1959.
37. W. G. Knauss, Trans. Soc. Rheology, 13, 291 (1969).
38. P. Mason, J. Appl. Phys., 29, 1146 (1958).
39. J. C. Halpin, J. Appl. Phys., 35, 3133 (1964).
40. J. C. Halpin, Rubber Chem. Technol. (Review Issue), 38, 1007 (1965).
41. F. Bueche, J. Appl. Phys., 26, 1133 (1955).
42. T. L. Smith, J. Polymer Sci., 32, 99 (1958).
43. M. Braden and A. N. Gent, J. Appl. Polymer Sci., 3, 100 (1960).
44. D. H. Kaelble, J. Appl. Pol. Sci., 9, pp. 1215-1225 (1965).
45. G. M. Bartenev and L. S. Briukhanova, J. Tech. Phys. USSR, 3, 262 (1958).
46. K. Siegbahn, et. al., ESCA: Atomic, Molecular and Solid State Structure Studied by Means of Electron Spectroscopy, Almqvist and Wiksell's Boktryckeri AB, Upsala, 1967.